Analysis and Optimization for Over-the-Air Federated Learning with Energy Harvesting

Caijuan Chen

Doctor of Philosophy

Department of Informatics

School of Multidisciplinary Sciences

The Graduate University for Advanced Studies, SOKENDAI

September 2023

Acknowledgments

Firstly, I would like to express my sincere gratitude to my advisor Professor Yusheng Ji, for her continuous support throughout my Ph.D. study and related research. Her guidance has illuminated the direction of my academic career like a brilliant light. The patience and wisdom of her are the qualities I aspire to in my own life.

I would also want to express my thanks to the co-authors: Professor John C.S. Lui, Professor Hai Lin, and especially Assistant Professor Yi-Han Chiang, who has great support and always give me helpful comments throughout my research progress.

In addition to my advisor, I would like to thank the rest of my thesis committee, Professor Kensuke Fukuda, Professor Koibuchi Michihiro, Associate Professor Megumi Kaneko, and Professor Mianxiong Dong, for their insightful comments and unique advice from their areas of expertise.

I am grateful for the financial, academic, and technical support of SOKEDAI (The Graduate University for Advanced Studies, Japan) and NII (National Institute of Informatics, Japan). Additionally, the financial support and warm regards from MEXT (Ministry of Education, Culture, Sports, Science and Technology, Japan) and JSPS (Japan Society for the Promotion of Science) have helped me through my past three years in Japan.

I want to express my gratitude to the students and visitors from the laboratory for their invaluable advice, unwavering support, and delightful snacks that kept me going during difficult times. I wish everyone a future filled with brightness, happiness, exciting challenges, and enjoyable experiences.

Lastly, I would like to express my gratitude to my cat, who always tried to bite off the network cable during my presentations but never succeeded. I would also like to thank my parents for their support, and Dr. Chaofeng Zhang, who stood by my side

and tried to pull me away from my inner world to realism like a barge hauler of the Volga River.

Abstract

Recently, federated learning (FL) has gained considerable attention as a promising training framework that effectively leverages distributed data and computational resources while addressing communication and privacy issues. The communication bottleneck is a significant challenge in the classical FL system for edge-intelligent networks, stemming from the iterative updating of high-dimensional model parameters between the parameter server (PS) and local clients. This issue arises due to the frequent back-and-forth communication required during the iterative FL process. The over-the-air (OTA) computation has been applied to the FL system as the PS only requires the average of local model updates instead of the individual updates.

However, the resources of local clients are usually limited in terms of battery capacity, which will have impacts on the convergence performance of the OTA FL system. Besides, replacing batteries of local clients is inconvenient and labor-intensive. In this thesis, we aim to apply energy harvesting techniques for the energy-constrained OTA FL system to realize durable training, green computation, and fast convergence. Besides, we also try to thoroughly investigate the impacts of the energy harvesting settings on the convergence performance of the OTA FL system.

To this end, we first try to optimize the client selection and energy management to realize fast convergence for the OTA FL system with energy harvesting clients under the network setting of single-input single-output (SISO) wireless channels, i.e., each client and the PS are equipped with a single antenna. We conduct the convergence analysis of the OTA FL system based on the OTA FL model, communication model, energy consumption and harvesting models. Then, the client selection problem is formulated based on the convergence analysis. To solve the client selection problem, we define the channel-energy-data (CED) coefficient to quantitatively characterize the influence of

selecting one certain client on the convergence rate and then propose a client selection algorithm that jointly considers channel state information, residual battery capacity, and dataset size. The simulation results demonstrate that the proposed solution outperforms other comparison schemes due to wisely selecting clients according to the CED coefficient. In addition, the proposed solution remains superior even if the impacts of noisy channels become pronounced.

Then, the single-input multiple-output (SIMO) network setting is considered for the OTA FL system with energy harvesting clients. We focus on optimizing client selection, receive beamforming, and energy management for the OTA FL system with transmission power control. We first derive the expression of the optimality gap regarding client selection and receive beamforming design. To minimize the optimality gap, a mixed-integer nonlinear programming (MINLP) problem is formulated and decomposed into two sub-problems. Next, the semidefinite relaxation method and the CED-based method are developed to optimize the receive beamforming sub-problem and client selection sub-problem iteratively. An alternative optimization method is proposed to deal with the decoupled sub-problems for obtaining the solutions to the original MINLP problem. Our simulation results demonstrate that the proposed solution is superior to other comparison schemes in various parameter settings.

In summary, in this thesis, we aim to improve the convergence performance of the OTA FL system. The optimization of client selection, receive beamforming, and transmission power control under the energy constraint is considered for the OTA FL system with energy harvesting clients. The simulation results show that the proposed method can outperform comparison schemes under both the SISO and the SIMO network settings.

Contents

List of Figures

List of Tables

List of Abbreviations

AWGN Additive White Gaussian Noise

CED Channel-Energy-Data

CNN Convolutional Neural Network

CP Channel-Prioritized

DC Difference-of-Convex-functions

DNN Deep Neural Network

EP Energy-Prioritized

FL Federated Learning

FLOPs Floating Point Operations

IoT Internet of Things

MINLP Mixed-Integer NonLinear Programming

NIP Nonlinear Integer Programming

OTA Over-the-Air

PS Parameter Server

QCQP Quadratically Constrained Quadratic Programming

RIS Reconfigurable Intelligent Surface

SDR Semidefinite Relaxation

SIMO Single-Input Multiple-Output

SISO Single-Input Single-Output

SNR Signal-to-Noise Ratio

SVM Support Vector Machine

1 Introduction

1.1 Background and motivation

Due to the increase in the number of deployed Internet of Things (IoT) devices, a great amount of data is continuously generated by them. Developers typically resort to deep learning techniques to extract meaningful information from these data. Moreover, with the development of hardware, the computing and storage capabilities of end devices, such as smartphones, smartwatches, and other intelligent IoT devices, have been significantly enhanced, which makes it possible to train models locally. Federated learning (FL) [1] has been proposed as an effective technique for distributed training on distributed IoT devices while preserving privacy.

FL allows multiple devices to collaboratively train a shared model using their local data, while a central parameter server (PS) coordinates the training process. This decentralized approach ensures that sensitive data remains on individual devices, thereby reducing the risk of privacy leakage. Moreover, by minimizing the need for extensive communication between devices and the central PS, FL can optimize resource

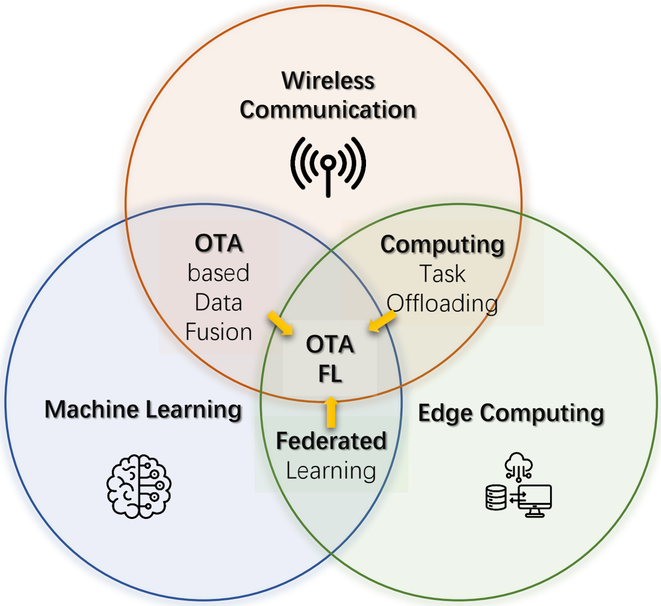

Figure 1.1: The relationships of the OTA FL with machine learning, edge computing, and wireless communication.

utilization and reduce communication overhead. Overall, FL offers a promising solution for training models in a distributed and privacy-preserving manner.

Under the typical FL paradigm, clients collaborate to train a shared model with their local data and send the updates to the PS. Then, the PS aggregates the received signals and broadcasts the averaged updates to the selected clients. The communication resources between clients and PS are usually constrained and the clients are required to interact with the PS multiple rounds during the training processes. As a result, the communication bottleneck becomes a significant problem that needs to be solved for FL. Some strategies have been proposed to impose communication efficiency for FL such as adjusting the number of local epochs [1] and client selection [2, 3, 4]. In [1], the communication cost can be reduced for FL by carrying out multiple local epochs at the client side before communication. In [2, 3, 4], the authors jointly optimize client selection and bandwidth allocation for FL to realize fast convergence and communication efficiency.

Different from the above works, which are implemented with digital transmission for FL, some studies adopt over-the-air (OTA) computation to reduce the communication cost for FL [5, 6, 7, 8, 9]. Compared with digital transmission, clients can share the same wireless channel via analog transmission due to the superposition property of the multiple access channel. The communication overhead can be reduced for OTA FL by making full utilization of the spectrum resources when clients send the gradients to PS. In addition, the privacy leakage from the client to the PS can be avoided for OTA FL since the signals received at the PS side through OTA computation are aggregated signals. Figure 1.1 illustrates that OTA FL is a combination of wireless communication, deep learning, and edge computing. The proliferation of IoT devices and the continuous advancements in the computational capabilities of IoT devices have propelled the demand for distributed computing to realize low latency, privacy protection, high scalability, and communication efficiency for mobile computing systems. As a result, FL has emerged as a solution by combining machine learning and edge computing. Besides, to improve the communication efficiency for FL, OTA FL has gained more and more attention by applying OTA to FL to make full use of the spectrum resources.

Recent research studies for OTA FL focus on client selection [10], power control [11], data heterogeneity [12], and energy constraint [13]. The authors in [10] conduct the convergence analysis for OTA FL and develop a client selection scheme when transmission power control is taken into consideration. In [11], the authors optimize the transmission power control to directly maximize the convergence speed of the OTA FL system with convergence analysis. In [12], the convergence analysis of the OTA FL system with heterogeneous data is given, and the authors conclude that convergence can be guaranteed for OTA FL with heterogeneous data and fading channels. Besides, due to the limited battery capacity of IoT intelligent devices, the energy constraint is a key issue that needs to be addressed. The authors in [13] first derive the convergence analysis for OTA FL when energy constraint is considered for local clients. Then, they formulate an online optimization client selection problem and employ the Lyapunov optimization technique to optimize a stable client selection scheme by solving the nonlinear integer programming (NIP) problem.

However, in most of the current studies, energy harvesting technologies have not been considered for the OTA FL system. Energy harvested from the environment such as wind, solar power, and human motion can enable local clients to perform sustained training and achieve green computing. There are some prior research studies have successfully applied energy harvesting techniques to wireless transmission

[14, 15], task offloading, and resource allocation [16, 17] for mobile edge computing. The authors in [17] aim to minimize energy consumption while meeting the quality of services for local clients with energy harvesting by optimizing task offloading and resource scheduling among the local clients, edge server, and cloud. There are also some prior works regarding FL with energy harvesting clients via traditional digital transmission [18, 19]. In [18], the time-division duplex is used for gradient transmission for typical FL. The authors formulate one integer linear program for client selection and client association and employ the branch and bound algorithm to minimize the training loss when multiple base stations exist. In [19], two different energy harvesting modes are investigated which include deterministic energy arrivals and stochastic energy arrivals. They conclude that energy harvesting technology can realize sustainable distributed learning. In [20], the authors investigate the energy harvesting technique for OTA FL, and two distributions of energy arrival processes including Bernoulli distribution and uniform distribution are discussed.

Different from the previous studies [18, 19, 20] that merely focus on the typical FL [18] or make client selection decisions based on the distribution of the harvested energy arrivals [19, 20], we propose a novel energy-aware OTA FL system that incorporates the energy harvesting technique to supply power to local clients and make client selection decisions based on the channel-energy-data (CED) coefficient. Instead of considering energy consumption as the constraint for the typical FL in [18, 19], we try to quantify the impact of energy consumption and energy harvesting on the convergence performance of OTA FL. Instead of simply giving the convergence analysis of the optimality gap for OTA FL regarding client selection in [20], we give the convergence analysis of the optimality gap for OTA FL regarding energy harvesting, energy consumption, receive beamforming, client selection, and data size. The overall goal of this thesis is to realize fast convergence by optimizing client selection, receive beamforming design, energy management, and transmission power control for OTA FL with energy harvesting clients.

1.2 Contributions

In this thesis, we apply energy harvesting techniques to the OTA FL system to realize durable computation and reduce reliance on conventional battery sources. We have two objectives as follows:

- Objective 1: For single-input single-output (SISO) OTA FL systems, we try to improve the convergence performance by optimizing the client selection with energy harvesting clients.
- Objective 2: For single-input multiple-output (SIMO) OTA FL systems, we try to improve the convergence performance by jointly optimizing receive beamforming, client selection, and transmission power control under the energy constraint.

In Chapter 3, we consider one SISO OTA FL system with energy harvesting clients, and the client selection problem under the energy constraint is formulated as a NIP problem to improve the system performance. The CED coefficient is defined to quantify the impacts of the channel gain, transmission energy, and data size on the convergence speed of the OTA FL system. Then, the discrete search method is adopted to solve the NIP problem. The simulation results validate that the proposed method is effective for the client selection scheme in the OTA FL system.

In Chapter 4, we consider one SIMO OTA FL system with energy harvesting and energy constraint, we aim to optimize the joint problem of client selection, receive beamforming design, and energy management to improve the system performance. We first derive the optimality gap between the actual loss and the optimal loss for OTA FL and quantify the impacts of energy harvesting, energy consumption, client selection, and receive beamforming design on the optimality gap. To minimize the optimality gap, we formulate a mixed-integer nonlinear programming (MINLP) problem based on the convergence analysis. Then, the original intractable MINLP problem is transformed into an online MINLP problem. By decomposing the online MINLP problem, two sub-problems can be obtained one for client selection and the other for receive beamforming design. To address the MINLP problem, we introduce several optimization strategies, encompassing a semidefinite relaxation (SDR) approach for the receive beamforming design sub-problem, a CED-based technique for the client selection sub-problem, and an alternative optimization method to jointly optimize the decoupled sub-problems. We conduct a thorough theoretical analysis of the proposed scheme and validate its performance via simulation experiments. A comparative evaluation with other comparison schemes reveals that our proposed approach exhibits substantial advantages in terms of convergence performance for OTA FL. Besides, we also evaluate the impact of design parameters on the learning performance of OTA FL.

1.3 Outline of thesis

The chapters of this thesis are organized as follows. In Chapter 2, the background knowledge regarding FL and OTA computation is introduced and the previous studies related to OTA FL, energy-aware FL, and energy harvesting for mobile edge computing are listed. In Chapter 3, the client selection scheme is designed to realize fast convergence for OTA FL under the SISO configuration setting with energy harvesting. Chapter 4 focuses on the OTA FL with energy harvesting under the SIMO setting, the client selection and receive beamforming are jointly optimized to improve the convergence performance of the OTA FL system. In Chapter 5, the conclusion of this thesis is given by summarizing the contributions. Besides, some potential research directions are listed as future work to further improve our current research.

2
Background and related work

This chapter introduces the background and previous studies related to OTA FL with energy harvesting. Section 2.1 introduces some preliminary knowledge including FL and OTA computation. Section 2.2 reviews some previous literature related to OTA FL and energy-aware FL. In Section 2.3, we highlight the differences and novelty of the thesis compared with the related work.

2.1 Background

In this section, the basic knowledge related to FL and OTA computation is given in subsections.

2.1.1 Federated learning

FL is proposed as the distributed machine learning technique that leverages the power of local devices to generate a global model without the need for centralized data

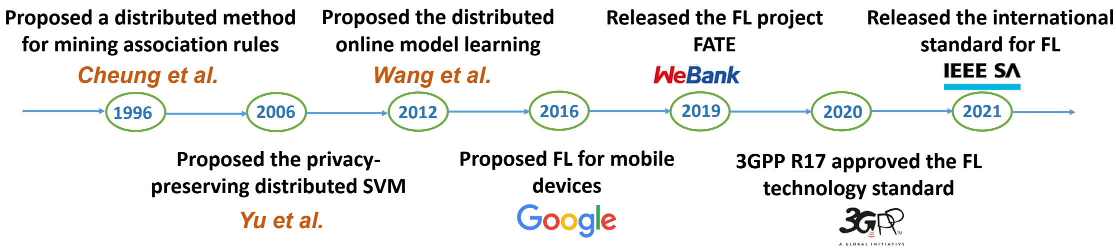

Figure 2.1: The roadmap of FL.

storage. The technical and theoretical foundations of FL can be traced back to various research contributions over the years, which is summarized in Figure 2.1. In [21], the authors first proposed association rule mining techniques for distributed databases, which laid the groundwork for distributed data mining approaches that later influenced FL. In 2006, Yu et al. [22] introduced distributed support vector machine (SVM) model with privacy protection on horizontally partitioned data, highlighting the importance of privacy-preserving techniques in distributed learning. In [23], the authors proposed concepts such as online machine learning with distributed privacy protection. In 2016, the Google AI team introduced the first FL framework [1], specifically targeting privacy protection for local clients. The WeBank AI team proposed federated transfer learning by combining FL with transfer learning. They released the open-source system FATE [24], which has been widely used in the industry. Subsequently, in 2021, IEEE released the first international standard IEEE 3652.1-2020 for FL [25], which provides guidelines for the architecture and application of FL. These research studies have significantly influenced the development and advancement of FL.

Figure 2.2 illustrates the operation of a FL system, where multiple decentralized edge clients contribute to the creation of a global model through on-device training. This collaborative approach is applicable in diverse domains such as healthcare [26], autonomous vehicles [27], financial services [28], and sensor data analysis [29]. The local models trained by each client are then combined to generate a global model that captures the shared knowledge of all clients. FL offers several advantages, including scalability, data privacy, and reduced storage space [30, 31]. The technique allows for efficient training of models on decentralized data sources without requiring data to be shared or transferred to a central server, thus maintaining the privacy and security of client data. Additionally, FL can be used to train models on large and diverse data sets,

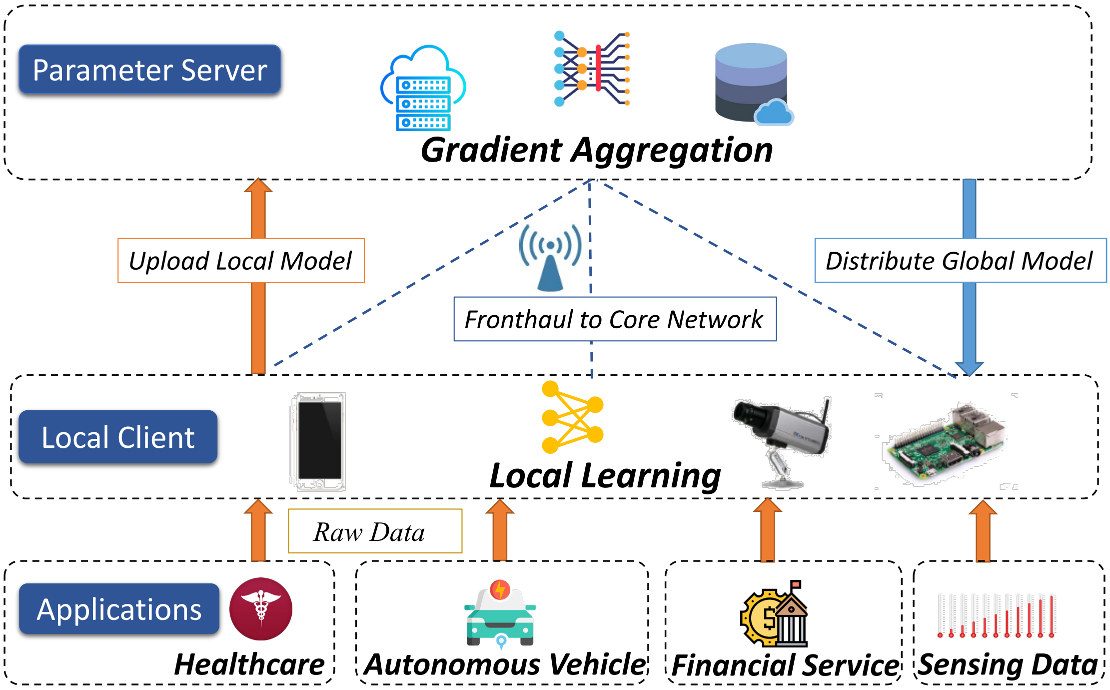

Figure 2.2: Implementations of FL in different application scenarios.

which would otherwise be difficult to manage in a centralized setting.

Figure 2.3 shows the basic flowchart of wireless network-based FL, which includes five main steps: client selection, global model broadcast, local model update, local model upload, and global model aggregation. Global broadcast updates can be performed simultaneously each time. Due to issues such as network latency and device computing power, there may be differences in the model upload time after the local updates are completed. The cloud needs to coordinate with the clients to update the model as synchronously as possible to improve device utilization efficiency. To address the common issues and guarantee the convergence efficiency, the classical FL system named FedAvg is proposed in [1], which is illustrated clearly in Algorithm 2.1. The detailed procedures of the FedAvg algorithm at the t-th training round are listed as follows:

- *Client selection*: At first, a subset of clients $\mathcal{K}_t$ are selected from the total client set $\mathcal{K}$ by the PS to join in the training.

- *Global model broadcast*: The current global model $\boldsymbol{w}_t \in \mathbb{R}^S$ is broadcast to the selected local clients, where S represents the total number of model parameters.

- *Local model update*: The selected local client k update the local model $\boldsymbol{w}_{k,t}$ as

$$\begin{aligned}\boldsymbol{w}_{k,t} &= \boldsymbol{w}_t \\ \boldsymbol{g}_{k,t}^{bs} &= \nabla f\left(\boldsymbol{w}_{k,t}, bs\right) \\ \boldsymbol{w}_{k,t+1} &= \boldsymbol{w}_{k,t} - \eta \boldsymbol{g}_{k,t}^{bs},\end{aligned} \tag{2.1}$$

  where $\boldsymbol{g}_{k,t}^{bs}$ is the local gradients calculated with the local data with batch-size bs and local model $\boldsymbol{w}_{k,t}$, and $\nabla f\left(\boldsymbol{w}_{k,t}, bs\right)$ is the corresponding gradients.

- *Local model upload*: After the training process is completed, the selected client k transmits the local gradients $\boldsymbol{g}_{k,t}$ to the PS.

- *Model aggregation*: After receiving the signals, the global gradient $\boldsymbol{g}_t$ can be represented as

$$\boldsymbol{g}_t = \frac{\sum_{k \in \mathcal{K}_t} D_k \boldsymbol{g}_{k,t}^{bs}}{\sum_{k \in \mathcal{K}_t} D_k}, \tag{2.2}$$

  where D_k is local data size at the selected client k. Let η denote the fixed learning rate, the global model is updated as

$$\boldsymbol{w}_{t+1} = \boldsymbol{w}_t - \eta \boldsymbol{g}_t. \tag{2.3}$$

The aforementioned steps will be iterated for T rounds, ultimately resulting in a model that is sufficiently distributed for training on the data from K clients.

The common challenges facing the classical FL algorithm FedAvg include communication overhead [32, 33], system heterogeneity [34, 35, 36, 37], statistical heterogeneity [38], and energy constraints of local clients [39], such as laptops, IoT devices, and wearable sensors [40]. The key point to effectively implementing FL in a wireless network environment is to consider these challenges and develop solutions that can mitigate their impacts on the learning process. The most widely concerned topics recently include communication efficiency [41, 42, 43], client scheduling [44, 45, 46, 47, 48, 49], and resource allocation [50, 51, 52, 53, 54] for FL systems, which are explained in detail

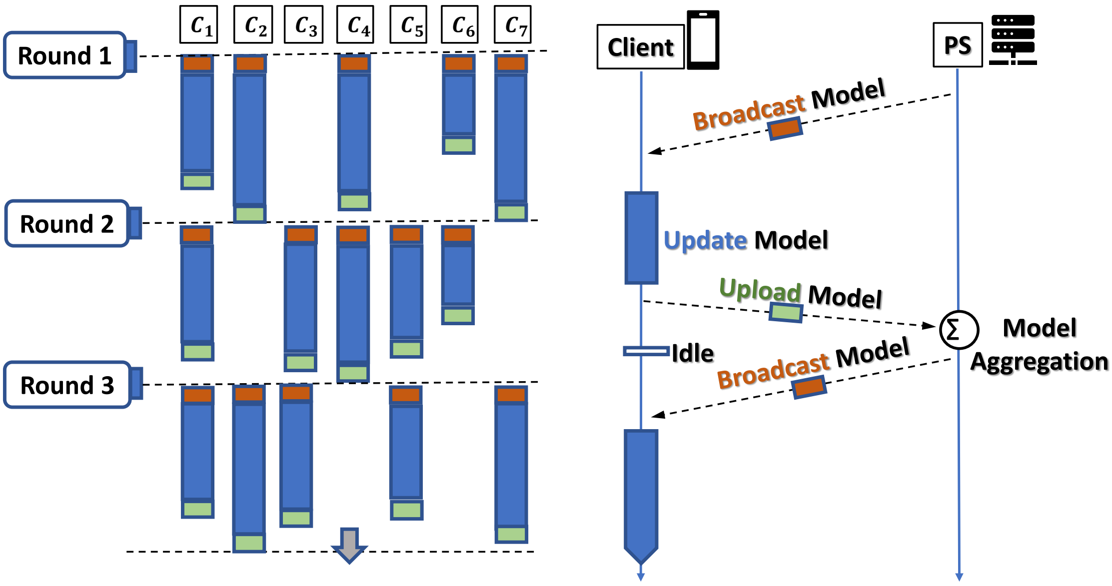

Figure 2.3: Illustration of the procedures for FL, which includes five main steps: client selection, global model broadcast, local model update, local model upload, and global model aggregation.

as follows.

- *Communication efficiency*: Although mobile devices' computational capabilities have grown significantly, the shortage of radio resources remains a persistent issue. In the FL system, local model transmission is crucial for collaborative learning, emphasizing the need to develop novel wireless communication techniques that can enhance FL efficiency. Researchers are currently investigating and creating innovative approaches to tackle radio resource constraints which include communication compression [55] and analog transmission [56], intending to improve the effectiveness of FL on mobile devices.

- *Client selection*: For the FL system, participant selection involves the process of selecting clients that will take part in each training round. This is typically done through random selection by the PS for FedAvg algorithm, which then aggregates parameter updates from all participants and takes a weighted average of the models. However, the training progress of FL is often constrained by the slowest participating devices, also known as stragglers [57]. To overcome this bottleneck, researchers are exploring new participant selection protocols that

Algorithm 2.1 The FedAvg Algorithm

Require: Local mini-batch size BS, number of participants $|\mathcal{K}_t|$ per iteration, number of local epochs E, local data set D_k at client k, learning rate η, and the total number of training rounds T.
Ensure: Global model $\boldsymbol{w}_T$.

```
Server side:
Initialize the global model w_0.
for t = 1, 2, ..., T do
    Select a subset K_t of the local clients to join in the training.
    for k ∈ K_t do
        g_{k,t} ←client k
    end for
    The gradient aggregation is computed as in (2.2) and the global model update
    is conducted as in (2.3).
end for
Client k side:
for each local epoch ep = 1, 2, ..., E do
    for each batch bs ∈ D_k do
        The local model is updated as in (2.1)
    end for
end for
```

can improve training efficiency in FL [58].

- *Resource allocation*: Due to the system heterogeneity and statistical heterogeneity of the local clients for the FL system, the resource heterogeneity has several dimensions that need to be considered, including variations in computation and communication capabilities and the data quality of local clients for local model training. Some strategies such as the bandwidth allocation [39, 59], power control [60] and the learning rate optimization [61] can improve the system convergence for the FL system.

These above-mentioned techniques aim to optimize the utilization of available resources while minimizing the negative impact on local clients. By carefully considering these issues, successful and efficient FL implementations can be achieved.

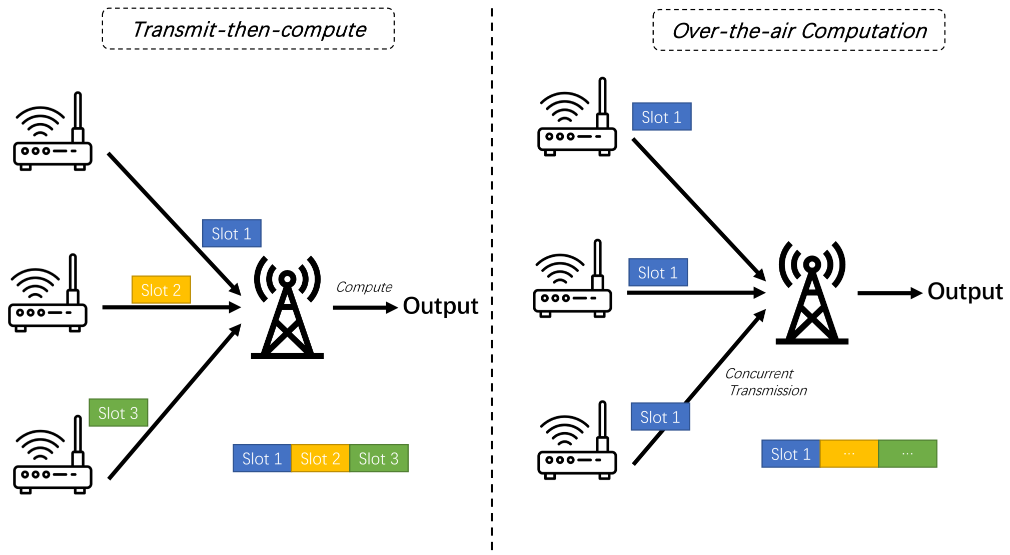

Figure 2.4: The comparison of the traditional wireless transmission and OTA computation.

2.1.2 Over-the-air computation

OTA computation is a novel approach to computing that utilizes the superposition property of wireless multiple-access channels to perform mathematical functions. As illustrated in Figure 2.4, traditional computing technique requires the acquisition of local data from edge devices, such as smartphones, laptops, tablets, vehicles, or sensors over orthogonal channels [62, 63], and the computation is conducted at the server side after receiving all information from all devices over the traditional transmission. Different from the traditional computing technique, for OTA computation, the wireless channels are used to directly perform computation tasks, leveraging the simultaneous transmission of multiple signals over the same frequency band. This approach offers several advantages, including reduced latency, increased energy efficiency, and improved privacy, as sensitive data does not need to be transmitted over separate channels. Although still in its early stages, OTA computation has the potential to transform various fields, including wireless communication, data processing, and edge computing.

Commonly, the procedures include the pre-processing and post-processing steps when OTA computation is applied to wireless communication and edge computing.

Table 2.1: Some example functions for OTA computation.

Operation	Pre-processing	Post-processing	Function
Arithmetic mean	$s_{k,t}$	$\frac{1}{K}$	$f_t = \frac{1}{K}\sum_{k=1}^{K} s_{k,t}$
Weighted sum	$a_{k,t}s_{k,t}$	1	$f_t = \sum_{k=1}^{K} a_{k,t}s_{k,t}$
Geometric mean	$log(s_{k,t})$	exp	$f_t = (\prod_{k=1}^{K} s_{k,t})^{1/K}$
Polynomial	$a_{k,t}s_{k,t}^{i_{k,t}}$	1	$f_t = \sum_{k=1}^{K} a_{k,t}s_{k,t}{}^{i_{k,t}}$

As shown in Figure 2.4, assuming that there are K sensors in the wireless sensor network and the generated initial signal at the node k during the time slot t is $s_{k,t}$, the pre-processing operation for the input signal is $\varphi_{k,t}$ and the post-processing operation is ς_t, where the pre-processing $\varphi_{k,t}$ is conducted at the local node k in time slot t and the post-processing ς_t is conducted at the server side after server receives the aggregated signal. The OTA computation function f_t is conducted as

$$f_t = \varsigma_t(\varphi_{k,t}(s_{k,t})). \tag{2.4}$$

As shown in Table 2.1, some common functions including arithmetic mean, weighted sum, geometric mean, and polynomial that can be computed via OTA computation, where $a_{k,t}$ means the weight of signal $s_{k,t}$ and $i_{k,t}$ means the index of signal $s_{k,t}$.

Wireless systems have gained significant attention due to their potential to enable various applications, such as environmental monitoring, structural health monitoring, and industrial automation. These applications often require the computation of various functions, such as maximum, minimum, mean, norm, and polynomial functions, which can be challenging to perform on resource-constrained sensor nodes. To address this challenge, researchers have explored the use of OTA computation, which involves utilizing the channel's characteristics to perform computations and performs computations in a distributed manner, enabling distributed sensing and optimizing in the distributed wireless system. By adopting OTA computation to compute these nomographic functions, wireless sensor network can effectively perform various computation-intensive tasks. This can help improve the overall performance and accuracy of wireless sensor networks, making them a valuable tool for a range of applications. As such, OTA computation is an exciting area of research that holds significant promise for the future of wireless sensor systems.

The OTA computation has been investigated in various fields, such as distributed localization [64], wireless control systems [65], wireless sensor networks [66, 67], wireless data center networks [68], wireless intra-chip computation [69], wireless communication [70], and physical layer security [71]. The authors in [65] apply the OTA computation to the wireless control system and try to minimize the effect of the wireless channel on the control system under the transmit power control. In [66], the authors adopt the OTA computation to compute the arithmetic mean of temperatures measured by 250 sensors for environmental monitoring. To realize the scalability and communication efficiency for the data central network, OTA computation is proposed to compute the arithmetic mean of the symbols at K source nodes for a wireless data central network in [68]. To realize scaling-out wired interconnects for hyperdimensional computing, OTA computation is exploited and a similarity-search task via multiple in-memory computing cores is proposed in [69]. In [70], the authors use the compute-and-forward scheme to harness the collisions for massive access channels, and the nodes forward a linear combination of the messages to the base station along with the corresponding coefficients for decoding. In [71], the authors propose the use of OTA computation for the multiplication of Gaussian prime numbers, which is then utilized to compute a secret key that can be applied in various encryption processes. Additionally, this approach can be used to generate keys using predetermined key-generation functions.

2.2 Related work

2.2.1 Over-the-air federated learning

As discussed in the previous subsection, OTA computation is highly suitable for distributed optimization systems, and the FL system is the prime example of such a system. Due to the limited wireless network resources and the presence of a large number of distributed devices in FL systems, the adoption of OTA computation can be

Table 2.2: The comparison of OTA FL with traditional FL.

Comparison	Traditional FL	OTA FL
Transmission scheme	digital transmission	analog transmission
Computation mode	transmit-then-compute	OTA computation
Privacy protection	low	high
Communication cost	high	low

highly beneficial for effectively utilizing network bandwidth. Furthermore, the process of aggregating model parameters in FL can be incorporated into the model parameter uploading process. By doing so, OTA computation can be leveraged to further optimize the overall performance of the system. As listed in Table 2.2, the OTA FL system can achieve communication efficiency, transmission along with aggregation, and privacy protection compared with the traditional FL via digital transmission. Recently, OTA FL has been proposed for communication-efficient distributed learning by making full use of the spectrum resources [61, 72, 73, 74, 75, 76, 77, 78, 79]. Most of the recent articles focus on the transmission power control [73, 74, 75], client selection scheme design [6, 13, 56, 77], and receive beamforming design [61, 76, 80, 81, 82] for the OTA FL system.

The design of transmission power for local clients can mitigate aggregation errors and improve the convergence speed for OTA FL. In [73], the authors adopt the successive convex approximation method and the trust region method to optimize transmission power for OTA FL when non-uniform channel fading exists. In [74], the authors optimize the transmission power to minimize the aggregation error for OTA FL when taking gradient statistics into account. In [75], the authors try to optimize the number of local iterations and adjust the transmission power to improve the convergence rate.

The presence of heterogeneous local clients, characterized by varying computational capabilities, current battery levels, and dynamic network conditions, can significantly affect the final performance of the OTA FL system. Therefore, the client selection scheme is important to achieve optimal outcomes. Some previous studies have focused on the client selection design for OTA FL. In [6], the authors adopt the difference-of-convex-functions (DC) method to mitigate the influence of system heterogeneity and network heterogeneity for OTA FL. Specifically, the optimization of client selection and receive beamforming for OTA FL is realized by minimizing the model aggregation error and maximizing the number of selected clients. In addition, the diverse energy constraints are investigated in [13] and the client selection scheme is designed with the Lyapunov optimization to realize fast convergence. In [56], the clients with weak channels are neglected for the broadband situation and the authors prove that the latency for OTA FL is smaller compared with the FL via digital transmission. The work [77] adopts the SDR technique to minimize the optimality gap of the training loss by jointly optimizing client selection and power control for OTA FL.

Multi-antenna beamforming is another way to improve the performance for OTA FL [61, 76, 80, 81, 82]. The work [61] jointly optimizes the receive beamforming design and learning rate with the combined method of DC method and exhaustive search method. In [76], the receive beamforming is optimized with the DC method, and the client selection is designed with the Gibbs sampling method for reconfigurable intelligent surface-assisted OTA FL system. The authors in [80] try to optimize the transmission power control and adapt the learning rate design for the OTA FL system. The research paper [81] introduces a novel and compatible framework that integrates non-orthogonal multiple access and OTA FL through concurrent communication. This framework enables efficient communication and cooperative learning among multiple devices in a wireless network. In [82], the authors adopt the SDR technique to deal with the receive beamforming design, and the client selection is solved with the DC method.

2.2.2 Energy-aware federated learning

FL assumes the availability of communication and computation resources at the local clients, as the training process requires significant computational power and parameter exchange between local clients and the PS. However, the distributed nature of FL can exacerbate the demands on edge devices, which often have limited resources. As a result, implementing FL can lead to issues such as slow convergence, decreased accuracy, or even model training failure. Therefore, it is crucial to consider the resource availability of edge devices when implementing FL, especially concerning battery life.

For the typical FL system, the energy consumption at local clients includes the computation energy consumption for the local model training procedure and the communication energy consumption for gradient upload procedure. Let e_k^{tot}, e_k^{cmp} and

e_k^{com} denote the total energy consumption, computation energy consumption, and communication energy consumption for client k, respectively. The number of the floating point operations (FLOPs) is used to measure the computation complexity of the energy consumption model according to [83]. Let a denote the number of the FLOPs for each data during the local update, which is a constant value. Let C_k denote the number of FLOPs in one CPU cycle. According to [16, 51, 83], the computation energy consumption e_k^{cmp} is calculated as

$$e_k^{cmp} = \frac{aD_k}{C_k} \iota_k I_k (f_k)^2, \tag{2.5}$$

where ι_k is the effective switched capacitance decided by the chip architecture, I_k is the number of local iterations and f_k means the number of CPU cycles per second. The communication energy consumption e_k^{com} is calculated as

$$e_k^{com} = t_k p_k, \tag{2.6}$$

where t_k is the communication time which is decided by the wireless transmission rate and signal size, and p_k is the average transmission power of local client k. The total energy consumption is calculated as

$$e_k^{tot} = e_k^{cmp} + e_k^{com}. \tag{2.7}$$

In the training procedures of the FL system, the energy consumption is usually constrained by the available battery of local clients. There are some previous studies that focus on the energy-constrained FL system [51, 55, 84, 85, 86, 87, 88, 89]. In [51], the authors investigate the energy-efficient resource allocation for FL with wireless communication networks. The authors in [55] try to enhance the energy efficiency of FL in mobile edge networks, allowing for heterogeneous participating devices without compromising the learning performance. In this regard, they propose one FL algorithm that guarantees convergence and enables flexible communication compression to achieve this objective. The work in [84] aims to minimize energy consumption while guaranteeing the system performance by optimizing bandwidth allocation and client selection for FL system. The problem of joint user association, task allocation, and power allocation in FL system is posed as an optimization problem with the objective of minimizing energy consumption for both task computation and transmission in [85]. In study [86], the authors tackle an optimization problem that seeks to determine the optimal allocation of resources for users for FL system, including the precise selection of relevant training samples, bandwidth, transmission power, beamforming weights, and processing speed, all with the aim of minimizing the total energy consumption, while adhering to a deadline constraint on the communication rounds of FL system. In [87], the authors formulate two problems for FL system with energy constraint clients, the first one is to optimize the learning performance under the energy consumption constraint for FL system and the second one is to minimize the energy consumption of the local clients with the learning performance requirement for FL system.

2.3 Summary

In this chapter, the background knowledge and related studies of the OTA FL system with energy harvesting are introduced. Different from the previous studies that only focus on transmission power control for OTA FL, we investigate the influence of energy harvesting on the learning performance of OTA FL in this thesis. Besides, we derive the optimality gap of the OTA FL system, which is related to energy management, client selection, receive beamforming design, and transmission power control.

3 Energy harvesting aware client selection for OTA FL

3.1 Introduction

As introduced in previous chapters, the OTA FL system can realize communication efficiency compared with the traditional FL system. However, the local clients still suffer from the energy constraint due to the communication energy consumption and computation energy consumption, which will influence the final convergence rate of the OTA FL system. While some efforts have been made to address energy constraints [13] and incorporate energy harvesting [20] in the OTA FL system, the effects of energy harvesting and client selection have not been thoroughly explored. In this chapter, we aim to solve the energy constraint problem of the OTA FL system and investigate the impacts of energy harvesting on the convergence performance of the OTA FL system. In this chapter, we first give some background knowledge in Section 3.2 about the system model. Specifically, Subsection 3.2.1 introduces the FL

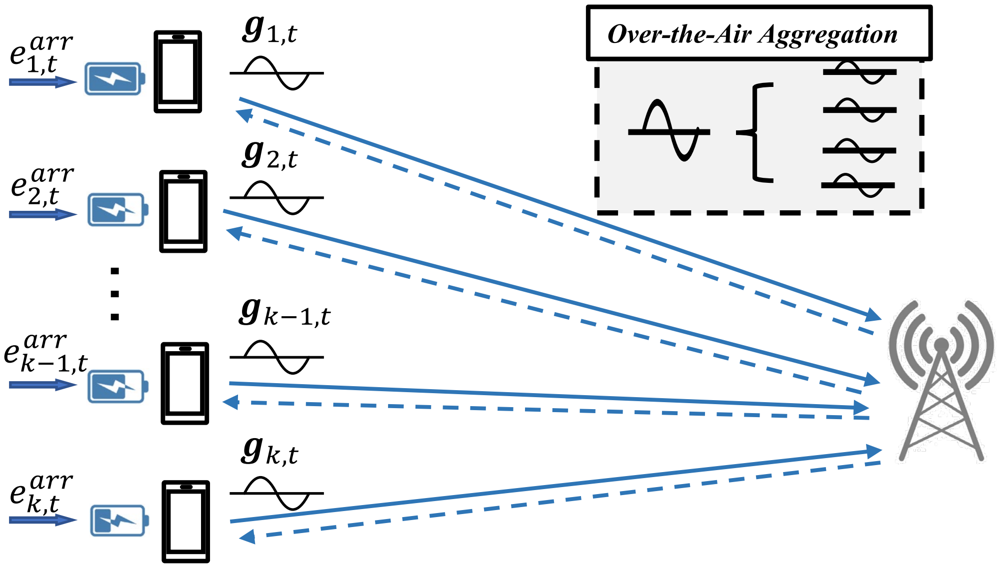

Figure 3.1: FL system via OTA computation with energy harvesting.

model, providing an overview of its key concepts and principles, Subsection 3.2.2 presents the communication model specific to the OTA FL system, outlining the key components and considerations, Subsection 3.2.3 describes the energy consumption and harvesting model, highlighting the factors influencing energy constraints in the OTA FL system, Subsection 3.2.4 formulates the initial problem, which aims to minimize the optimality gap of the training loss by optimizing client selection under energy constraints. Based on the information of the system model, we try to analyze the convergence performance of the OTA FL system in the presence of energy harvesting in Subsection 3.3.1. Subsequently, in Subsection 3.3.2, we transform the initial client selection problem into the NIP problem, taking into consideration the energy constraint and energy harvesting. To address the formulated NIP problem, in Section 3.4, we propose a client selection and energy management method based on CED coefficients for the OTA FL system, which involves clients that harvest energy. In Section 3.5, the proposed client selection scheme is evaluated for the OTA FL system with the simulations. Besides, the impacts of the energy harvesting settings on the OTA FL system are discussed in the simulations.

3.2 System model

In this section, we first provide some background knowledge about the FL model, the communication model, the energy consumption and harvesting model. Then, we formulate the problem to minimize the optimality gap by jointly optimizing the client selection and energy management for the OTA FL system.

3.2.1 Federated learning model

We consider the OTA FL system that consists of K single-antenna clients and one single-antenna PS, which is depicted in Figure 3.1. The set of all clients is denoted as $\mathcal{K}$. Each client $k \in \mathcal{K}$ has a number of feature-label pairs, which can be denoted as $\mathcal{D}_k = \left\{\left(\boldsymbol{x}_{k,i}, y_{k,i}\right), i \in \{1, \ldots, D_k\}\right\}$, where $\boldsymbol{x}_{k,i}$ is the feature vector, $y_{k,i}$ is the ground-truth label, and D_k is the total number of local training samples owned by client k. The total number of samples for all clients is $D = \sum_{k\in\mathcal{K}} D_k$. Clients can harvest energy from various energy harvesting resources.

We assume that the total number of training rounds is T for the traditional FL system, and the information will continue to be exchanged between the local client side and the PS side during this period. Just like the FedAvg algorithm in Subsection 2.1.1, at the t-th training round, the traditional FL system conducts the following steps: client selection, global model broadcast, local model update, local model upload, and global model aggregation. First, it is assumed that a subset of clients $\mathcal{K}_t$ are selected from $\mathcal{K}$ by the PS to join in the training. Let $\boldsymbol{\beta}_t = [\beta_{1,t}, \beta_{2,t}, \ldots, \beta_{K,t}]$ denote the client selection vector, and $\beta_{k,t} \in \{0, 1\}$ represents a binary indicator. If client k is selected at the t-th training round, $\beta_{k,t} = 1$, otherwise, $\beta_{k,t}$ is set as 0, thus $\mathcal{K}_t = \left\{k|\beta_{k,t} = 1, k \in \mathcal{K}\right\}$. Then, the selected local client k update the local model $\boldsymbol{w}_{k,t}$ as $\boldsymbol{w}_{k,t} = \boldsymbol{w}_t$. Suppose that $f\left(\boldsymbol{w}_{k,t}, \boldsymbol{x}_{k,i}, y_{k,i}\right)$ is the loss function for the corresponding local training sample $\left(\boldsymbol{x}_{k,i}, y_{k,i}\right)$, $i \in \{1, \ldots, D_k\}$ at client k. The local loss for all samples at client k is calculated as

$$F_{k,t}\left(\boldsymbol{w}_{k,t}, \mathcal{D}_k\right) = \frac{1}{D_k}\sum_{i=1}^{D_k} f\left(\boldsymbol{w}_{k,t}, \boldsymbol{x}_{k,i}, y_{k,i}\right). \tag{3.1}$$

Let $\nabla f\left(\boldsymbol{w}_{k,t}, \boldsymbol{x}_{k,i}, y_{k,i}\right)$ denote the gradient of $f\left(\boldsymbol{w}_{k,t}, \boldsymbol{x}_{k,i}, y_{k,i}\right)$. The local gradient $\boldsymbol{g}_{k,t} \in$

$\mathbb{R}^S$ is calculated as

$$\boldsymbol{g}_{k,t} = \frac{1}{D_k} \sum_{i=1}^{D_k} \nabla f\left(\boldsymbol{w}_{k,t}, \boldsymbol{x}_{k,i}, y_{k,i}\right). \tag{3.2}$$

After the training process is completed, the selected client k transmits the local gradients $\boldsymbol{g}_{k,t}$ to the PS. After receiving the signals, the global gradient can be represented as

$$\boldsymbol{g}_t = \frac{\sum_{k\in\mathcal{K}_t} D_k \boldsymbol{g}_{k,t}}{\sum_{k\in\mathcal{K}_t} D_k}. \tag{3.3}$$

Let η denote the fixed learning rate. The global model is updated as

$$\boldsymbol{w}_{t+1} = \boldsymbol{w}_t - \eta \boldsymbol{g}_t. \tag{3.4}$$

The global loss for the selected clients can be given by

$$F_t\left(\boldsymbol{w}_t, \mathcal{K}_t\right) = \frac{\sum_{k\in\mathcal{K}_t} D_k F_{k,t}\left(\boldsymbol{w}_{k,t}, \mathcal{D}_k\right)}{\sum_{k\in\mathcal{K}_t} D_k}. \tag{3.5}$$

The main differences between the OTA FL system and the traditional FL system are the procedures of local model transmission and global model aggregation. In the next subsection, the communication model which includes the local model transmission and global model aggregation is introduced.

3.2.2 Communication model

For the OTA FL system, clients need to upload their gradients to the PS with the shared wireless channel synchronously. In this chapter, we assume that the channel coefficients are quasi-static during the same training round, but they may fluctuate in different training rounds. Let $\hat{h}_{k,t} \in \mathbb{C}$ represent the channel coefficient of client k at the t-th training round, and $h_{k,t}$ means the magnitude of $\hat{h}_{k,t}$. Let $p_{k,t}$ denote the power control factor of client k at the t-th training round. The pre-processing operation for local gradients $\boldsymbol{g}_{k,t}$ at client k during the t-th training round is as follows:

$$\boldsymbol{\varphi}_{k,t} = p_{k,t} \beta_{k,t} \boldsymbol{g}_{k,t}. \tag{3.6}$$

The received gradients vector $\boldsymbol{r}_t \in \mathbb{C}^s$ at the PS side via OTA computation at the t-th training round is calculated as follows:

$$\begin{aligned} \boldsymbol{r}_t &= \sum_{k\in\mathcal{K}} h_{k,t}\boldsymbol{\varphi}_{k,t} + \boldsymbol{z}_t \\ &= \sum_{k\in\mathcal{K}} \beta_{k,t}h_{k,t}p_{k,t}\boldsymbol{g}_{k,t} + \boldsymbol{z}_t, \end{aligned} \tag{3.7}$$

where $\boldsymbol{z}_t = [z_t^1, z_t^2, \ldots, z_t^s] \in \mathbb{C}^s$ represents the additive white Gaussian noise (AWGN) vector, and z_t^s follows the distribution $\mathcal{CN}\left(0, \sigma^2\right)$. To obtain the averaged gradients of the OTA FL system, the PS conducts the post-processing operation for the received aggregated gradients [10]. The post-processing for aggregated gradients is as follows:

$$\bar{\boldsymbol{r}}_t = \frac{\boldsymbol{r}_t}{\alpha_t \sum_{k\in\mathcal{K}} \beta_{k,t}D_k}, \tag{3.8}$$

where α_t is the scaling factor for obtaining the transmission energy at the t-th training round. In addition, the averaged global gradients over an error-free channel are $\boldsymbol{g}_t$, which is calculated as (3.3). The mean squared error of the received global gradient $\bar{\boldsymbol{r}}_t$ via OTA computation and the error-free averaged global gradients $\boldsymbol{g}_t$ is calculated as

$$\begin{aligned} MSE(\bar{\boldsymbol{r}}_t, \boldsymbol{g}_t) &= E(|\bar{\boldsymbol{r}}_t - \boldsymbol{g}_t|^2) \\ &= E(|\frac{\sum_{k\in\mathcal{K}} \beta_{k,t}h_{k,t}p_{k,t}\boldsymbol{g}_{k,t} + \boldsymbol{z}_t}{\alpha_t \sum_{k\in\mathcal{K}} \beta_{k,t}D_k} - \frac{\sum_{k\in\mathcal{K}} \beta_{k,t}D_k\boldsymbol{g}_{k,t}}{\sum_{k\in\mathcal{K}} \beta_{k,t}D_k}|^2). \end{aligned} \tag{3.9}$$

To minimize the mean squared error between the received global gradients $\bar{\boldsymbol{r}}_t$ via OTA computation and the error-free global gradients $\boldsymbol{g}_t$, the power control factor $p_{k,t}$ needs to satisfy the requirement for the selected client k at the t-th training round as follows [62]:

$$p_{k,t} = \frac{\alpha_t D_k}{h_{k,t}}. \tag{3.10}$$

As a result, take (3.10) into (3.8), the received global gradients $\bar{\boldsymbol{r}}_t$ can be rewritten as follows:

$$\bar{\boldsymbol{r}}_t = \frac{\sum_{k\in\mathcal{K}} \beta_{k,t}D_k\boldsymbol{g}_{k,t} + \frac{\boldsymbol{z}_t}{\alpha_t}}{\sum_{k\in\mathcal{K}} \beta_{k,t}D_k}. \tag{3.11}$$

By comparing (3.11) with (3.3), we can infer that the difference between the OTA FL system and the error-free FL system is decided by the part of $\frac{z_t}{\alpha_t \sum_{k\in\mathcal{K}} \beta_{k,t} D_k}$, specifically, the aggregation error is decided by the noise signal vector $\boldsymbol{z}_t$, the channel state information vector $\boldsymbol{h}_t$, the power control vector $\boldsymbol{p}_t$, the client selection indicator vector $\boldsymbol{\beta}_t$, and the dataset size vector $\boldsymbol{D}$.

3.2.3 Energy consumption and harvesting model

Let $e_{k,t,i}$ denote the computation energy consumption for each sample at local client k. Let a denote the number of FLOPs for each data during the local update. Let C_k denote the number of FLOPs in one CPU cycle, and ι_k denote the effective switched capacitance decided by the chip architecture. The CPU frequency is denoted as f_k. According to [16, 51, 83], $e_{k,t,i}$ can be calculated as follows:

$$e_{k,t,i} = \frac{a}{C_k} \iota_k I_k (f_k)^2, \tag{3.12}$$

which is decided by the computation ability of the local clients and the complexity of the deep learning model. We assume that $e_{k,t,i}$ remains unchanged for client k, but $e_{k,t,i}$ varies across different clients because of client heterogeneity. The data size D_k for client k may also be different across different clients. By combining (3.10), the total energy consumption $e_{k,t}^{\mathrm{tot}}$ for client k during the t-th training round can be obtained as follows [13]:

$$\begin{aligned} e_{k,t}^{\mathrm{tot}} &= D_k e_{k,t,i} + ||p_{k,t} \boldsymbol{g}_{k,t}||^2 \\ &= \underbrace{D_k e_{k,t,i}}_{\text{Computation energy consumption}} + \underbrace{\frac{\alpha_t^2 D_k^2}{h_{k,t}^2} \left\| \boldsymbol{g}_{k,t} \right\|_2^2}_{\text{Transmission energy consumption}}. \end{aligned} \tag{3.13}$$

We assume that each client can harvest energy from its resources. The energy harvesting process is built based on a successive energy arrival model. The newly arrived energy at the t-th training round is as follows: $\boldsymbol{e}_t^{\mathrm{arr}} = [e_{1,t}^{\mathrm{arr}}, \ldots, e_{K,t}^{\mathrm{arr}}]$, where $e_{k,t}^{\mathrm{arr}}$ follows a Poisson process with the parameter $\bar{e}_k$. For each client, the harvested energy can be stored in the battery and used for further operations. The current battery energy is denoted as $b_{k,t}$ at the initial time of the t-th training round for client k. The maximum battery capacity for client k is denoted as $B^{\max}$.

For each selected client k at the t-th training round, the total energy consumption cannot exceed the residual battery capacity, which is denoted as follows:

$$e_{k,t}^{\text{tot}} \leq b_{k,t}. \tag{3.14}$$

The energy harvested during the t-th training round can be used in the following training rounds, and the updated battery energy of the client k is less than the maximum capacity $B^{\max}$. The battery level update process after the t-training round $b_{k,t+1}$ is decided by the minimum value of the updated energy and maximum battery, which can be expressed as follows:

$$b_{k,t+1} = \min \left\{ b_{k,t} - e_{k,t}^{\text{tot}} + e_{k,t}^{\text{arr}}, B^{\max} \right\}, \tag{3.15}$$

where $b_{k,1} = B_k^1$ is the initial battery energy at client k.

3.2.4 Problem formulation

The total number of training rounds is set as T. Let $\boldsymbol{w}^*$ indicate the optimal global mode of the OTA FL system, and let $F(\boldsymbol{w}^*)$ represent the global loss of the optimal global model. The initial global model is denoted as $\boldsymbol{w}_1$. The optimality gap of the actual training loss and optimal training loss is defined as $\mathbb{E}[F(\boldsymbol{w}_{T+1})] - F(\boldsymbol{w}^*)$ after T training rounds. If the optimality gap of the training loss $\mathbb{E}[F(\boldsymbol{w}_{T+1})] - F(\boldsymbol{w}^*)$ is smaller, the convergence performance of the OTA FL system is better. Our goal is to minimize the optimality gap $\mathbb{E}[F(\boldsymbol{w}_{T+1})] - F(\boldsymbol{w}^*)$ within the energy constraint via client selection optimization for the OTA FL system. The optimization problem is formulated as follows:

$$
\begin{aligned}
\mathcal{P}_1: \quad \min_{\boldsymbol{\beta}} \quad & \mathbb{E}[F(\boldsymbol{w}_{T+1})] - F(\boldsymbol{w}^*) && \text{(3.16a)}\\
\text{s.t.} \quad & e_{k,t}^{\text{tot}} \leq b_{k,t}, \quad \forall k \in \mathcal{K}, 1 \leq t \leq T, && \text{(3.16b)}\\
& \beta_{k,t} \in \{0,1\}, \quad \forall k \in \mathcal{K}, 1 \leq t \leq T. && \text{(3.16c)}
\end{aligned}
$$

where the first constraint denotes that the total energy consumption at the t-th training round for each selected client k is less than its residual battery capacity, and the second constraint indicates the binary client selection vector at the t-th training round.

3.3 Convergence analysis and problem transformation

In this section, we present the convergence analysis of the OTA FL system. Note that energy consumption and energy harvesting of the local clients are introduced into the convergence analysis. The derived convergence result can measure the impacts of the channel state information $h_{k,t}$, the residual battery capacity $(b_{k,t} - e_{k,t,i} D_k)$, and the dataset size D_k of the selected client k on the convergence rate of the OTA FL system. Based on the convergence result, the transformed problems are rebuilt from $\mathcal{P}_1$.

3.3.1 Convergence analysis

According to (3.4) and (3.11), the global weight parameters for the OTA FL system are updated as follows:

$$\boldsymbol{w}_{t+1} = \boldsymbol{w}_t - \eta \bar{\boldsymbol{r}}_t. \tag{3.17}$$

For the convenience of convergence analysis, we make the following three assumptions on the training loss function for the OTA FL system as used in [3, 10].

Assumption 1 *(**l-Smoothness**) This indicates that a nonnegative constant l exists for parameters $\boldsymbol{w}$ and $\boldsymbol{v}$ to make the inequality satisfy the following:*

$$F(\boldsymbol{w}) - F(\boldsymbol{v}) \leq (\boldsymbol{w} - \boldsymbol{v})^T \nabla F(\boldsymbol{v}) + \frac{l}{2} \|\boldsymbol{w} - \boldsymbol{v}\|_2^2. \tag{3.18}$$

Assumption 2 *(**PL Inequality**) For a nonnegative μ constant, the Polyak-Lojasiewicz (PL) condition should hold the following:*

$$\|\nabla F(\boldsymbol{w})\|_2^2 \geq 2\mu \left[F(\boldsymbol{w}) - F(\boldsymbol{w}^*)\right]. \tag{3.19}$$

Assumption 3 *(**Gradient Bound**) The local gradients have the bound constraint of the* *global gradients as follows:*

$$\|\nabla f(\boldsymbol{w})\|_2^2 \leq \lambda_1 + \lambda_2 \|\nabla F(\boldsymbol{w})\|_2^2. \tag{3.20}$$

where $\lambda_1 \geq 0$ *and* $\lambda_2 \geq 0$.

The optimality gap at the t-th training round is defined as $\mathbb{E}[F(\boldsymbol{w}_{t+1})] - F(\boldsymbol{w}^*)$. We can derive the relationship of the optimality gap for two adjacent rounds as in Lemma 3.1.

Lemma 3.1 *Based on Assumptions 1-3, when the learning rate satisfies* $\eta = \frac{1}{l}$, *given the residual battery capacity vector* $\boldsymbol{b}_t$ *and the client selection vector* $\boldsymbol{\beta}_t$, *the optimality gap at the* t*-th training round within the energy constraint can be represented as follows*

$$\mathbb{E}[F(\boldsymbol{w}_{t+1})] - F(\boldsymbol{w}^*) \leq \psi_t \left(\mathbb{E}[F(\boldsymbol{w}_t)] - F(\boldsymbol{w}^*)\right) + \frac{\lambda_1}{l}\phi_t, \tag{3.21}$$

where ψ_t *and* ϕ_t *can be expressed as follows:*

$$\psi_t = 1 - \frac{\mu}{l} + \frac{2\mu\lambda_2\phi_t}{l}, \tag{3.22}$$

$$\phi_t = \frac{s\sigma^2}{2\left(\sum_{k\in\mathcal{K}} D_k\beta_{k,t}\right)^2}\left(\max_{k\in\mathcal{K}} \frac{\beta_{k,t}D_k^2}{h_{k,t}^2\left(b_{k,t} - D_k e_{k,t,i}\right)}\right) + \frac{2\left(D - \sum_{k\in\mathcal{K}}\beta_{k,t}D_k\right)^2}{D^2}. \tag{3.23}$$

Proof. Let $\boldsymbol{o}$ denote the errors that are introduced by client selection and noisy channels for the OTA FL system, then $\boldsymbol{o}$ can be represented as

$$\begin{aligned}\boldsymbol{o} &= \nabla F(\boldsymbol{w}_t) - \bar{\boldsymbol{r}}_t \\ &= \underbrace{\nabla F(\boldsymbol{w}_t) - \frac{\sum_{k\in\mathcal{K}}\beta_{k,t}D_k\boldsymbol{g}_{k,t}}{\sum_{k\in\mathcal{K}}\beta_{k,t}D_k}}_{\text{Client selection related error}} + \underbrace{\frac{-\boldsymbol{z}_t}{\alpha_t\sum_{k\in\mathcal{K}}\beta_{k,t}D_k}}_{\text{Noise related error}}.\end{aligned} \tag{3.24}$$

When Assumption 1 exists, by incorporating (3.4) into (3.18), we have

$$F(\boldsymbol{w}_{t+1}) \leq F(\boldsymbol{w}_t) - \eta\left(\nabla F(\boldsymbol{w}_t) - \boldsymbol{o}\right)^T \nabla F(\boldsymbol{w}_t) + \frac{l\eta^2}{2}\left\|\left(\nabla F(\boldsymbol{w}_t) - \boldsymbol{o}\right)\right\|_2^2. \tag{3.25}$$

By accessing the expected values of (3.25) and setting the learning rate to $\eta = \frac{1}{l}$, we have

$$\mathbb{E}\left[F\left(\boldsymbol{w}_{t+1}\right)\right] \leq \mathbb{E}\left[F\left(\boldsymbol{w}_{t}\right)\right] - \frac{1}{2l}\left\|\nabla F\left(\boldsymbol{w}_{t}\right)\right\|_2^2 + \frac{1}{2l}\mathbb{E}\left[\|\boldsymbol{o}\|_2^2\right]. \tag{3.26}$$

Let $\mathcal{K}_t = \left\{k|\beta_{k,t} = 1, k \in \mathcal{K}, t \in \{1, \ldots, T\}\right\}$ denote the set of selected clients and $\widetilde{\mathcal{K}}_t = \left\{k|\beta_{k,t} = 0, k \in \mathcal{K}, t \in \{1, \ldots, T\}\right\}$ denote the set of unselected clients according to [3], and then $\mathbb{E}\left[\|\boldsymbol{o}\|_2^2\right]$ is bounded as

$$\begin{aligned}
&\mathbb{E}\left[\|\boldsymbol{o}\|_2^2\right] \\
&= \mathbb{E}\left[\left\|\nabla F(\boldsymbol{w}_t) - \frac{\sum_{k\in\mathcal{K}}\beta_{k,t}D_k\boldsymbol{g}_{k,t}}{\sum_{k\in\mathcal{K}}\beta_{k,t}D_k} - \frac{\boldsymbol{z}_t}{\alpha_t\sum_{k\in\mathcal{K}}\beta_{k,t}D_k}\right\|_2^2\right] \\
&\leq \mathbb{E}\left[\left\|\frac{\sum_{k\in\mathcal{K}}\sum_{i=1}^{D_k}\nabla f(\boldsymbol{w}_{k,t}, x_{k,i}, y_{k,i})}{\sum_{k\in\mathcal{K}}D_k} - \frac{\boldsymbol{z}_t}{\alpha_t\sum_{k\in\mathcal{K}}\beta_{k,t}D_k}\right.\right. \\
&\qquad \left.\left. - \frac{\sum_{k\in\mathcal{K}}\sum_{i=1}^{D_k}\beta_{k,t}\nabla f(\boldsymbol{w}_{k,t}, x_{k,i}, y_{k,i})}{\sum_{k\in\mathcal{K}}\beta_{k,t}D_k}\right\|_2^2\right] \\
&\leq \mathbb{E}\left[\left\|\frac{-(D - \sum_{k\in\mathcal{K}}\beta_{k,t}D_k)}{D\sum_{k\in\mathcal{K}}\beta_{k,t}D_k}\sum_{k\in\mathcal{K}_t}\sum_{i=1}^{D_k}\nabla f(\boldsymbol{w}_{k,t}, x_{k,i}, y_{k,i})\right.\right. \\
&\qquad \left.\left. + \frac{\sum_{k\in\widetilde{\mathcal{K}}_t}\sum_{i=1}^{D_k}\nabla f(\boldsymbol{w}_{k,t}, x_{k,i}, y_{k,i})}{D}\right\|_2^2\right] \\
&\quad + \frac{S\sigma^2}{\|\alpha_t\sum_{k\in\mathcal{K}}\beta_{k,t}D_k\|^2} \\
&\leq \mathbb{E}\left[\frac{(D - \sum_{k\in\mathcal{K}}\beta_{k,t}D_k)}{D\sum_{k\in\mathcal{K}}\beta_{k,t}D_k}\sum_{k\in\mathcal{K}_t}\sum_{i=1}^{D_k}\nabla f(\boldsymbol{w}_{k,t}, x_{k,i}, y_{k,i})\right. \\
&\qquad \left. + \frac{\sum_{k\in\widetilde{\mathcal{K}}_t}\sum_{i=1}^{D_k}\nabla f(\boldsymbol{w}_{k,t}, x_{k,i}, y_{k,i})}{D}\right]^2 \\
&\quad + \frac{S\sigma^2}{\|\alpha_t\sum_{k\in\mathcal{K}}\beta_{k,t}D_k\|^2}.
\end{aligned} \tag{3.27}$$

Compared to the traditional FL system [3], the difference for the OTA FL system lies in the introduced aggregation error part $\frac{S\sigma^2}{\|\alpha_t\sum_{k\in\mathcal{K}}\beta_{k,t}D_k\|^2}$ caused by noise. Based on

Assumption 3, we can get

$$
\begin{aligned}
&\mathbb{E}\left(\|\boldsymbol{o}\|_2^2\right)\\
&\leq \mathbb{E}\left[\frac{2(D-\sum_{k\in\mathcal{K}}\beta_{k,t}D_k)}{D}\sqrt{(\lambda_1+\lambda_2\|\nabla F(\boldsymbol{w}_t)\|_2^2)}\right]^2+\frac{S\sigma^2}{\|\alpha_t\sum_{k\in\mathcal{K}}\beta_{k,t}D_k\|^2}\\
&\leq \frac{4}{D^2}\left(D-\sum_{k\in\mathcal{K}}\beta_k D_k\right)^2\left(\lambda_1+\lambda_2\|\nabla F\left(\boldsymbol{w}_t\right)\|_2^2\right)+\frac{S\sigma^2}{\left\|\alpha_t\sum_{k\in\mathcal{K}}D_k\beta_{k,t}\right\|_2^2}.
\end{aligned}
\tag{3.28}
$$

By incorporating (3.28) into (3.26) and subtracting $F\left(\boldsymbol{w}^*\right)$ from both sides of (3.26), we have

$$
\begin{aligned}
\mathbb{E}\left[F\left(\boldsymbol{w}_{t+1}\right)\right]-F\left(\boldsymbol{w}^*\right)\leq{}&\mathbb{E}\left[F\left(\boldsymbol{w}_t\right)\right]-F\left(\boldsymbol{w}^*\right)\\
&+\frac{2}{lD^2}\left(D-\sum_{k\in\mathcal{K}}\beta_{k,t}D_k\right)^2\left(\lambda_1+\lambda_2\|\nabla F\left(\boldsymbol{w}_t\right)\|_2^2\right)\\
&+\frac{S\sigma^2}{2l{\alpha_t}^2(\sum_{k\in\mathcal{K}}\beta_{k,t}D_k)^2}-\frac{1}{2l}\left\|\nabla F\left(\boldsymbol{w}_t\right)\right\|_2^2.
\end{aligned}
\tag{3.29}
$$

According to (3.13) and (3.14), which represent the calculation of the total energy consumption $e_{k,t}^{\mathrm{tot}}$ and the energy consumption constraint caused by available battery $b_{k,t}$, the normalization scaling factor α_t at the t-th training round needs to satisfy the following condition:

$$
\alpha_t\leq\min_{k\in\mathcal{K}}\left(\frac{\beta_{k,t}h_{k,t}\sqrt{b_{k,t}-D_k e_{k,t,i}}}{D_k\left\|\boldsymbol{g}_{k,t}\right\|_2}\right).
\tag{3.30}
$$

The variable α_t can also be expressed as follows:

$$
\alpha_t=\min_{k\in\mathcal{K}}\left(\frac{\beta_{k,t}h_{k,t}\sqrt{b_{k,t}-D_k e_{k,t,i}}}{D_k\left\|\boldsymbol{g}_{k,t}\right\|_2}\right).
\tag{3.31}
$$

Based on Assumption 2 and Assumption 3, we have

$$
\|\nabla F(\boldsymbol{w}_t)\|_2^2\geq 2\mu\left[F(\boldsymbol{w}_t)-F(\boldsymbol{w}^*)\right],
\tag{3.32}
$$

and

$$\|\boldsymbol{g}_{k,t}\|^2 \le \lambda_1 + \lambda_2 \|\nabla F(\boldsymbol{w})\|^2. \tag{3.33}$$

By incorporating (3.30), (3.32), and (3.33) into (3.29), we finally obtain

$$\mathbb{E}\left[F\left(\boldsymbol{w}_{t+1}\right)\right] - F\left(\boldsymbol{w}^*\right) \le \psi_t \left[\mathbb{E}\left[F\left(\boldsymbol{w}_t\right)\right] - F\left(\boldsymbol{w}^*\right)\right] + \frac{\lambda_1}{l}\phi_t. \tag{3.34}$$

The proof of Lemma 3.1 has been completed. □

By repeatedly applying Lemma 3.1 and collecting terms, we have the optimality gap after T training rounds as in Theorem 3.1.

Theorem 3.1 ***(Optimality Gap)*** *We assume that the total training round is T and the initial global model is $\boldsymbol{w}_1$. The optimality gap after T training rounds of the OTA FL system can be expressed as follows:*

$$\mathbb{E}\left[F\left(\boldsymbol{w}_{T+1}\right)\right] - F\left(\boldsymbol{w}^*\right) \le \Omega_T\left(\boldsymbol{\beta}\right), \tag{3.35}$$

where

$$\Omega_T\left(\boldsymbol{\beta}\right) = \prod_{t=1}^{T} \psi_t \left(\mathbb{E}\left[F\left(\boldsymbol{w}_1\right)\right] - F\left(\boldsymbol{w}^*\right)\right) + \frac{\lambda_1}{l}\left(\sum_{t=1}^{T-1}\prod_{j=t+1}^{T}\psi_j\phi_t + \phi_T\right). \tag{3.36}$$

Proof. By recursive operation for (3.34), we can get cumulative optimality gap after T training rounds as

$$\begin{aligned}
&\mathbb{E}\left[F(\boldsymbol{w}_{T+1})\right] - F(\boldsymbol{w}^*) \\
&\le \psi_T\left[\mathbb{E}\left[F(\boldsymbol{w}_T)\right] - F(\boldsymbol{w}^*)\right] + \frac{\lambda_1}{l}\phi_T \\
&\le \psi_T\left(\psi_{T-1}\left(\mathbb{E}\left[F(\boldsymbol{w}_{T-1})\right] - F(\boldsymbol{w}^*)\right) + \frac{\lambda_1}{l}\phi_{T-1}\right) + \frac{\lambda_1}{l}\phi_T \\
&\le \cdots \\
&\le \prod_{t=1}^{T}\psi_t\left(\mathbb{E}\left[F\left(\boldsymbol{w}_1\right)\right] - F\left(\boldsymbol{w}^*\right)\right) + \frac{\lambda_1}{l}\left(\sum_{t=1}^{T-1}\prod_{j=t+1}^{T}\psi_j\phi_t + \phi_T\right).
\end{aligned} \tag{3.37}$$

The proof of Theorem 3.1 has been completed. □

3.3.2 Problem transformation

According to Theorem 3.1, the optimality gap is related to the client selection vector $\boldsymbol{\beta}_t$. If more clients are selected to upload the gradients, the loss decreases faster. However, due to the energy constraint, the induced noise increases when more clients are selected. In contrast from $\mathcal{P}_1$, the energy constraint is added into the convergence analysis for $\mathcal{P}_2$. When the total training round is T, we can formulate $\mathcal{P}_2$ as follows:

$$\mathcal{P}_2: \quad \min_{\boldsymbol{\beta}} \quad \Omega_T(\boldsymbol{\beta}) \tag{3.38a}$$

$$\text{s.t.} \quad \beta_{k,t} \in \{0,1\}, \quad \forall k \in \mathcal{K}, 1 \le t \le T. \tag{3.38b}$$

It is difficult to solve $\mathcal{P}_2$ directly due to the stochasticity of the channel state information $\boldsymbol{h}_t$ and the harvested energy $\boldsymbol{e}_t^{\mathrm{arr}}$ for each training round t. We focus on solving the problem via an online pattern based on Lemma 3.1. The optimality gap $\mathbb{E}[F(\boldsymbol{w}_{t+1})] - F(\boldsymbol{w}^*)$ at the t-th training round can be represented by ϕ_t when $\mathbb{E}[F(\boldsymbol{w}_t)] - F(\boldsymbol{w}^*)$ is known. Therefore, $\mathcal{P}_2$ can be transformed to $\mathcal{P}_3$ to minimize ϕ_t, which can be formulated as follows:

$$\mathcal{P}_3: \quad \min_{\boldsymbol{\beta}_t} \quad \phi_t(\boldsymbol{\beta}_t) \tag{3.39a}$$

$$\text{s.t.} \quad \beta_{k,t} \in \{0,1\}, \quad \forall k \in \mathcal{K}. \tag{3.39b}$$

Note that $\mathcal{P}_3$ is in essence one NIP problem. Besides, by analyzing (3.23), there is an inverse correlation between the objective value $\phi_t(\boldsymbol{\beta}_t)$ and the maximum constraint part $\max_{k\in\mathcal{K}}\left(\frac{\beta_{k,t}D_k^2}{h_{k,t}^2\left(b_{k,t}-D_k e_{k,t,i}\right)}\right)$. To analyze the impact of the maximum constraint part on the objective value $\phi_t(\boldsymbol{\beta}_t)$, we define the CED coefficient for client k at the t-th training round as follows:

$$q_{k,t} = \frac{\beta_{k,t}D_k^2}{h_{k,t}^2\left(b_{k,t} - D_k e_{k,t,i}\right)}, \tag{3.40}$$

which is decided by the channel state information $h_{k,t}$, residual battery capacity $b_{k,t}$ and the dataset size D_k. The list of CED coefficients is denoted as $\boldsymbol{Q}_t = [q_{1,t}, q_{2,t}, \ldots, q_{K,t}]$.

Algorithm 3.1 The Joint Channel-Energy-Data (CED)-based Client Selection Algorithm

Require: $\boldsymbol{h}_t$, $\boldsymbol{b}_t$, $\boldsymbol{c}_t$, $\boldsymbol{D}$, and D.
Ensure: $\boldsymbol{\beta}_t$.

for $k = 1, \ldots, K$ **do**
    Calculate $q_{k,t}$ based on (3.40);
end for
Sort $\boldsymbol{Q}_t$ in ascending order to obtain $\boldsymbol{Q}'_t$;
Let $q'_{k,t}$ be the k-th smallest value in $\boldsymbol{Q}'_t$, and let $\mathcal{S}^{[k]}$ be the client subset decided by the k smallest values of $\boldsymbol{Q}'_t$;
for $k = 1, \ldots, K$ **do**;
    Calculate $\phi_t^{[k]}$ based on (3.41);
end for
Calculate $k^* = \arg\min_{k \in \mathcal{K}} \phi_t^{[k]}$;
for $k = 1, \ldots, K$ **do**
    if $q_{k,t} \leq q_{k^*,t}$ **then**
        Set $\beta_{k,t} \leftarrow 1$;
    else
        Set $\beta_{k,t} \leftarrow 0$.
    end if
end for

The maximum value in $\boldsymbol{Q}_t$ is defined as follows: $Q_t^{\max} = \max_{k \in \mathcal{K}} q_{k,t}$. If the selected clients have the less available battery, worse channel quality, and larger data size, $Q_t^{\max}$ becomes larger, which leads to a larger objective value $\phi_t(\boldsymbol{\beta}_t)$ and worse performance of the OTA FL system.

3.4 Algorithm design

By analyzing the problem $\mathcal{P}_3$, we can observe that there is a trade-off between $\sum_{k \in \mathcal{K}} D_k \beta_{k,t}$ and $Q_t^{\max}$. If more clients participate in the training, $\sum_{k \in \mathcal{K}} D_k \beta_{k,t}$ will be larger, which will make the objective value smaller and the global loss converge faster. However, if more clients are selected, $Q_t^{\max}$ will be larger, which will lead to one larger objective value and slow convergence of the OTA FL system. As a result, we need to design an effective client selection scheme for the OTA FL system with energy harvesting clients and energy constraint.

The proposed solution is referred to as Algorithm 3.1. First, we sort $\boldsymbol{Q}_t$ in ascending order to obtain Q_t'. Let $q_{k,t}'$ be the k-th smallest value in Q_t', and let $\mathcal{S}^{[k]}$ be the subset consisting of k clients selected according to the k smallest values of Q_t'. There are K possible client selection decisions, and the final client selection decision is based on the following:

$$\phi_t^{[k]} = \frac{S\sigma^2 q_{k,t}'}{2\left(\sum_{i\in\mathcal{S}^{[k]}} D_i\right)^2} + \frac{2\left(D - \sum_{i\in\mathcal{S}^{[k]}} D_i\right)^2}{D^2}. \tag{3.41}$$

We obtain the indicator k^* by calculating the index of the minimum value of $\phi_t^{[k]}$ as follows:

$$k^* = \arg\min_{k\in\mathcal{K}} \phi_t^{[k]}. \tag{3.42}$$

The client can be selected if $k \leq k^*$ for the sorted queue Q_t', which means $q_{k,t} \leq q_{k^*,t}$. The complete process of the OTA FL system at the t-th training round includes the following procedures:

1. At the beginning of the t-th training round, the PS selects a subset of the clients based on Algorithm 3.1.

2. The PS sends the global model to the selected clients $\mathcal{K}_t$.

3. Local clients update the global model and upload the gradients to the PS via OTA computation.

4. The PS obtains the aggregated gradients based on (3.11).

5. Clients obtain the energy from the energy resources and update the current batter level queue based on (3.15). The clients send current battery level $b_{k,t+1}$ to the PS.

The above-mentioned procedures will conduct for T training rounds for the OTA FL system. The time complexity of Algorithm 3.1 is mainly determined by the sorting process (see Line 3 therein), which takes $O(K\log K)$ operations. In addition, as Algorithm 3.1 is conducted T times for convergence, the overall time complexity is given by $O\left(TK\log K\right)$.

Table 3.1: The notations in Chapter 3.

Notation	Description
K	number of clients
T	total number of training rounds
S	total number of weight parameters
D	total number of training samples of all clients
η	learning rate
$\mathcal{K}$	local client set
$\mathcal{K}_t$	the selected client set at the t-th training round
$\boldsymbol{\beta}_t$	client selection indicator at the t-th training round
$\boldsymbol{w}_{k,t}$	local model for client k at the t-th training round
$\boldsymbol{w}_t$	global model at the beginning of the t-th training round
D_k	number of training samples at client k
$\boldsymbol{g}_{k,t}$	local gradient vector of client k at the t-th training round
$\boldsymbol{g}_t$	global gradient vector at the t-th training round
$p_{k,t}$	power control factor of client k at the t-th training round
$h_{k,t}$	channel coefficient magnitude of client k at the t-th training round
α_t	scaling factor at the t-th training round
$\boldsymbol{r}_t$	the received gradients at the t-th training round
$\bar{\boldsymbol{r}}_t$	gradients after post-processing at the t-th training round
$\boldsymbol{z}_t$	additive white Gaussian noise at the t-th training round
$e_{k,t,i}$	computation energy consumption per sample of client k
$e_{k,t}^{\text{tot}}$	energy consumption of client k at the t-th training round
$b_{k,t}$	residual battery capacity of client k at the t-th training round
$B^{\max}$	maximum battery capacity for all clients
$e_{k,t}^{\text{arr}}$	energy harvested by client k at the t-th training round
a	the number of FLOPs for each data during the local update
C_k	the number of FLOPs in one CPU cycle
ι_k	the effective switched capacitance decided by the chip architecture
f_k	CPU cycle frequency
$\tilde{h}_{k,t}$	the estimated channel coefficient of client k at the t-th training round
$\delta_{k,t}^{h}$	error estimation of client k's channel at the t-th training round
σ_h^2	variance of the channel estimation error

3.5 Performance evaluation

3.5.1 Simulation setup

In the simulation, as shown in Figure 3.2, there are 40 clients randomly located within the range of a circle with a radius of 250 meters, and the PS is located at $(0, 0, 10)$. The average channel gain for the free-space path loss model is calculated as $\bar{h}_k = G_P G_C \left(\frac{3\times10^8}{4\pi f_c L_k}\right)^{\rho}$, where $G_P = 5$ dBi is the antenna gain of the PS, $G_C = 0$ dBi is

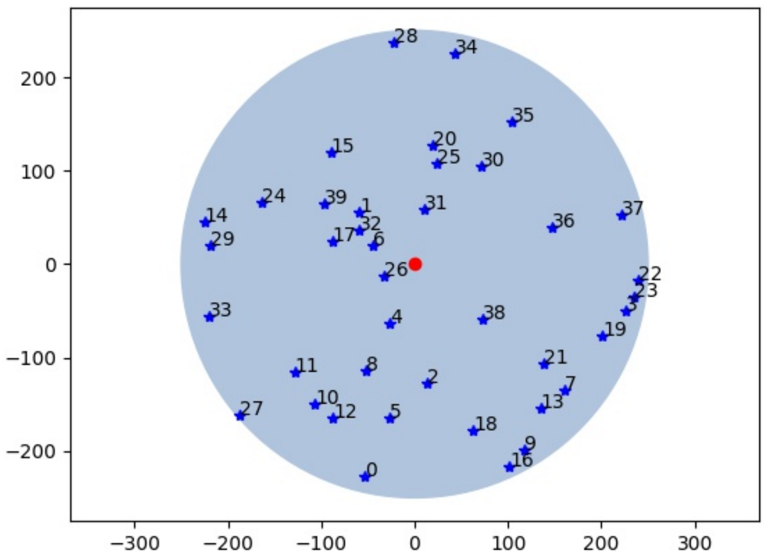

Figure 3.2: The locations of the local clients.

the antenna gain of clients, $f_c = 915$ MHz is the carrier frequency, L_k is the distance between client k and the PS, and the pass loss exponent is $\rho = 2.7$. The channel gain $h_{k,t}$ during the t-th training round is calculated as $h_{k,t} = \bar{h}_k \gamma_{k,t}$, where $\gamma_{k,t}$ is generated from the Gaussian distribution with zero-mean and unit-variance. The noise power is set as -100 dB by default. Table 3.1 lists the notations used for this chapter.

We use the convolutional neural network (CNN) for training, which is composed of two 5×5 convolutional layers, each followed by one 2×2 max-pooling layer, one fully-connected layer with 50 units, and one softmax layer. The structure of the CNN model is illustrated in Figure 3.3. The learning rate η is set as 0.01. Several studies have investigated the estimation of computational complexity of deep neural network (DNN) model [90, 91]. Similar to the DNN model, the number of FLOPs for different layers in the CNN model is calculated as in [92]. The number of FLOPs for the convolutional layer is calculated as

$$\mathcal{N}_{conv} = 2 \times \mathcal{N}_{ci} \times \mathcal{N}_k^2 \times \mathcal{N}_{ho} \times \mathcal{N}_{wo} \times \mathcal{N}_{co}, \tag{3.43}$$

where $\mathcal{N}_{ci}$ is the number of input channel, $\mathcal{N}_k$ is the kernel size, $\mathcal{N}_{ho} \times \mathcal{N}_{wo}$ is the

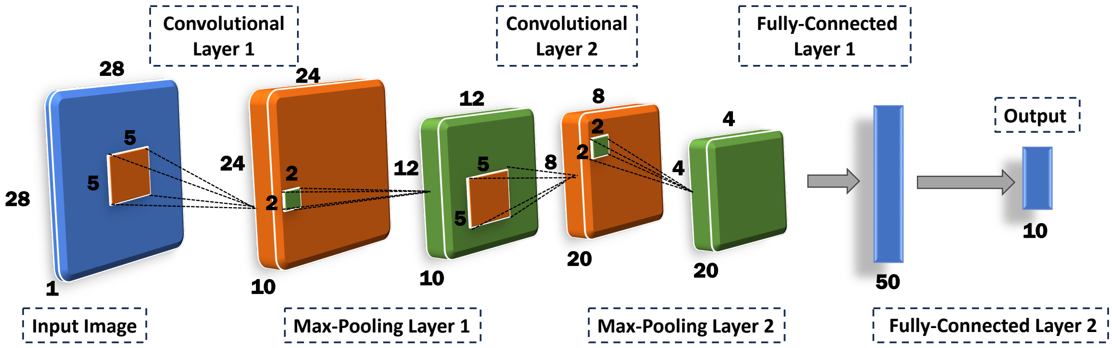

Figure 3.3: The structures of the CNN model.

output feature map size, and $\mathcal{N}_{co}$ is the output channel size. The number of FLOPs for the max-pooling layer is calculated as

$$\mathcal{N}_{pooling} = \mathcal{N}_k^2 \times \mathcal{N}_{ho} \times \mathcal{N}_{wo} \times \mathcal{N}_{co}. \tag{3.44}$$

Let $\mathcal{N}_o$ be the number of output neurons. The number of FLOPs for the ReLU activation layer is calculated as

$$\mathcal{N}_{ReLU} = \mathcal{N}_o, \tag{3.45}$$

where $\mathcal{N}_o$ is equal to $\mathcal{N}_{ho} \times \mathcal{N}_{wo} \times \mathcal{N}_{co}$ if the ReLU activation is conducted after the CNN layer, and $\mathcal{N}_o$ is equal to $\mathcal{N}_{co}$ if the ReLU activation is conducted after the fully-connected layer. The number of FLOPs for the fully-connected layer is calculated as

$$\mathcal{N}_{fc} = 2 \times \mathcal{N}_{ci} \times \mathcal{N}_{co}. \tag{3.46}$$

The number of FLOPs of different layers for the CNN model is calculated in Table 3.2. The total number of FLOPs is 9.6985×10^5. For the convenience of calculation, we set a approximately as 10^6 for the CNN model used in this thesis. According to (3.12), the energy consumption for one sample local update is set as 0.001 J when the effective switched capacitance ι_k is set as 10^{-26}, the CPU cycle frequency is set as 1 GHz, and the number of FLOPs in one CPU cycle C_k is set as 10. The Poisson parameter $\bar{e}_k$ for client k regarding the arrivals of the harvested energy is set in the range of 0.1 J to 1 J.

Table 3.2: The FLOPs of different layers for CNN model.

Layers	**Operation**	**FLOPs**
Convolutional layer 1	$2 \times 1 \times 5^2 \times 24 \times 24 \times 10$	288000
Max-pooling layer 1	$2^2 \times 12 \times 12 \times 10$	5760
ReLU layer	$12 \times 12 \times 10$	1440
Convolutional layer 2	$2 \times 10 \times 5^2 \times 8 \times 8 \times 20$	640000
Max-pooling layer 2	$2^2 \times 4 \times 4 \times 20$	1280
ReLU layer	$4 \times 4 \times 20$	320
Fully-connected layer 1	$2 \times 320 \times 50$	32000
ReLU layer	50	50
Fully-connected layer 2	$2 \times 50 \times 10$	1000
Total		969850

We conduct the simulations with Python 3.8 and carry out the experiments with the Fashion-MNIST dataset [93]. There are two kinds of settings regarding the data distribution among clients according to [94]. The first setting is a balanced data setting which is denoted as 'B', in which, the number of samples is equal among all clients and the number is set as 800. The second setting is the unbalanced data setting which is denoted as 'UnB', in which, the number of samples per client is randomly from [100, 200] for half of the clients and the number of samples per client is randomly from [1000, 2000] for the other clients.

We compare the proposed algorithm (denoted as CED) with the following comparison methods:

1. Channel-Prioritized (CP) [95]: we select k_{avg} clients with better channels and sufficient energy from $\mathcal{K}$, where k_{avg} is the averaged number of the selected clients of the proposed method.

2. Energy-Prioritized (EP): k_{avg} clients with more energy are selected from $\mathcal{K}$ at the t-th training round.

We chose these two comparison methods based on the convergence analysis of the optimality gap, which reveals that the client selection scheme is primarily affected by the variations in channel conditions and the available energy of local clients. Therefore, the CP method and the EP method are considered as the baseline methods for our comparative analysis.

3.5.2 Evaluating the test accuracy

Figure 3.4(a) and Figure 3.4(b) demonstrate the test accuracy for the OTA FL system of the three methods under the balanced data setting and unbalanced data setting respectively. The proposed CED method is better than the CP method and the EP method for both settings for the OTA FL system. The reason for this is that the CP method may select clients with less energy, and the EP method may select clients with worse channels, which may introduce more noise and make the gradients deviate from the correct values. The EP method performs worst as the channel has a larger impact on the convergence performance for the OTA FL system compared with the energy under the current simulation setting.

3.5.3 Evaluating the battery utility

Figure 3.5(a) and Figure 3.5(b) give the cumulative probability density of the residual battery for 3000 training rounds. The two data settings have similar trends under the current energy harvesting setting and energy consumption setting for the OTA FL system. It can be observed that the residual battery of the CED method is lower than that of the EP method and the CP method. This is because the communication energy is higher for the CED method, which also reveals that the CED method can make full utilization of the harvested energy to improve the system performance.

3.5.4 Evaluating the channel noise

Figure 3.6(a) and Figure 3.6(b) show the test accuracy for the proposed CED method with different noise settings. It is evident that the test accuracy of the OTA FL system decreases when noise power increases for both data settings. This is because the induced noise makes the gradients deviate from true values for each training round. When the noise is set too large, the OTA FL system even can not converge.

3.5.5 Evaluating the parameters of the CED coefficient

As the client selection is decided mainly based on the CED coefficient $q_{k,t}$, which is related to $D_k/h_{k,t}$ and the available battery $(b_{k,t} - D_k e_{k,t,i})$. The available battery is mainly decided by the averaged arrival rate of the energy harvesting process $\bar{e}_k$.

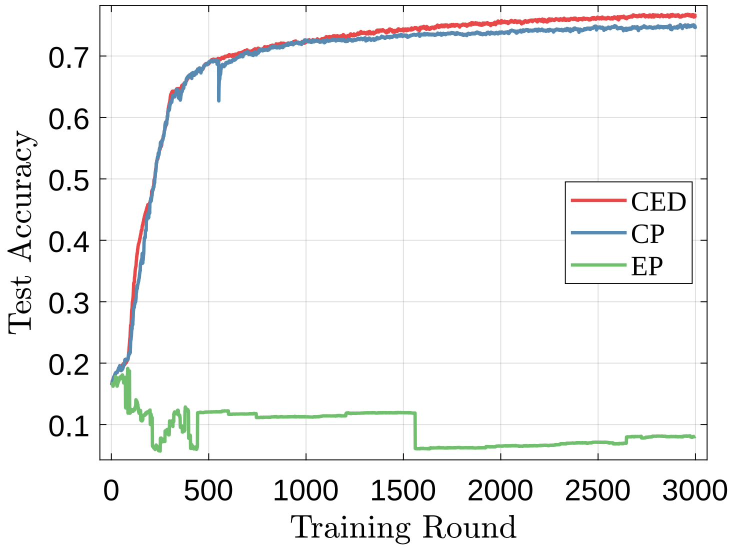

(a) Balanced data setting

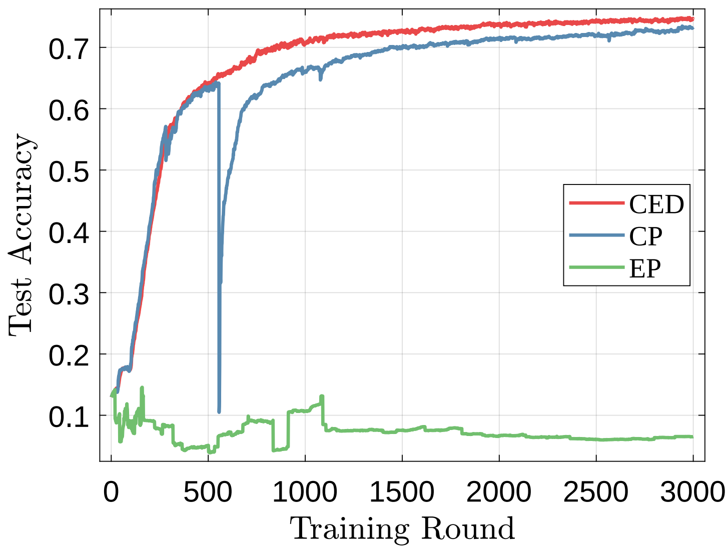

(b) Unbalanced data setting

Figure 3.4: Test accuracy comparison.

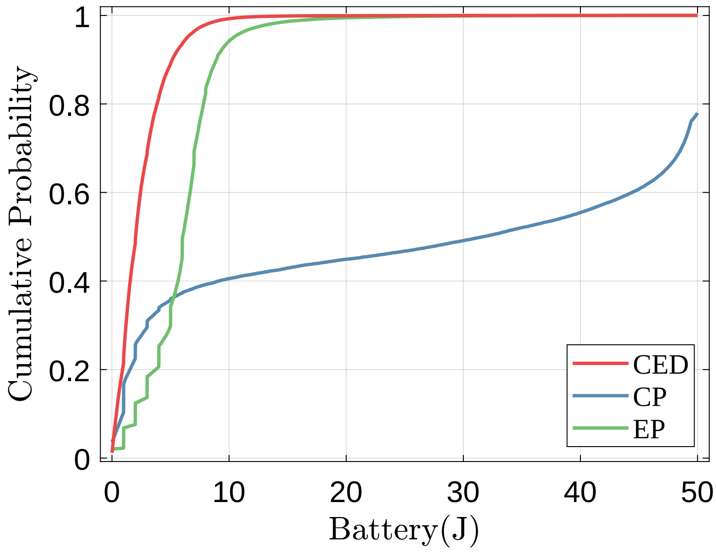

(a) Balanced data setting

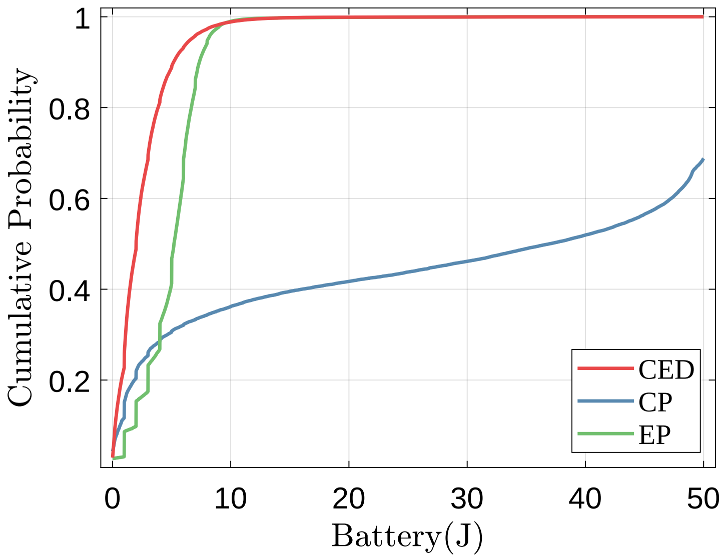

(b) Unbalanced data setting

Figure 3.5: Residual battery comparison.

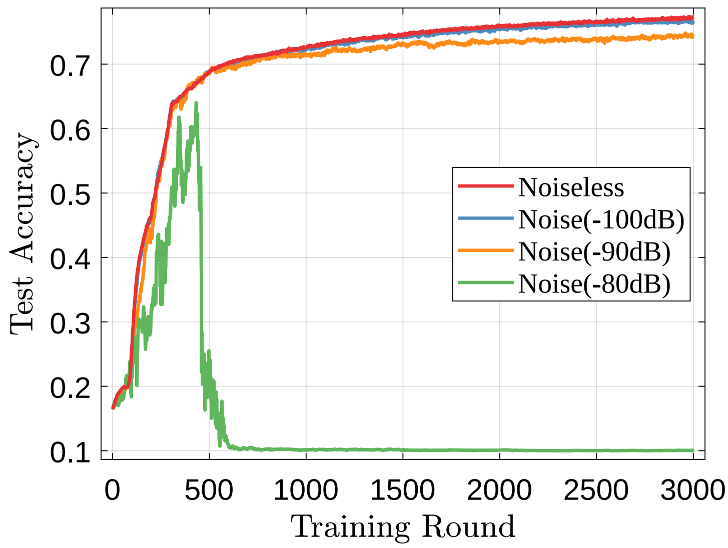

(a) Balanced data setting

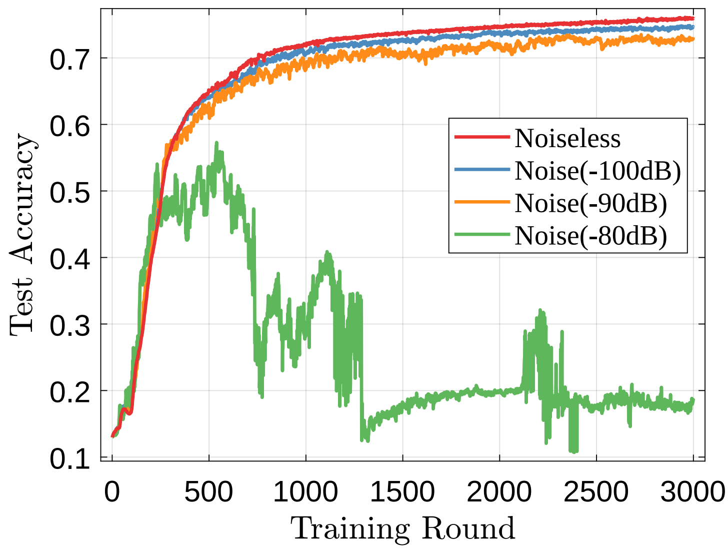

(b) Unbalanced data setting

Figure 3.6: The impacts of noise power.

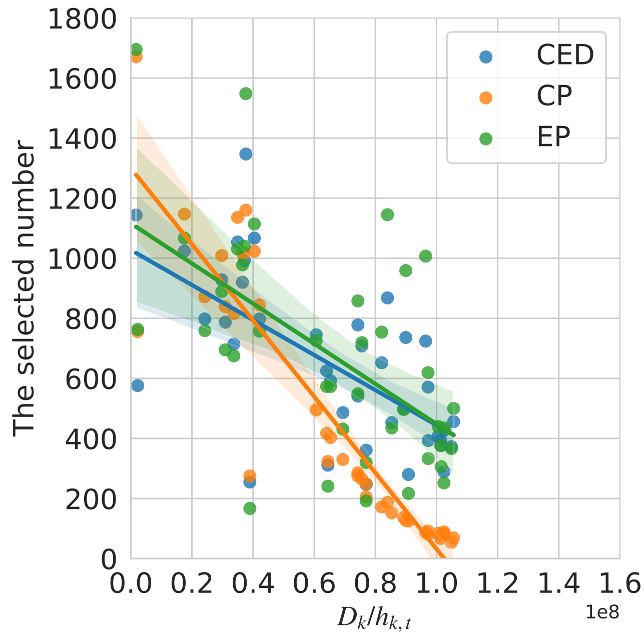

(a) The impacts of the data size and channel gain

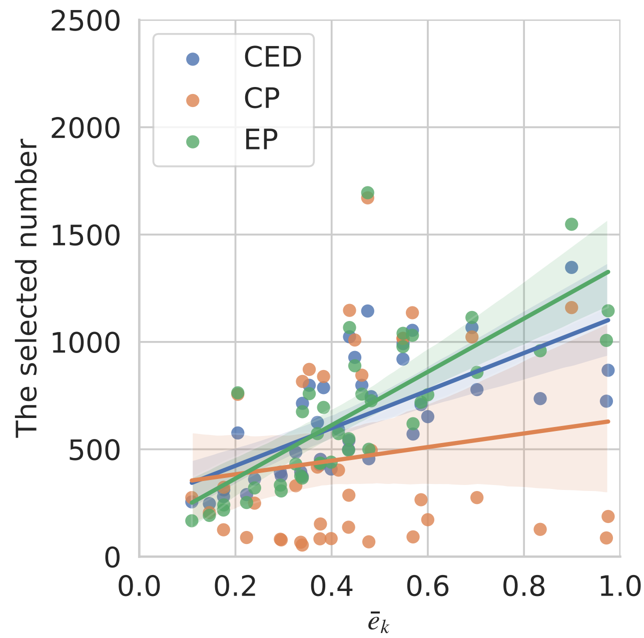

(b) The impact of the average arrival rate of energy harvesting

Figure 3.7: The impacts of the parameters on the client selection decision under the balanced data setting.

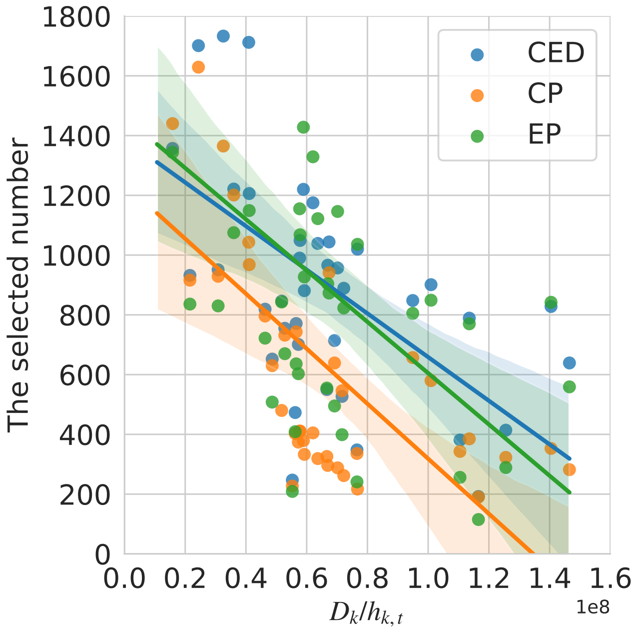

(a) The impacts of the data size and channel gain

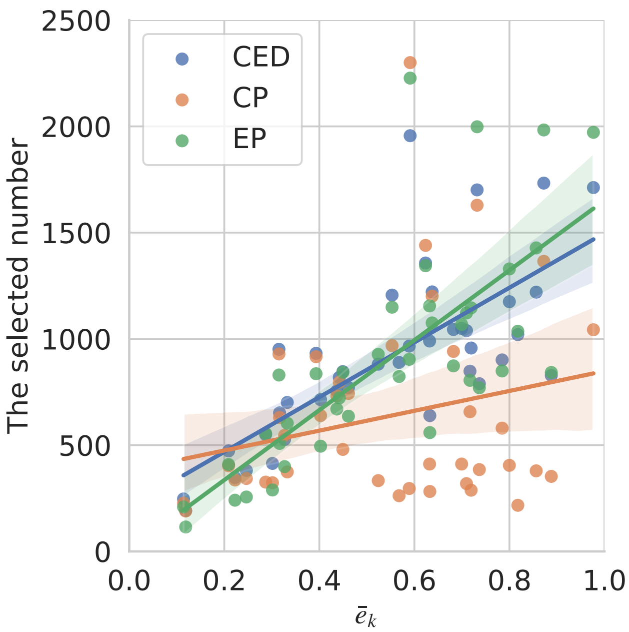

(b) The impact of the average arrival rate of energy harvesting

Figure 3.8: The impacts of the parameters on the client selection decision under the unbalanced data setting.

Therefore, in this subsection, we investigate the impacts of the parameter $D_k/h_{k,t}$ and $\bar{e}_k$ on the client selection decision of the three different methods under two different data settings for OTA FL system.

Figure 3.7(a) shows the influence of $D_k/h_{k,t}$ on the selected number of the local clients for three different methods, and Figure 3.7(b) shows the influence of the harvested energy on the selected number of the local clients for three different methods. As the local clients have the same amount of training samples, the parameter $D_k/h_{k,t}$ reveals the impacts of the channel gain $h_{k,t}$ on the client selection decision. In Figure 3.7(a), it is clear that the CP method is more related to the parameter $D_k/h_{k,t}$ compared with the CED method and CP method for that the client selection is not only decided by the channel gain but also by the arrival rate of the harvested energy. However, in Figure 3.7(b), it is observed that the EP method and the CED method are more related to the average arrival rate of the harvested energy as the CP method only makes client selection decision based on the channel state information.

Figure 3.8(a) shows the influence of $D_k/h_{k,t}$ on the selected number of the local clients for three different methods under the unbalanced data setting, and Figure 3.8(b) shows the influence of the harvested energy on the selected number of the local clients for three different methods under the unbalanced data setting, which have the similar trends with the Figure 3.7(a) and Figure 3.7(b). In Figure 3.8(a), three different methods have similar trends. Besides, if $D_k/h_{k,t}$ is higher for client k, the selected probability is lower. Therefore, if the client k has a smaller data size and better channel gain, the client k is easier to be selected. In Figure 3.8(b), the EP method and the CED method are more related to the average arrival rate of the harvested energy compared with the CP method. Besides, if the average arrival rate of the harvested energy is higher, the selection probability is higher. Therefore, for a certain client k, if the client has a smaller data size, better channel gain, and larger average arrival rate of the harvested energy, the client k tends to be selected.

3.5.6 Evaluating the proposed method with imperfect channel state information

In edge-intelligent networks, it is only able to obtain partial channel state information due to imperfect channel estimation or feedback. Thus, it is necessary to take channel uncertainty into consideration for joint client selection and transceiver design, namely robust transmission scheme design. There are also some studies that focus on the blind OTA FL system [96, 97]. However, few studies combine the imperfect channel state information with the energy management for the OTA FL system. In this subsection, we plan to derive the convergence performance of the OTA FL system with imperfect channel state information and energy constraint.

We assume that the error estimation of client k's channel at the t-th training round, denoted as $\delta^h_{k,t}$, follows a random distribution with zero mean and variance σ_h^2. Let $\tilde{h}_{k,t}$ denote the estimated channel coefficient at client k during the t-th training round, and the estimated channel can be represented as

$$\tilde{h}_{k,t} = h_{k,t} + \delta^h_{k,t}. \tag{3.47}$$

As only the estimated channel $\tilde{h}_{k,t}$ is available on the client side, the formula (3.10) related with power control factor $p_{k,t}$ is rewritten as

$$p_{k,t} = \frac{\alpha_t D_k}{\tilde{h}_{k,t}}, \tag{3.48}$$

The received global gradients can be rewritten as

$$\begin{aligned} \bar{\boldsymbol{r}}_t &= \frac{\sum_{k\in\mathcal{K}} \frac{h_{k,t}}{\tilde{h}_{k,t}} \beta_{k,t} D_k \boldsymbol{g}_{k,t} + \frac{z_t}{\alpha_t}}{\sum_{k\in\mathcal{K}} \beta_{k,t} D_k} \\ &= \frac{\sum_{k\in\mathcal{K}} (1 - \frac{\delta^h_{k,t}}{\tilde{h}_{k,t}}) \beta_{k,t} D_k \boldsymbol{g}_{k,t} + \frac{z_t}{\alpha_t}}{\sum_{k\in\mathcal{K}} \beta_{k,t} D_k}. \end{aligned} \tag{3.49}$$

By analyzing (3.49), it is observed that gradient error is not only related to the noisy channel but also related to the channel estimation error.

The gradient error $\boldsymbol{o}$ which is decided by client selection, channel error estimate, and the noisy channels for the OTA FL system is rewritten as

$$\begin{aligned}\boldsymbol{o} &= \nabla F(\boldsymbol{w}_t) - \bar{\boldsymbol{r}}_t \\ &= \underbrace{\nabla F(\boldsymbol{w}_t) - \frac{\sum_{k\in\mathcal{K}} \beta_{k,t} D_k \boldsymbol{g}_{k,t}}{\sum_{k\in\mathcal{K}} \beta_{k,t} D_k}}_{\text{Client selection related error}} + \underbrace{\frac{\sum_{k\in\mathcal{K}} \frac{\delta^h_{k,t}}{\tilde{h}_{k,t}} \beta_{k,t} D_k \boldsymbol{g}_{k,t}}{\sum_{k\in\mathcal{K}} \beta_{k,t} D_k}}_{\text{Channel estimation related error}} + \underbrace{\frac{-\boldsymbol{z}_t}{\alpha_t \sum_{k\in\mathcal{K}} \beta_{k,t} D_k}}_{\text{Noise related error}}. \end{aligned} \tag{3.50}$$

As a result, $\mathbb{E}\left[\|\boldsymbol{o}\|_2^2\right]$ is bounded as

$$\begin{aligned}&\mathbb{E}\left[\|\boldsymbol{o}\|_2^2\right] \\ &= \mathbb{E}\left[\left\|\nabla F(\boldsymbol{w}_t) - \frac{\sum_{k\in\mathcal{K}} \beta_{k,t} D_k \boldsymbol{g}_{k,t}}{\sum_{k\in\mathcal{K}} \beta_{k,t} D_k} + \frac{\sum_{k\in\mathcal{K}} \frac{\delta^h_{k,t}}{\tilde{h}_{k,t}} \beta_{k,t} D_k \boldsymbol{g}_{k,t}}{\sum_{k\in\mathcal{K}} \beta_{k,t} D_k} - \frac{\boldsymbol{z}_t}{\alpha_t \sum_{k\in\mathcal{K}} \beta_{k,t} D_k}\right\|_2^2\right] \\ &\le \mathbb{E}\left[\frac{(D - \sum_{k\in\mathcal{K}} \beta_{k,t} D_k)}{D\sum_{k\in\mathcal{K}} \beta_{k,t} D_k} \sum_{k\in\mathcal{K}_t} \sum_{i=1}^{D_k} \nabla f(\boldsymbol{w}_{k,t}, x_{k,i}, y_{k,i}) + \frac{\sum_{k\in\widetilde{\mathcal{K}}_t} \sum_{i=1}^{D_k} \nabla f(\boldsymbol{w}_{k,t}, x_{k,i}, y_{k,i})}{D}\right]^2 \\ &\quad + \frac{S\sigma^2}{\|\alpha_t \sum_{k\in\mathcal{K}} \beta_{k,t} D_k\|^2} + \frac{\sigma_h^2 (\sum_{k\in\mathcal{K}} \frac{1}{\tilde{h}_{k,t}} \beta_{k,t} D_k g_{k,t})^2}{(\sum_{k\in\mathcal{K}} \beta_{k,t} D_k)^2}. \end{aligned} \tag{3.51}$$

According to (3.51), when channel estimate error $\delta^h_{k,t}$ is considered in the convergence analysis of the OTA FL system, the Lemma 3.1 can be rewritten as Lemma 3.2.

Lemma 3.2 *Based on Assumptions 1-3, when the learning rate satisfies* $\eta = \frac{1}{l}$*, given the residual battery capacity vector* $\boldsymbol{b}_t$*, the client selection vector* $\boldsymbol{\beta}_t$*, and the estimated channel* $\tilde{h}_{k,t}$ *with variance* σ_h^2*, the optimality gap at the t-th training round within the energy constraint can be represented as follows*

$$\mathbb{E}[F(\boldsymbol{w}_{t+1})] - F(\boldsymbol{w}^*) \le \psi_t \left(\mathbb{E}[F(\boldsymbol{w}_t)] - F(\boldsymbol{w}^*)\right) + \frac{\lambda_1}{l}\phi_t, \tag{3.52}$$

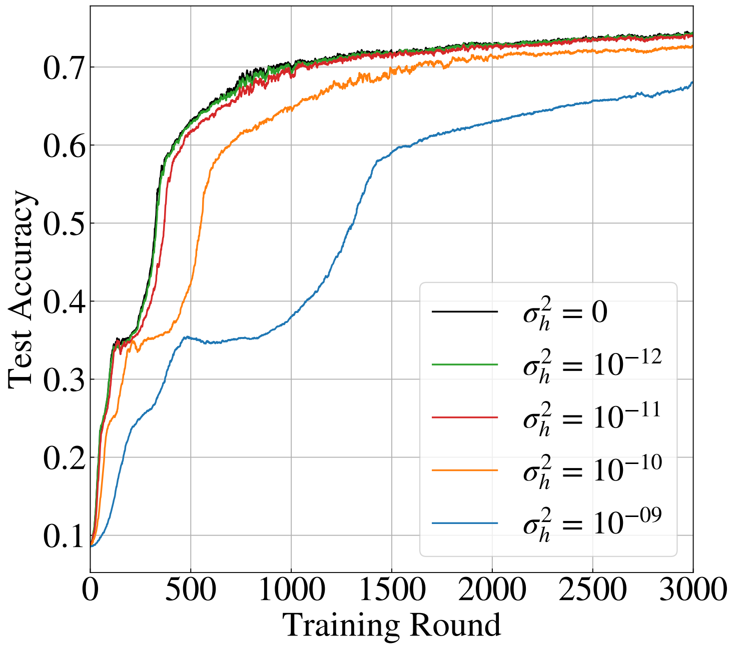

(a) Balanced data setting

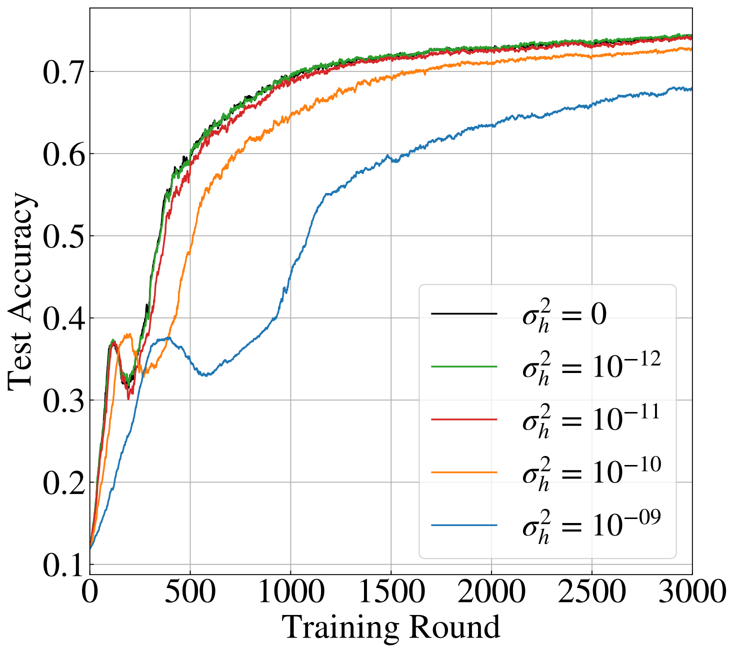

(b) Unbalanced data setting

Figure 3.9: The impacts of the channel estimation error on the test accuracy.

where ψ_t and ϕ_t can be expressed as follows:

$$\psi_t = 1 - \frac{\mu}{l} + \frac{2\mu\lambda_2\phi_t}{l}, \tag{3.53}$$

$$\phi_t = \frac{s\sigma^2}{2\left(\sum_{k\in\mathcal{K}} D_k\beta_{k,t}\right)^2}\left(\max_{k\in\mathcal{K}} \frac{\beta_{k,t}D_k^2}{\tilde{h}_{k,t}^2\left(b_{k,t} - D_k e_{k,t,i}\right)}\right) + \frac{2\left(D - \sum_{k\in\mathcal{K}} \beta_{k,t}D_k\right)^2}{D^2}$$
$$+\frac{\sigma_h^2(\sum_{k\in\mathcal{K}} \frac{1}{\tilde{h}_{k,t}}\beta_{k,t}D_k)^2}{2(\sum_{k\in\mathcal{K}} \beta_{k,t}D_k)^2}. \tag{3.54}$$

Lemma 3.2 indicates that the OTA FL system remains capable of achieving convergence even in the presence of channel estimation error. Furthermore, as the variance of the channel estimation error σ_h^2 increases, the convergence speed of the OTA FL system decreases.

To validate the proposed method for the OTA FL system with imperfect channel state information, we conduct simulations to assess the performance of the OTA FL system with the channel estimation error under both balanced and unbalanced data settings. Figure 3.9(a) and Figure 3.9(b) illustrate the test accuracy of the OTA FL system with imperfect channel state information. The results clearly demonstrate that a larger variance σ_h^2 in the channel estimation error leads to the decrease in the test accuracy of the OTA FL system, as evident from both figures. Notably, when the channel estimation error variance σ_h^2 is set to 0, representing an absence of channel estimation error, the system achieves its best performance.

3.6 Summary

In this chapter, our primary focus is on addressing the client selection problem in the OTA FL system that involves energy harvesting clients. We aim to derive a convergence analysis for the OTA FL system considering both energy constraint and energy harvesting. Based on the convergence analysis, we formulate a problem that aims to minimize the optimality gap of the training loss by optimizing the client selection decision. To tackle the formulated problem, we introduce the concept of the CED coefficient and propose a discrete search method to solve the NIP problem in an online mode. Through extensive simulations, we demonstrate the effectiveness of the proposed method in achieving fast convergence for the OTA FL system that incorporates energy harvesting clients.

4

Joint receive beamforming and client selection for OTA FL with energy harvesting

4.1 Introduction

The SISO setting for the OTA FL system is considered in Chapter 3. To improve the system performance under the weak channels, the SIMO setting is considered in this chapter and the receive beamforming design is optimized to realize fast convergence for the OTA FL system. Besides, in addition to the energy constraint, the power control is also considered to make the system more realistic for the OTA FL system with energy harvesting. The MINLP problem is formulated based on the convergence analysis for the OTA FL system. To optimize the client selection and receive beamforming design under the energy constraint and power control, the joint optimization method is proposed for the MINLP problem via online mode. Specifically, the CED-based

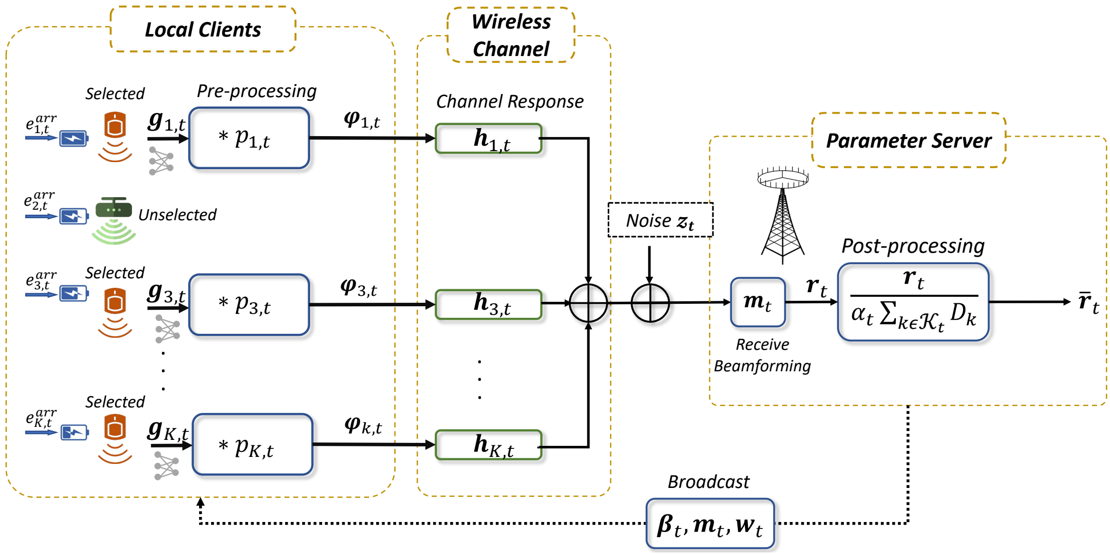

Figure 4.1: FL system via OTA computation with energy harvesting.

method proposed in Chapter 3 is used for client selection, and the SDR-based method is used for the receive beamforming design. The simulation results show that the joint optimization method can achieve better performance compared with other baselines.

4.2 System model

In this chapter, we consider the OTA FL system which is composed of a PS with N antennas and K single-antenna local clients. The data distribution setting of the local clients has the same setting as in Chapter 3. Besides, the FL model has the same structure and setting as in Chapter 3. In the following, we will introduce some background knowledge related to the communication model, and the energy consumption and harvesting models, which mainly focus on the differences between this chapter and Chapter 3.

4.2.1 Communication model

For the OTA FL system, the communication process includes the global model broadcasting from the PS to the selected clients and the local model uploading from the selected clients to the PS. In this chapter, we assume that the global model can be broadcast correctly from the PS to clients. In the upload process via OTA computation, the selected clients need to send their updated gradients to PS synchronously with the shared wireless channel. Let $p_{k,t}$ represent the power control factor of client k at the t-th training round. The pre-processing operation for local gradients $\boldsymbol{g}_{k,t}$ at client k during the t-th training round is as follows:

$$\boldsymbol{\varphi}_{k,t} = p_{k,t}\boldsymbol{g}_{k,t}. \tag{4.1}$$

Let $\boldsymbol{h}_{k,t} \in \mathbb{C}^N$ denote the channel coefficient of client k at the t-th training round, where N is the number of receive antennas at the PS side, and $\boldsymbol{m}_t \in \mathbb{C}^N$ denote the receive beamforming vector at the t-th training round. We assume that the channel coefficients may fluctuate in different training rounds but stay quasi-static during the same training round. Let $\boldsymbol{z}_t = [\boldsymbol{z}_t^{[1]}, \boldsymbol{z}_t^{[2]}, \ldots, \boldsymbol{z}_t^{[S]}] \in \mathbb{C}^{N\times S}$ represent AWGN matrix, in which, $\boldsymbol{z}_t^{[s]}$ denotes the induced noise for s-th gradient signal. Each element of $\boldsymbol{z}_t^{[s]}$ follows the complex normal distribution of $\mathcal{CN}\left(0, \sigma^2\right)$. The PS receives the aggregated gradients vector $\boldsymbol{r}_t \in \mathbb{C}^S$ at the t-th training round as

$$\boldsymbol{r}_t = \sum_{k\in\mathcal{K}_t} \boldsymbol{m}_t^H \boldsymbol{h}_{k,t}\boldsymbol{\varphi}_{k,t} + \boldsymbol{m}_t^H \boldsymbol{z}_t. \tag{4.2}$$

To get the averaged gradients of the OTA FL system, the PS post-processes the received aggregated gradients [10] as

$$\bar{\boldsymbol{r}}_t = \frac{\boldsymbol{r}_t}{\alpha_t \sum_{k\in\mathcal{K}_t} D_k}, \tag{4.3}$$

where α_t represents the normalization scaling factor at the t-th training round. Then, the error estimate $\boldsymbol{\epsilon}_t$ between the aggregated gradients $\bar{\boldsymbol{r}}_t$ and the error-free gradients $\boldsymbol{g}_t$ at the t-th training round can be expressed as

$$\boldsymbol{\epsilon}_t = \frac{\sum_{k\in\mathcal{K}_t}\left(\frac{\boldsymbol{m}_t^H \boldsymbol{h}_{k,t} p_{k,t}}{\alpha_t} - D_k\right)\boldsymbol{g}_{k,t}}{\sum_{k\in\mathcal{K}_t} D_k} + \frac{\boldsymbol{m}_t^H \boldsymbol{z}_t}{\alpha_t \sum_{k\in\mathcal{K}_t} D_k}. \tag{4.4}$$

According to [62], to minimize the mean squared error, the uniform forcing technology is used for OTA computation. The mean squared error of the global gradients is calculated as

$$\begin{aligned} MSE(\boldsymbol{\epsilon}_t) &= E(|\boldsymbol{\epsilon}_t|^2) \\ &= E(|\frac{\sum_{k\in\mathcal{K}_t}\left(\frac{\boldsymbol{m}_t^H\boldsymbol{h}_{k,t}p_{k,t}}{\alpha_t} - D_k\right)\boldsymbol{g}_{k,t}}{\sum_{k\in\mathcal{K}_t}D_k} + \frac{\boldsymbol{m}_t^H\boldsymbol{z}_t}{\alpha_t\sum_{k\in\mathcal{K}_t}D_k}|^2). \end{aligned} \tag{4.5}$$

As a result, the power control factor $p_{k,t}$ needs to satisfy the requirement for the selected client k at the t-th training round as follows:

$$p_{k,t} = \frac{\alpha_t D_k(\boldsymbol{m}_t^H\boldsymbol{h}_{k,t})^H}{||\boldsymbol{m}_t^H\boldsymbol{h}_{k,t}||^2}. \tag{4.6}$$

Unlike in Chapter 3, in this chapter, we introduce a new assumption regarding the transmission power of client k during the t-th training round, and we assume that the average transmission power is limited by a maximum transmission power value P_0 as follows:

$$\frac{\left\|p_{k,t}\boldsymbol{g}_{k,t}\right\|^2}{S} \le P_0. \tag{4.7}$$

Take (4.6) into (4.3), the averaged gradients can be rewritten as follows:

$$\bar{\boldsymbol{r}}_t = \frac{\sum_{k\in\mathcal{K}_t}D_k\boldsymbol{g}_{k,t} + \frac{\boldsymbol{m}_t^H\boldsymbol{z}_t}{\alpha_t}}{\sum_{k\in\mathcal{K}_t}D_k}. \tag{4.8}$$

4.2.2 Energy consumption and harvesting models

According to [98], the transmission time of each training round for the OTA FL system is calculated as

$$\tau_{\mathrm{tr}} = \left\lceil\frac{S}{R}\right\rceil T_{\mathrm{slot}}, \tag{4.9}$$

where T_{slot} is the transmission time for each resource block and R is the number of the transmitted signals for each resource block. Let $e_{k,t,i}$ denote the computation energy consumption for one training sample of client k. The data size D_k for client k may be varied across different clients because of the heterogeneous data distribution.

The total energy consumption includes the computation energy consumption and transmission energy consumption. In this chapter, the number of local epochs is set as 1 for simplicity. By combining (4.6) and (4.9), the total energy consumption $e_{k,t}^{\mathrm{tot}}$ [13] for local client k during the t-th training round can be calculated as

$$\begin{aligned} e_{k,t}^{\mathrm{tot}} &= D_k e_{k,t,i} + \frac{\tau_{\mathrm{tr}} \left\| p_{k,t} \boldsymbol{g}_{k,t} \right\|^2}{S} \\ &= D_k e_{k,t,i} + \frac{\tau_{\mathrm{tr}} \alpha_t^2 D_k^2}{S ||\boldsymbol{m}_t^H \boldsymbol{h}_{k,t}||^2} \left\| \boldsymbol{g}_{k,t} \right\|^2. \end{aligned} \tag{4.10}$$

We assume that the local client k can harvest energy from the surrounding environment. The energy harvesting process is constructed based on a successive energy arrival model. Let $\boldsymbol{e}_t^{\mathrm{arr}} = [e_{1,t}^{\mathrm{arr}}, \ldots, e_{K,t}^{\mathrm{arr}}]$ denote the newly arrived energy vector during the t-th training round, and $e_{k,t}^{\mathrm{arr}}$ means the arrived energy for client k during the t-th training round. For each local client, the energy harvested from the surrounding environment can be stored in the battery and used to supply subsequent computation and transmission energy consumption.

Let $b_{k,t}$ represent the battery capacity at the beginning of the t-th training round for local client k. The maximum battery capacity for all clients is set as B^{max}. At the t-th training round, the total energy consumption cannot exceed the residual battery capacity for each selected client k, which is represented as

$$e_{k,t}^{\mathrm{tot}} \leq b_{k,t}. \tag{4.11}$$

The updated battery capacity of each client can not exceed the maximum battery capacity B^{max} during each training round. The updated battery level $b_{k,t+1}$ for client k at the end of the t-th training round can be expressed as follows:

$$b_{k,t+1} = \min \left\{ b_{k,t} - e_{k,t}^{\mathrm{tot}} + e_{k,t}^{\mathrm{arr}}, B^{\mathrm{max}} \right\}. \tag{4.12}$$

The transmission energy consumption is constrained by the residual battery capacity and maximum transmission power. Based on (4.7) (4.10), and (4.11), the transmission energy for client k at the t-th training round can not be larger than the transmission

Table 4.1: The new notations in Chapter 4.

Notation	Description
N	number of antennas equipped at the PS
$\boldsymbol{h}_{k,t}$	channel coefficient of client k at the t-th training round
$\boldsymbol{m}_t$	receive beamforming vector at the t-th training round
τ_{tr}	transmission time for one training round
P_0	maximum transmission power
$\Delta_{k,t}^{\max}$	transmission energy threshold of client k at the t-th training round

energy threshold $\Delta_{k,t}^{\max}$, which is calculated as

$$\Delta_{k,t}^{\max} = \min \left\{ b_{k,t} - D_k e_{k,t,i}, \tau_{\text{tr}} P_0 \right\}. \tag{4.13}$$

4.2.3 Problem formulation

In this chapter, we formulate the problem $\mathcal{P}1$, which focuses on minimizing the optimality gap after T training rounds in the context of a SIMO OTA FL system. The problem involves optimizing both the client selection scheme and the receive beamforming design for the OTA FL system while considering energy constraints and transmission power control. The formulation of $\mathcal{P}1$ is similar to the problem $\mathcal{P}1$ presented in subsection 3.2.4. The formulated problem $\mathcal{P}_1$ can be represented as

$$\begin{aligned}
\mathcal{P}_1: \quad \min_{\boldsymbol{\beta},\boldsymbol{m}} \quad & \mathbb{E}[F(\boldsymbol{w}_{T+1})] - F(\boldsymbol{w}^*) && \text{(4.14a)}\\
\text{s.t.} \quad & e_{k,t}^{\text{tot}} \le b_{k,t}, \quad \forall k \in \mathcal{K}, 1 \le t \le T, && \text{(4.14b)}\\
& \frac{\left\| p_{k,t} \boldsymbol{g}_{k,t} \right\|^2}{S} \le P_0, \quad \forall k \in \mathcal{K}, 1 \le t \le T, && \text{(4.14c)}\\
& \beta_{k,t} \in \{0,1\}, \quad \forall k \in \mathcal{K}, 1 \le t \le T, && \text{(4.14d)}\\
& \boldsymbol{m}_t \in \mathbb{C}^N, \quad 1 \le t \le T. && \text{(4.14e)}
\end{aligned}$$

The formulated problem $\mathcal{P}_1$ includes the following constraints:

1) The total energy consumption is bounded by the available battery capacity.

2) The transmission power is limited by the maximum transmission power.

3) The client selection is represented by a binary vector, indicating the selection or non-selection of each client.

4) The receive beamforming vector is a complex value, reflecting the beamforming coefficients for signal reception.

These constraints ensure that the energy consumption, transmission power, client selection, and receive beamforming adhere to their respective limitations in the OTA FL system.

The presence of channel fading and the introduced noise make the received gradient signals deviate from their actual values for the OTA FL system. The client selection and receive beamforming design both have impacts on the received signals for the OTA FL system because of the energy constraint, channel fading, and communication error. In the next section, we derive the impact of the convergence performance of the OTA FL system regarding the client selection matrix $\boldsymbol{\beta}$, the receive beamforming matrix $\boldsymbol{m}$, and the transmission energy threshold $\Delta_{k,t}^{\max}$. Table 4.1 lists the new notations used for this chapter except the notations used in Chapter 3.

4.3 Convergence analysis and problem transformation

The convergence analysis of the OTA FL system is given in this section. Note that the energy constraint and transmission power control are both introduced into the convergence analysis for OTA FL. The derived convergence results reveal that the channel coefficient, the transmission energy threshold, and the data size all have impacts on the convergence rate of the OTA FL system. Based on the convergence result, the non-convex MINLP problem is built as $\mathcal{P}_2$ to minimize the optimality gap of the training loss of the OTA FL system. Because of the stochasticity of the channel coefficient and energy harvesting, the offline problem $\mathcal{P}_2$ is transformed into the online non-convex MINLP problem $\mathcal{P}_3$.

4.3.1 Convergence analysis

According to (3.4) and (4.3), the global model for the OTA FL system at the t-th training round is updated through

$$\boldsymbol{w}_{t+1} = \boldsymbol{w}_t - \eta \bar{\boldsymbol{r}}_t. \tag{4.15}$$

In this chapter, we also use the same three assumptions as in Chapter 3 regarding loss functions [3, 10] for ease of convergence analysis.

Let $F(\boldsymbol{w}^*)$ denote the optimal loss, and the optimality gap between the actual loss and the optimal loss at the t-th training round can be formally represented as $\mathbb{E}[F(\boldsymbol{w}_{t+1})] - F(\boldsymbol{w}^*)$. A smaller optimality gap represents better learning performance for the OTA FL system. The relationship of the optimality gap for two adjacent rounds is given in Lemma 4.1.

Lemma 4.1 *When Assumptions 1-3 are satisfied, with the learning rate $\eta = \frac{1}{l}$, the given client selection vector $\boldsymbol{\beta}_t$, the given receive beamforming vector $\boldsymbol{m}_t$, and the transmission energy threshold $\Delta_{k,t}^{\max} = \min\left\{b_{k,t} - D_k e_{k,t,i}, \tau_{\rm tr} P_0\right\}$, the optimality gap $\mathbb{E}[F(\boldsymbol{w}_{t+1})] - F(\boldsymbol{w}^*)$ at the t-th training round within the energy constraint is given by*

$$\mathbb{E}[F(\boldsymbol{w}_{t+1})] - F(\boldsymbol{w}^*) \leq \psi_t \left(\mathbb{E}[F(\boldsymbol{w}_t)] - F(\boldsymbol{w}^*)\right) + \frac{\lambda_1}{l}\phi_t, \tag{4.16}$$

where ψ_t and ϕ_t can be represented as follows:

$$\psi_t = 1 - \frac{\mu}{l} + \frac{2\mu\lambda_2\phi_t}{l}, \tag{4.17}$$

$$\phi_t = \frac{\sigma^2 \tau_{\rm tr}}{2\left(\sum_{k\in\mathcal{K}} D_k \beta_{k,t}\right)^2} \left(\max_{k\in\mathcal{K}} \frac{\beta_{k,t} D_k^2 ||\boldsymbol{m}_t||^2}{\Delta_{k,t}^{\max} ||\boldsymbol{m}_t^H \boldsymbol{h}_{k,t}||^2}\right) + \frac{2\left(D - \sum_{k\in\mathcal{K}} \beta_{k,t} D_k\right)^2}{D^2}. \tag{4.18}$$

Proof. The proof process for Lemma 4.1 is similar to the proof process of the Lemma 3.1, the main differences lie in that the introduced receive beamforming vector

$\boldsymbol{m}_t$. As a result, the formula (3.29) is rewritten as

$$\begin{aligned}\mathbb{E}\left[F\left(\boldsymbol{w}_{t+1}\right)\right]-F\left(\boldsymbol{w}^*\right)\leq\ &\mathbb{E}\left[F\left(\boldsymbol{w}_t\right)\right]-F\left(\boldsymbol{w}^*\right)\\ &+\frac{2}{lD^2}\left(D-\sum_{k\in\mathcal{K}}\beta_{k,t}D_k\right)^2\left(\lambda_1+\lambda_2\|\nabla F\left(\boldsymbol{w}_t\right)\|_2^2\right)\\ &+\frac{S\sigma^2\|\boldsymbol{m}_t^H\|^2}{2l{\alpha_t}^2\left(\sum_{k\in\mathcal{K}}\beta_{k,t}D_k\right)^2}-\frac{1}{2l}\|\nabla F\left(\boldsymbol{w}_t\right)\|_2^2.\end{aligned} \tag{4.19}$$

According to (4.10), (4.11), and (4.13), which represent the calculation of the total energy consumption $e_{k,t}^{\text{tot}}$, energy consumption constraint caused by available battery $b_{k,t}$, and the definition of the transmission energy threshold $\Delta_{k,t}^{\max}$, the normalization scaling factor α_t at the t-th training round needs to satisfy the following condition:

$$\alpha_t\leq\left(\frac{\beta_{k,t}\|\boldsymbol{m}_t^H\boldsymbol{h}_{k,t}\|\sqrt{S\Delta_{k,t}^{\max}}}{\sqrt{\tau_{\text{tr}}}D_k\left\|\boldsymbol{g}_{k,t}\right\|_2}\right),k\in\mathcal{K}. \tag{4.20}$$

The variable α_t can also be expressed as follows:

$$\alpha_t=\min_{k\in\mathcal{K}}\left(\frac{\beta_{k,t}\|\boldsymbol{m}_t^H\boldsymbol{h}_{k,t}\|\sqrt{S\Delta_{k,t}^{\max}}}{\sqrt{\tau_{\text{tr}}}D_k\left\|\boldsymbol{g}_{k,t}\right\|_2}\right). \tag{4.21}$$

By incorporating (3.32), (3.33), and (4.21), into (4.19), we finally obtain

$$\mathbb{E}\left[F\left(\boldsymbol{w}_{t+1}\right)\right]-F\left(\boldsymbol{w}^*\right)\leq\psi_t\left[\mathbb{E}\left[F\left(\boldsymbol{w}_t\right)\right]-F\left(\boldsymbol{w}^*\right)\right]+\frac{\lambda_1}{l}\phi_t. \tag{4.22}$$

The proof of Lemma 4.1 has been completed. □

By comparing the Lemma 4.1 with Lemma 3.1, it is clear to observe that the convergence rate of the OTA FL system for SIMO setting is influenced by many parameters such as the client selection vector, the receive beamforming design, the available battery, the energy harvesting setting, and the transmission power control.

Lemma 4.1 reveals that the upper bound of the optimality gap at the t-th training round $\mathbb{E}[F(\boldsymbol{w}_{t+1})]-F(\boldsymbol{w}^*)$ is related with the optimality gap at the $(t-1)$-th training round $\mathbb{E}[F(\boldsymbol{w}_t)]-F(\boldsymbol{w}^*)$, ψ_t, and ϕ_t. By repeatedly applying Lemma 4.1 and collecting terms, we have the optimality gap after the total number of T training rounds as in Theorem 4.1. Different from Lemma 4.1, Theorem 4.1 illustrates the relationship between the optimality gap after T training rounds and the initial optimality gap.

Theorem 4.1 *Suppose that the total number of training rounds is set as T and the initial global model is set as $\mathbf{w}_1$. The optimality gap after T training rounds of the OTA FL system is given by*

$$\mathbb{E}\left[F\left(\boldsymbol{w}_{T+1}\right)\right]-F\left(\boldsymbol{w}^*\right) \leq \Omega_T\left(\boldsymbol{\beta}, \boldsymbol{m}\right), \tag{4.23}$$

where

$$\Omega_T\left(\boldsymbol{\beta}, \boldsymbol{m}\right)=\prod_{t=1}^{T} \psi_t\left(\mathbb{E}\left[F\left(\boldsymbol{w}_1\right)\right]-F\left(\boldsymbol{w}^*\right)\right)+\frac{\lambda_1}{l}\left(\sum_{t=1}^{T-1} \prod_{j=t+1}^{T} \psi_j \phi_t+\phi_T\right). \tag{4.24}$$

Proof. The proof process is the same as the proof process with Theorem 3.1. □

Theorem 4.1 reveals that the optimality gap is upper-bounded by $\Omega_T\left(\boldsymbol{\beta}, \boldsymbol{m}\right)$. When the initial optimality gap $\mathbb{E}\left[F\left(\boldsymbol{w}_1\right)\right]-F\left(\boldsymbol{w}^*\right)$ and the parameters μ, l, λ_1, and λ_2 of Assumptions 1-3 are known, the upper bound of the optimality gap is decided by ψ_1, $\phi_1, \ldots, \psi_T$ and ϕ_T.

4.3.2 Problem transformation

According to Theorem 4.1, the optimality gap after T training rounds $\mathbb{E}\left[F\left(\boldsymbol{w}_{T+1}\right)\right]-F\left(\boldsymbol{w}^*\right)$ is influenced by the client selection vector $\boldsymbol{\beta}_t$, the receive beamforming vector $\boldsymbol{m}_t$, and the transmission energy threshold $\Delta_{k,t}^{\max}$, which are obtained from each training round t and each selected client k. The transmission power control and energy constraint are both introduced into the convergence analysis process of the optimality gap. To minimize the optimality gap after T training rounds, the problem $\mathcal{P}_1$ can be transformed to the problem $\mathcal{P}_2$, which is

$$\begin{aligned}
\mathcal{P}_2: \quad & \min_{\boldsymbol{\beta}, \boldsymbol{m}} \quad \Omega_T\left(\boldsymbol{\beta}, \boldsymbol{m}\right) && \text{(4.25a)}\\
& \text{s.t.} \quad \beta_{k,t} \in \{0,1\}, \quad \forall k \in \mathcal{K}, 1 \leq t \leq T, && \text{(4.25b)}\\
& \qquad\ \ \boldsymbol{m}_t \in \mathbb{C}^N, \qquad 1 \leq t \leq T. && \text{(4.25c)}
\end{aligned}$$

It is difficult to solve the problem $\boldsymbol{\mathcal{P}}_2$ directly because of the stochasticity of the channel coefficient $\boldsymbol{h}_t$ and the harvested energy vector $\boldsymbol{e}_t^{\text{arr}}$ for each training round t. We try to reformulate the problem $\boldsymbol{\mathcal{P}}_2$ and focus on solving the problem with an online pattern according to Lemma 4.1.

The optimality gap at the t-th training round $\mathbb{E}[F(\boldsymbol{w}_{t+1})] - F(\boldsymbol{w}^*)$ is defined as Θ_{t+1}. According to Lemma 4.1, we have

$$\begin{aligned}\Theta_{t+1} &\leq \left(1 - \frac{\mu}{l} + \frac{2\mu\lambda_2\phi_t}{l}\right)\Theta_t + \frac{\lambda_1}{l}\phi_t \\ &= \left(1 - \frac{\mu}{l}\right)\Theta_t + \left(\frac{2\mu\lambda_2}{l}\Theta_t + \frac{\lambda_1}{l}\right)\phi_t. \end{aligned} \tag{4.26}$$

One can observe that the optimality gap at the t-th training round Θ_{t+1} is decided by ϕ_t when the parameters of assumptions μ, l, λ_1, λ_2, and the optimality gap at the $(t-1)$-th training round Θ_t are known. Therefore, the problem $\boldsymbol{\mathcal{P}}_2$ can be transformed to $\boldsymbol{\mathcal{P}}_3$ to minimize ϕ_t with an online pattern, which can be formulated as follows:

$$\boldsymbol{\mathcal{P}}_3: \quad \min_{\boldsymbol{\beta}_t} \quad \phi_t\left(\boldsymbol{\beta}_t, \boldsymbol{m}_t\right) \tag{4.27a}$$

$$\text{s.t.} \quad \beta_{k,t} \in \{0,1\}, \quad \forall k \in \mathcal{K}, \tag{4.27b}$$

$$\boldsymbol{m}_t \in \mathbb{C}^N. \tag{4.27c}$$

The reformulated problem $\boldsymbol{\mathcal{P}}_3$ is one MINLP problem rather than the NIP problem in [99]. The receive beamforming design and transmission power control are both considered in $\boldsymbol{\mathcal{P}}_3$, which makes the problem more difficult to solve compared with [99].

By analyzing (4.8) and (4.18), one can observe that if more clients are selected to upload the gradients, the loss decreases faster. However, due to the constraint of the transmission power control and residual battery capacity, α_t will be smaller and the signal-to-noise ratio (SNR) will decrease when more clients are selected to participate in the training, which will make the convergence speed slower.

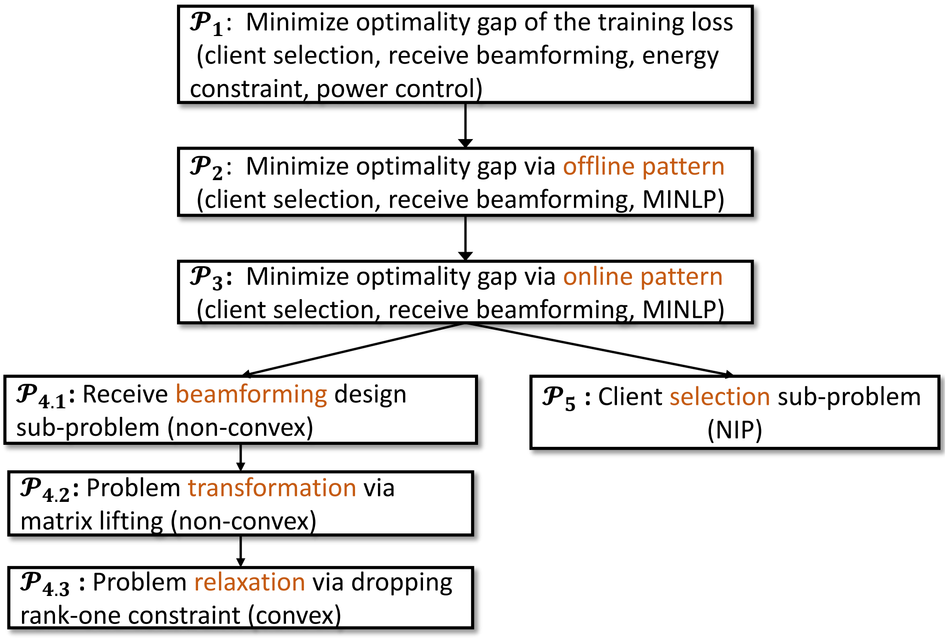

Figure 4.2: The relations of the problems.

4.4 Joint online optimization of client selection and receive beamforming

In this section, we propose an alternative optimization method to solve the problem $\mathcal{P}_3$. Specifically, the SDR programming method is adopted to optimize the receive beamforming when the client selection vector is given, and the discrete search method named the CED-based method is proposed to realize client selection with the given receive beamforming design. The process of the alternative optimization will iterate for a predefined number of iterations. Besides, we also give discussions about the computation complexity of the proposed algorithms.

4.4.1 Receive beamforming optimization

At the t-th training round, assuming that the client selection vector $\boldsymbol{\beta}_t$ is given. To optimize the receive beamforming design for the OTA FL system, the problem $\mathcal{P}_3$ can be simplified as

$$\mathcal{P}_{4.1}: \quad \min_{\boldsymbol{m}_t} \quad \max_{k \in \mathcal{K}} \frac{\beta_{k,t} D_k^2 ||\boldsymbol{m}_t||^2}{\Delta_{k,t}^{\max} ||\boldsymbol{m}_t^H \boldsymbol{h}_{k,t}||^2}. \tag{4.28}$$

For the convenience of the analysis, the min-max problem $\mathcal{P}_{4.1}$ is reformulated as one minimization problem $\mathcal{P}_{4.2}$, which is presented in Lemma 4.2.

Lemma 4.2 *By assuming that* $\boldsymbol{M}_t = \boldsymbol{m}_t \boldsymbol{m}_t^H$ *and* $\boldsymbol{H}_{k,t} = \boldsymbol{h}_{k,t} \boldsymbol{h}_{k,t}^H$*, the non-convex receive beamforming optimization problem* $\mathcal{P}_{4.1}$ *can be reformulated as*

$$\begin{aligned} \mathcal{P}_{4.2}: \quad \min_{\boldsymbol{M}_t} \quad & \operatorname{Tr}(\boldsymbol{M}_t) && \text{(4.29a)} \\ \text{s.t.} \quad & \operatorname{Tr}(\boldsymbol{M}_t \boldsymbol{H}_{k,t}) \geq \frac{\beta_{k,t} D_k^2}{\Delta_{k,t}^{\max}}, \forall k \in \mathcal{K}, && \text{(4.29b)} \\ & \boldsymbol{M}_t \succeq \boldsymbol{0}, && \text{(4.29c)} \\ & \operatorname{rank}(\boldsymbol{M}_t) = 1. && \text{(4.29d)} \end{aligned}$$

Proof. We assume that the introduced variable τ is set as $\min_k \frac{\Delta_{k,t}^{\max} ||\boldsymbol{m}_t^H \boldsymbol{h}_{k,t}||^2}{\beta_{k,t} D_k^2}$. The problem $\mathcal{P}_{4.1}$ is equivalent to

$$\begin{aligned} \min_{\boldsymbol{m}_t} \quad & \frac{||\boldsymbol{m}_t||^2}{\tau} && \text{(4.30a)} \\ \text{s.t.} \quad & \frac{||\boldsymbol{m}_t^H \boldsymbol{h}_{k,t}||^2}{\tau} \geq \frac{\beta_{k,t} D_k^2}{\Delta_{k,t}^{\max}}, \quad \forall k \in \mathcal{K}. && \text{(4.30b)} \end{aligned}$$

When another new variable $\tilde{\boldsymbol{m}}_t = \boldsymbol{m}_t / \sqrt{\tau}$ is given, the problem (4.30) can be reformulated as

$$\begin{aligned} \min_{\tilde{\boldsymbol{m}}_t} \quad & ||\tilde{\boldsymbol{m}}_t||^2 && \text{(4.31a)} \\ \text{s.t.} \quad & ||\tilde{\boldsymbol{m}}_t^H \boldsymbol{h}_{k,t}||^2 \geq \frac{\beta_{k,t} D_k^2}{\Delta_{k,t}^{\max}}, \quad \forall k \in \mathcal{K}. && \text{(4.31b)} \end{aligned}$$

Note that the problem (4.31) is the quadratically constrained quadratic programming (QCQP) problem. According to [62], when we assume that $\boldsymbol{M}_t = \boldsymbol{m}_t \boldsymbol{m}_t^H$ and $\boldsymbol{H}_{k,t} =$

$\boldsymbol{h}_{k,t}\boldsymbol{h}_{k,t}^{H}$ are satisfied, the problem (4.31) can be rewritten as

$$\min_{\boldsymbol{M}_t} \quad \mathrm{Tr}(\boldsymbol{M}_t) \tag{4.32a}$$

$$\text{s.t.} \quad \mathrm{Tr}(\boldsymbol{M}_t\boldsymbol{H}_{k,t}) \geq \frac{\beta_{k,t}D_k^2}{\Delta_{k,t}^{\max}}, \quad \forall k \in \mathcal{K}, \tag{4.32b}$$

$$\boldsymbol{M}_t \succeq \boldsymbol{0}, \tag{4.32c}$$

$$\mathrm{rank}\left(\boldsymbol{M}_t\right) = 1. \tag{4.32d}$$

The proof of Lemma 4.2 has been completed. □

One effective method to deal with the problem $\mathcal{P}_{4.2}$ is the SDR method, which obtains the convex relaxed problem by dropping the rank-one constraint. In this way, the problem $\mathcal{P}_{4.2}$ can be transformed to

$$\mathcal{P}_{4.3}: \min_{\boldsymbol{M}_t} \quad \mathrm{Tr}(\boldsymbol{M}_t) \tag{4.33a}$$

$$\text{s.t.} \quad \mathrm{Tr}(\boldsymbol{M}_t\boldsymbol{H}_{k,t}) \geq \frac{\beta_{k,t}D_k^2}{\Delta_{k,t}^{\max}}, \forall k \in \mathcal{K}, \tag{4.33b}$$

$$\boldsymbol{M}_t \succeq \boldsymbol{0}. \tag{4.33c}$$

Then, the approximate solution can be obtained by solving the convex problem $\mathcal{P}_{4.3}$ with CVX toolbox [100]. Assuming that $\boldsymbol{M}_t^*$ is the approximate optimal value of $\mathcal{P}_{4.3}$, then the eigenvalue decomposition for $\boldsymbol{M}_t^*$ is conducted as $\boldsymbol{M}_t^* = \boldsymbol{U}_t \sum \boldsymbol{U}_t^H$, where $\boldsymbol{U}_t = \left[\varrho_1, \varrho_2, ..., \varrho_N\right]$ is the matrix including the eigenvalue vectors and $\sum = diag(\rho_1, \rho_2, ..., \rho_N)$ is the diagonal matrix including the eigenvalue values. Let $\rho_{\max}$ be the maximum eigenvalue of $\boldsymbol{M}_t^*$ and $\varrho_{\max}$ be the corresponding eigenvector of $\boldsymbol{M}_t^*$. According to [62], if the constraint rank $\left(\boldsymbol{M}_t^*\right) = 1$ is satisfied, the optimal receive beamforming vector is $\boldsymbol{m}_t^* = \sqrt{\rho_{\max}}\varrho_{\max}$. If the constraint rank $\left(\boldsymbol{M}_t^*\right) = 1$ can not be satisfied for the relaxed problem, we adopt the Gaussian randomization [101] to get the candidate optimal values $\boldsymbol{m}_t^{[i]} = \boldsymbol{U}_t \sum^{1/2} \xi_t^{[i]}$, where $\xi_t^{[i]}$ is randomly generated from $\mathcal{CN}(0, \boldsymbol{I}_{N\times 1})$. We generate the total number of I candidates for the receive beamforming vector. Then, from the candidates $\boldsymbol{m}_t \in \left\{\boldsymbol{m}_t^{[1]}, \ldots, \boldsymbol{m}_t^{[I]}\right\}$, we get the optimal value $\boldsymbol{m}_t^*$

Algorithm 4.1 The SDR-based Receive Beamforming Algorithm

Require: $\boldsymbol{\beta}_t$, $\boldsymbol{h}_t$, $\boldsymbol{b}_t$, $\boldsymbol{c}_t$, $\boldsymbol{D}$, τ_{tr}, P_0, and I.
Ensure: $\boldsymbol{m}_t$.

Solve (4.33) to obtain $\boldsymbol{M}_t^*$.
if rank$(\boldsymbol{M}_t^*) = 1$ **then**
  $\boldsymbol{m}_t^* = \sqrt{\rho_{\max}}\varrho_{\max}$;
else
  Obtain the eigenvalue decomposition of $\boldsymbol{M}_t^* = \boldsymbol{U}_t \sum \boldsymbol{U}_t^H$;
  Generate the number of I random vectors, and the i-th vector is $\xi_t^{[i]} \in \mathcal{CN}(0, \boldsymbol{I}_{N\times 1})$;
  Obtain the candidate optimal values $\boldsymbol{m}_t^{[i]} = \boldsymbol{U}_t \sum^{1/2} \xi_t^{[i]}$;
  Obtain the optimal receive beamforming vector $\boldsymbol{m}_t^*$ according to (4.34).
end if
$\boldsymbol{m}_t = \boldsymbol{m}_t^*$.

which can get the minimum objective value according to

$$\boldsymbol{m}_t^* = \arg \min_{\boldsymbol{m}_t \in \left\{\boldsymbol{m}_t^{[1]},\dots,\boldsymbol{m}_t^{[I]}\right\}} \max_{k\in\mathcal{K}} \frac{\beta_{k,t} D_k^2 ||\boldsymbol{m}_t||^2}{\Delta_{k,t}^{\max} ||\boldsymbol{m}_t{}^H \boldsymbol{h}_{k,t}||^2}. \tag{4.34}$$

The process for designing the receive beamforming vector with SDR combined with the Gaussian randomization approach is summarized in Algorithm 4.1.

4.4.2 Client selection optimization

Given the optimized receive beamforming vector $\boldsymbol{m}_t$ obtained from Algorithm 4.1, to optimize the client selection decisions, the problem $\mathcal{P}_3$ can be simplified as

$$\mathcal{P}_5: \quad \min_{\boldsymbol{\beta}_t} \quad \phi_t\left(\boldsymbol{\beta}_t\right) \tag{4.35a}$$

$$\text{s.t.} \quad \beta_{k,t} \in \{0,1\}, \quad \forall k \in \mathcal{K}. \tag{4.35b}$$

Note that $\mathcal{P}_5$ is the NIP problem. There is an inverse correlation between the optimization objective value $\phi_t\left(\boldsymbol{\beta}_t\right)$ and the maximum constraint part $\max_{k\in\mathcal{K}}\left(\frac{\beta_{k,t} D_k^2}{\Delta_{k,t}^{\max}||\boldsymbol{m}_t^H \boldsymbol{h}_{k,t}||^2}\right)$.

Algorithm 4.2 The CED-based Client Selection Algorithm

Require: $\boldsymbol{m}_t$, $\boldsymbol{h}_t$, $\boldsymbol{b}_t$, $\boldsymbol{c}_t$, $\boldsymbol{D}$, σ^2, τ_{tr}, P_0, and D.
Ensure: $\boldsymbol{\beta}_t$.

```
for k = 1, ..., K do
    Calculate q_{k,t} based on (4.36);
end for
Sort Q_t in ascending order to obtain Q'_t;
Let q'_{k,t} be the k-th smallest value in Q'_t, and let S^{[k]} be the client subset decided by
    the k smallest values of Q'_t;
for k = 1, ..., K do;
    Calculate \tilde{φ}_{[t,k]} based on (4.37);
end for
Calculate k* = arg min_{k∈K} \tilde{φ}_{[t,k]};
for k = 1, ..., K do
    if q_{k,t} ≤ q_{k*,t} then
        Set β_{k,t} ← 1;
    else
        Set β_{k,t} ← 0.
    end if
end for
```

The CED coefficient for client k at the t-th training round is denoted as follows:

$$q_{k,t} = \frac{\beta_{k,t} D_k^2}{\Delta_{k,t}^{\max} ||\boldsymbol{m}_t^H \boldsymbol{h}_{k,t}||^2}, \tag{4.36}$$

which is decided by the channel coefficient $\boldsymbol{h}_{k,t}$, the transmission energy threshold $\Delta_{k,t}^{\max}$ and the dataset size D_k. Let $\boldsymbol{Q}_t = [q_{1,t}, q_{2,t}, \ldots, q_{K,t}]$ denote the list of CED coefficients. The maximum value of $\boldsymbol{Q}_t$ is calculated as $Q_t^{\max} = \max_{k \in \mathcal{K}} q_{k,t}$. One can observe that if the selected clients have worse channel quality, less available transmission energy, and larger data size, $Q_t^{\max}$ becomes larger.

By analyzing the problem $\mathcal{P}_5$, one can observe that there is a trade-off relationship between the total number of the selected training samples $\sum_{k \in \mathcal{K}} \beta_{k,t} D_k$ and $Q_t^{\max}$. If more clients are selected during the training process, the number of the training samples $\sum_{k \in \mathcal{K}} \beta_{k,t} D_k$ will be larger, which will make the global loss convergence speed be faster. However, if more clients are selected, $Q_t^{\max}$ will increase, which will lead to slow convergence. As a result, to improve the learning performance of the OTA FL

Algorithm 4.3 The Alternative Optimization Algorithm

Require: $\boldsymbol{h}_t, \boldsymbol{b}_t, \boldsymbol{c}_t, \boldsymbol{D}, \sigma^2, \tau_{\text{tr}}, P_0, D, I, J, j = 0$, and $\boldsymbol{\beta}_t\,(0)$.
Ensure: $\boldsymbol{\beta}_t, \boldsymbol{m}_t$.
1: **repeat**
2: Given $\boldsymbol{\beta}_t\,(j)$ and $(\boldsymbol{h}_t, \boldsymbol{b}_t, \boldsymbol{c}_t, \boldsymbol{D}, \tau_{\text{tr}}, P_0, I)$, obtain $\boldsymbol{m}_t\,(j+1)$ via Algorithm 4.1;
3: Given $\boldsymbol{m}_t\,(j+1)$ and $(\boldsymbol{h}_t, \boldsymbol{b}_t, \boldsymbol{c}_t, \boldsymbol{D}, \sigma^2, \tau_{\text{tr}}, P_0, D)$, obtain $\boldsymbol{\beta}_t\,(j+1)$ via Algorithm 4.2;
4: Update $\boldsymbol{m}_t = \boldsymbol{m}_t\,(j+1)$, $\boldsymbol{\beta}_t = \boldsymbol{\beta}_t\,(j+1)$, $j = j+1$;
5: **until** $j = J$.

system, an effective client selection scheme is required to minimize the problem $\mathcal{P}_4$.

The proposed discrete search method named the CED-based method for $\mathcal{P}_4$ is summarized in Algorithm 4.2. First, $\boldsymbol{Q}_t$ is sorted in ascending order to get the sorted queue $\boldsymbol{Q}'_t$. Let $q'_{k,t}$ be the k-th value in $\boldsymbol{Q}'_t$, and let $\mathcal{S}^{[k]}$ be the subset of the selected k clients according to the k smallest values of $\boldsymbol{Q}'_t$. There are K possible client selection decisions, and the final client selection is decided by

$$\tilde{\phi}_{[t,k]} = \frac{\sigma^2 \tau_{\text{tr}} ||\boldsymbol{m}_t||^2 q'_{k,t}}{2\left(\sum_{i\in\mathcal{S}^{[k]}} D_i\right)^2} + \frac{2\left(D - \sum_{i\in\mathcal{S}^{[k]}} D_i\right)^2}{D^2}. \tag{4.37}$$

The indicator k^* can be obtained by calculating the index of the minimum value of $\tilde{\phi}_{[t,k]}$ as

$$k^* = \arg\min_{k\in\mathcal{K}} \tilde{\phi}_{[t,k]}. \tag{4.38}$$

The client can be selected if the index k is smaller than k^* for the sorted queue $\boldsymbol{Q}'_t$, which denotes $q_{k,t} \leq q_{k^*,t}$.

4.4.3 The alternative optimization for client selection and receive beamforming

The proposed alternative optimization method to minimize the optimality gap of the OTA FL system is summarized in Algorithm 4.3. At the beginning of the t-th training round, all clients can be selected at the initial setup as $\boldsymbol{\beta}_t\,(0) = [1, 1, ..., 1]$. Then, the receive beamforming is optimized with the SDR method according to Algorithm 4.1.

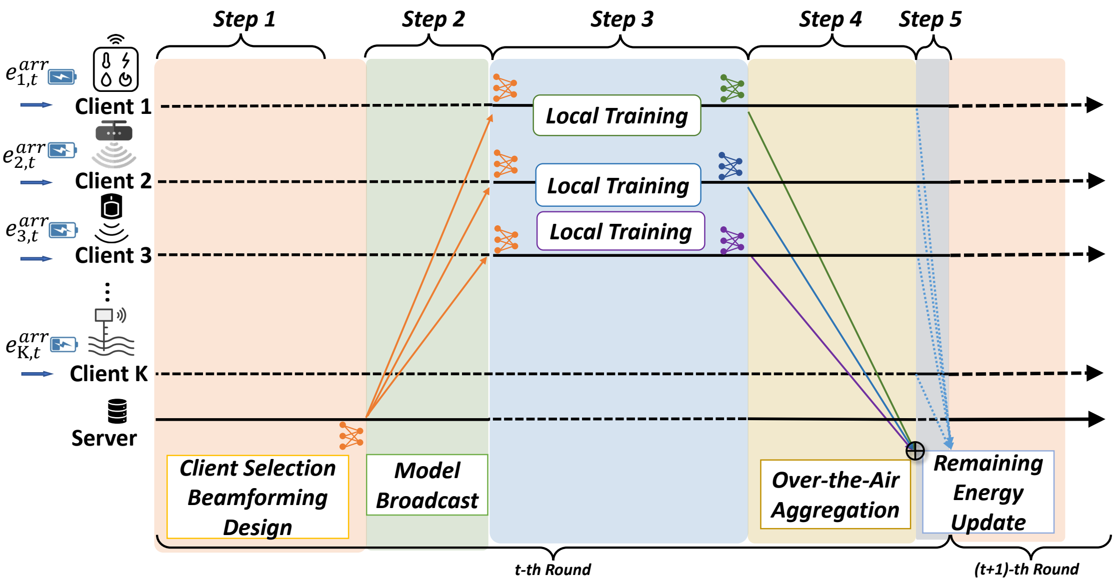

Figure 4.3: The procedures of the OTA FL system.

When the optimized receive beamforming vector $\boldsymbol{m}_t$ is obtained, the selected clients can be obtained based on Algorithm 4.2. These two steps are repeated for J times. When the joint optimization process is completed, the PS sends the global model to the selected clients. Then, local clients update the global model and upload the gradients via OTA computation. The PS obtains the aggregated gradients based on (4.3). Clients obtain the energy from the energy resources and update the current battery level queue based on (4.12).

The computational complexity of Algorithm 4.1 for designing the receive beamforming is mainly decided by the procedure of obtaining $\boldsymbol{M}_t^*$ with SDR algorithm (see Line 1 in Algorithm 4.1), which is $O\left((N^2+K)^{3.5}\right)$ [102]. The computational complexity of Algorithm 4.2 for optimizing client selection is mainly determined by the sorting process (see Line 3 in Algorithm 4.2), which takes $O(K\log K)$ operations. In addition, as Algorithm 4.3 is conducted T rounds during the training procedure and the alternative optimization is conducted for J iterations, the overall time complexity is given by $O\left(TJ((N^2+K)^{3.5}+(K\log K))\right)$.

Figure 4.2 is given to clearly illustrate the relations of the problems of the whole OTA FL system with energy harvesting. First of all, the problem $\mathcal{P}_2$ is formulated according to Theorem 4.1 to minimize the optimality gap after T training rounds for

OTA FL. Then, the intractable offline MINLP problem $\mathcal{P}_2$ is transformed to the online MINLP problem $\mathcal{P}_3$ to minimize the optimality gap at the t-th training round based on (4.26) and Lemma 4.1. To solve the problem $\mathcal{P}_3$, the MINLP problem is decoupled into two sub-problems as $\mathcal{P}_{4.1}$ for receive beamforming design and $\mathcal{P}_5$ for client selection. The SDR programming is used for optimizing receive beamforming sub-problem. Specifically, the problem $\mathcal{P}_{4.1}$ can be transformed to $\mathcal{P}_{4.2}$ via matrix lifting according to Lemma 4.2. Then, the non-convex problem $\mathcal{P}_{4.2}$ is relaxed to the convex problem $\mathcal{P}_{4.3}$ via dropping rank-one constraint. Then, the convex problem $\mathcal{P}_{4.3}$ can be solved via the CVX toolbox. For the client selection sub-problem, the discrete search method combined with the CED coefficient is proposed to deal with the NIP problem $\mathcal{P}_5$.

Figure 4.3 is given to clearly illustrate the procedures of the whole OTA FL system with energy harvesting at the t-th training round, which includes the following constraints:

1) In the proposed joint optimization method for the OTA FL system, the PS optimizes the client selection vector $\mathcal{K}_t$ and receive beamforming design $\boldsymbol{m}_t$.

2) The PS broadcasts the global model to the selected clients $\mathcal{K}_t$.

3) The selected clients $\mathcal{K}_t$ conduct the local training using their respective local datasets.

4) The local clients send the local gradients to PS via OTA computation.

5) The clients update their remaining energy levels by considering both energy consumption and energy harvesting.

These procedures will continue for a total of T training rounds.

4.5 Performance evaluation

In the simulation, the PS is located at $(0, 0, 10)$, and 40 clients are randomly located within the range of a circle with a radius of 250 meters. Let $\bar{h}_k = G_P G_C \left(\frac{3\times10^8}{4\pi f_c L_k}\right)^{\rho}$ denote the average channel gain for the free-space path loss model, where $G_P = 5$ dBi denotes the antenna gain of the PS, $G_C = 0$ dBi denotes the antenna gain of the local clients, $f_c = 915$ MHz means the carrier frequency, L_k means the distance between PS and client

k, and the pass loss exponent ρ is set as 3. The channel gain $\boldsymbol{h}_{k,t}$ for client k during the t-th training round is expressed as $\boldsymbol{h}_{k,t} = \sqrt{\bar{h}_k}\boldsymbol{\gamma}_{k,t}$, where $\boldsymbol{\gamma}_{k,t}$ is generated from the Gaussian distribution with zero-mean and unit-variance. The transmission slot for each resource block T_{slot} is set as 1 ms, and the number of the transmitted signals R is set as 14 [98]. Let $\bar{e}_k$ denote the average amount of harvested energy per round for client k, and the harvested energy for client k during the t-th training round is $e_{k,t}^{\text{arr}}$. The harvested energy for client k during the training processes is $[e_{k,1}^{\text{arr}}, e_{k,2}^{\text{arr}}, \ldots, e_{k,T}^{\text{arr}}]$, which follows a Poisson distribution with an average of $\bar{e}_k$ [103]. We assume that $\bar{e}_k$ is uniformly distributed between 0.1 J and 1 J for different clients. The computation energy consumption per sample $e_{k,t,i}$ is set as a constant value of 0.001 J for all clients, which is consistent with the information provided in Chapter 3. The maximum battery capacity B^{max} is set as 20 J, and the maximum transmission power P_0 is set as -10 dB. The total number of candidates I for receive beamforming vector is set as 5 in Algorithm 4.2. The iteration number J for the alternative optimization method is set as 20.

We use the Fashion-MNIST dataset [93] to conduct the experiments. Two kinds of settings regarding the data distribution among clients are taken into consideration according to [94]: balanced and unbalanced data settings. For both settings, the training samples at local clients are independent and identically distributed. For the balanced data setting, the number of samples is equal to 800 for all clients. For the unbalanced data setting, the sample size is set randomly in [100, 200] for half of the clients, and [1000, 2000] for the other half. By analyzing ϕ_t in (4.18), one can observe that the convergence rate of the optimality gap is influenced by the number of selected clients for the balanced data setting. However, for the unbalanced data setting, the convergence rate of the optimality gap is influenced not only by the number of selected clients but also by the data size of selected clients. We use two kinds of data settings to illustrate that by introducing the data size D_k of client k in our formulations, the proposed scheme can be applied to different data size distributions. The CNN model is adopted for training, which has the same structure as in Chapter 3. The total number of the model parameters is 21840, and the total number of training rounds is set as 1500. The learning rate η is set as 0.01 by default.

4.5.1 Comparison scheme

We compare the proposed solution CED+SDR with the following comparison methods:

- Perfect: all clients are selected in each training round and assuming that the perfect aggregation can be achieved with the error-free transmission.
- DC [6]: the client selection and receive beamforming is optimized with the two-step DC method, and the threshold of the mean squared error is set as 15 dB.
- CED only: clients are selected with the proposed CED method without beamforming optimization for each training round.
- SDR only: for the client selection sub-problem, the local clients with sufficient energy can be selected, which is similar to [19, 20]. Besides, the receive beamforming is optimized with the proposed SDR method.

Figure 4.4(a) and Figure 4.4(b) demonstrate the performance of the training loss and test accuracy of the proposed method with other baselines for the OTA FL system under the balanced data setting. The number of antennas for PS is set as 10 and the noise power is set as -70 dB. We omit the training loss of the DC method and SDR only method since they are too large compared with the other three methods. The training loss of the other three methods is depicted in Figure 4.4(a). It is observed that the proposed CED+SDR method performs better compared with the DC method and SDR only method from Figure 4.4(b). Besides, one can observe that the training loss of the proposed CED+SDR method decreases faster compared with the CED only method from Figure 4.4(a) even though the accuracy of these two methods is close in Figure 4.4(b). The DC method cannot converge as it only takes transmission power control into account and ignores the energy constraint of local clients for the OTA FL system. The SDR only method performs worst as the selected clients with SDR only method may have poor channels or inadequate energy. The performance of the CED only method performs better compared with the SDR only method, indicating that the client selection has a larger impact on the learning performance of OTA FL than the receive beamforming optimization.

Figure 4.5(a) and Figure 4.5(b) demonstrate the learning performance of the proposed method with other baselines for the OTA FL system under the unbalanced

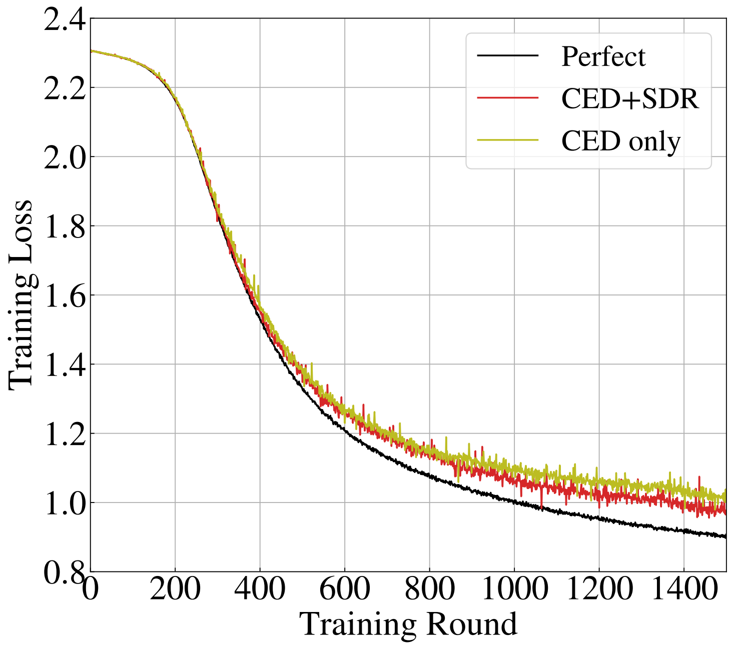

(a) Training Loss

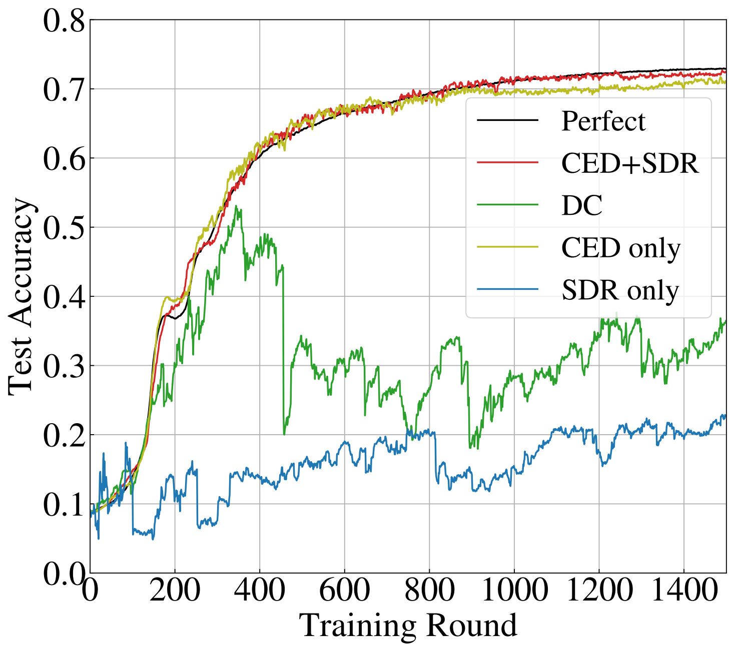

(b) Test Accuracy

Figure 4.4: The learning performance under the balanced data setting.

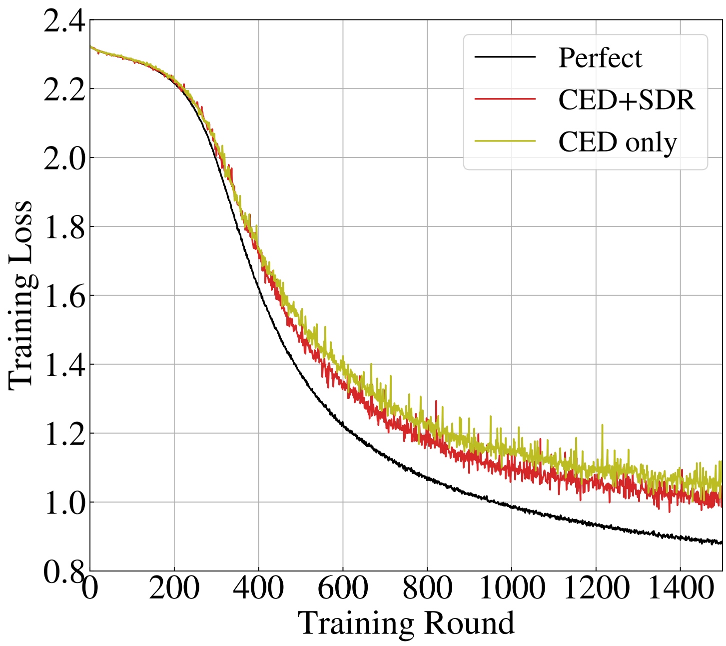

(a) Training Loss

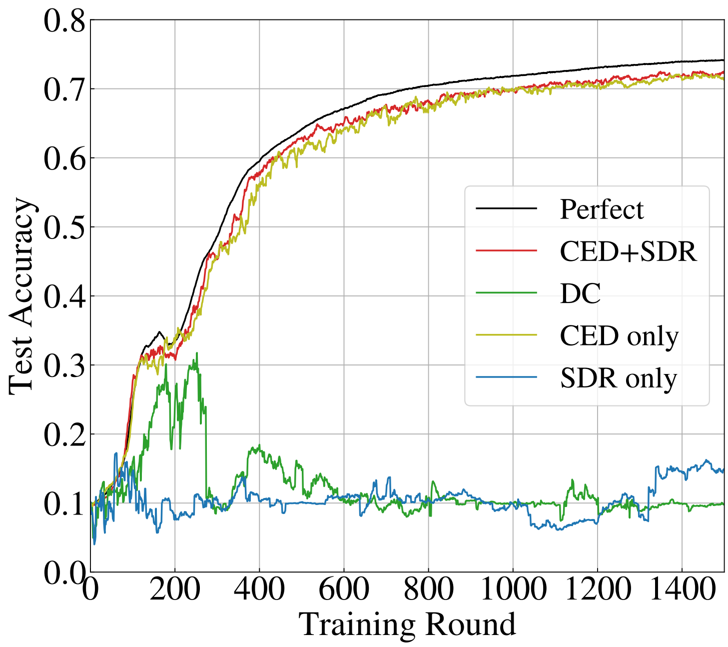

(b) Test Accuracy

Figure 4.5: The learning performance under the unbalanced data setting.

data setting, which has a similar trend to the balanced data setting. From Figure 4.4 and Figure 4.5, we can get the conclusion that the proposed scheme can be applied to different data size distributions.

4.5.2 Parameter analysis

In this subsection, the impacts of the noise power, the number of antennas at the PS side, and the average arrival rate of the harvested energy on the learning performance of the proposed CED+SDR method are discussed for the OTA FL system. We show the experimental results of the proposed method under the unbalanced data setting as examples since the results of the proposed method under the balanced data setting have similar trends to those under the unbalanced data setting.

In Figure 4.6(a) and Figure 4.6(b), different noise power settings are investigated for the proposed CED+SDR method under the unbalanced data setting for the OTA FL system. The PS is equipped with a total of 10 antennas. We can see that accuracy of the OTA FL system decreases when noise power increases for the proposed CED+SDR method under the unbalanced data setting. The reason is that the introduced noise makes the gradients deviate from the actual values in each training round for the OTA FL system. When the noise power is set too large such as -50 dB, the SNR is too low to make the OTA FL system converge. When the noise is set as -80 dB, the proposed CED+SDR method has a similar performance to the Perfect method.

In Figure 4.7(a) and Figure 4.7(b), the impacts of the number of antennas at the PS side are shown for the proposed CED+SDR method under the unbalanced data setting for the OTA FL system. The noise power is set as -60 dB for easily observing the impacts of the number of antennas at the PS side on the learning performance of the OTA FL system. We can see that the proposed CED+SDR method can converge even when the number of antennas at the PS side is set as 1. And with the number of antennas at the PS side increasing, the proposed method performs better, which indicates that the proposed SDR method is effective for the receive beamforming optimization of the OTA FL system.

To show the influence of the average arrival rate of the harvested energy $\bar{e}_k$ on the learning performance of the proposed CED+SDR method conveniently, we set $\bar{e}_k$ as the same value for all clients for the OTA FL system. Besides, the number of antennas

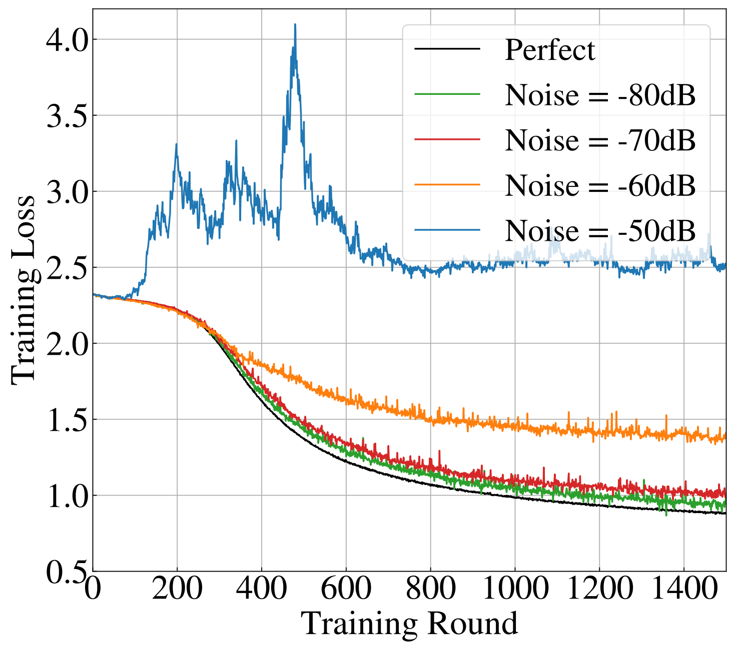

(a) Training Loss

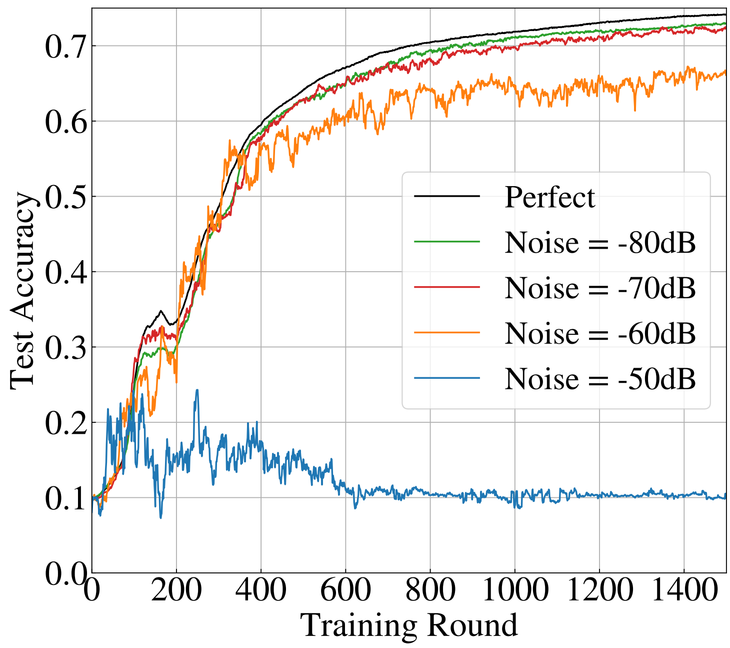

(b) Test Accuracy

Figure 4.6: The impacts of noise power on the learning performance under the unbalanced data setting.

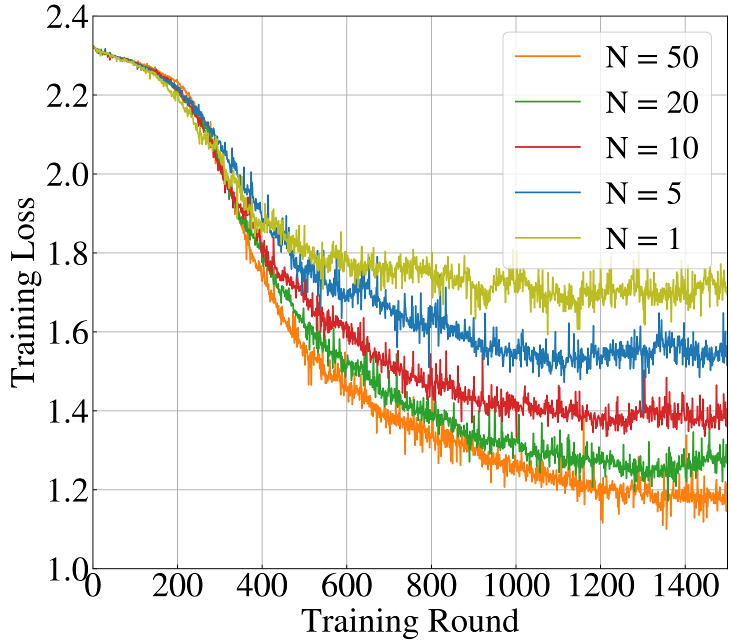

(a) Training Loss

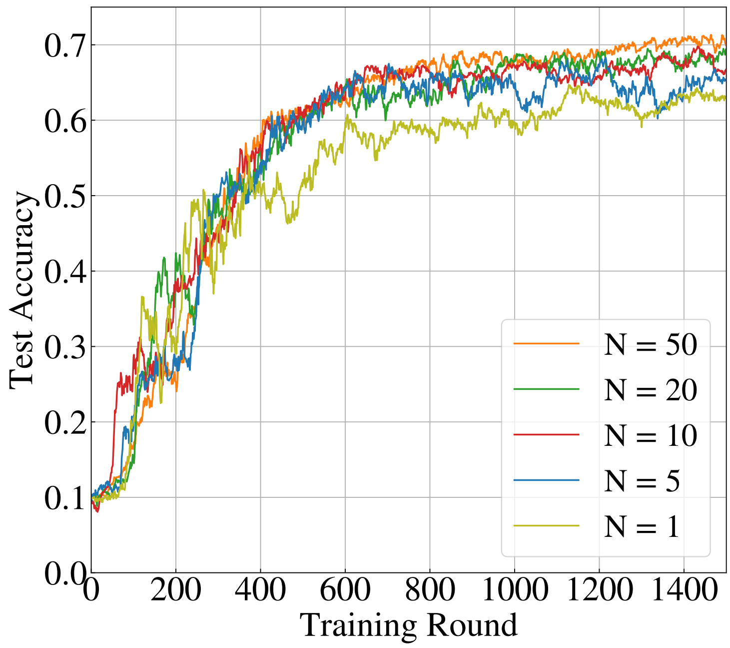

(b) Test Accuracy

Figure 4.7: The impacts of the number of antennas at the PS side on the learning performance under the unbalanced data setting.

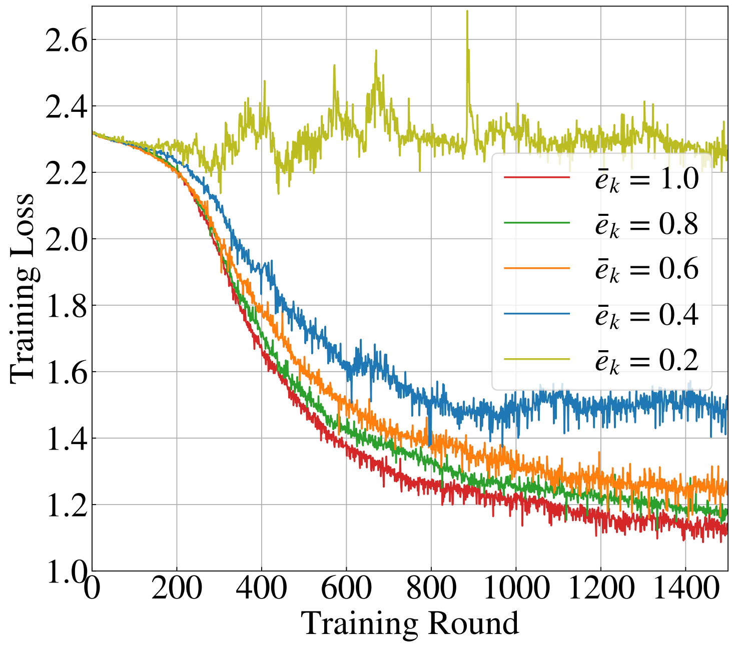

(a) Training Loss

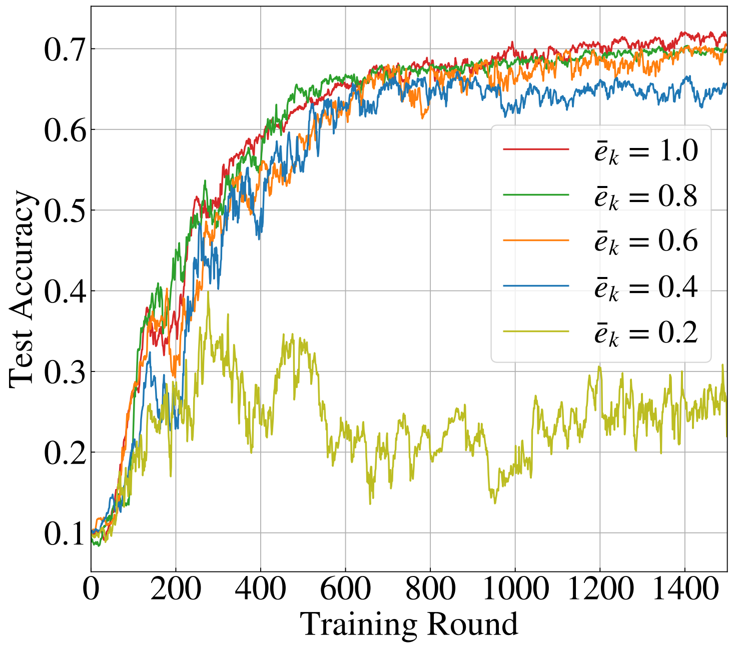

(b) Test Accuracy

Figure 4.8: The impacts of the average arrival rate of energy on the learning performance under the unbalanced data setting.

at the PS side is set as 10 and the noise power is set as −60 dB. Figure 4.8(a) and Figure 4.8(b) show the training loss and the test accuracy of the proposed CED+SDR method with different average arrival rate settings for energy harvesting. We can see that the accuracy increases when the average arrival rate of the harvested energy $\bar{e}_k$ increases for the OTA FL system under the unbalanced data setting. It is observed that when the average arrival rate of the harvested energy $\bar{e}_k$ is set too small such as 0.2, the proposed method cannot converge as the SNR is too low caused by the transmission energy constraint. However, if the average arrival rate of energy $\bar{e}_k$ is too large, the learning performance cannot continue to improve as the transmission energy of local clients is limited not only by the current battery capacity but also by the maximum transmission power.

4.5.3 Mini-batch gradient descent

In this subsection, the mini-batch gradient descent is considered rather than the batch gradient descent for the OTA FL system. When mini-batch gradient descent is adopted for local model update and the batch size is set as BS, the total data samples at client k are divided into $\lceil \frac{D_k}{BS} \rceil$ batches. Let $BS(1), BS(2)..., BS(\lceil \frac{D_k}{BS} \rceil)$ denote the sample data of batch $1, 2, ..., \lceil \frac{D_k}{BS} \rceil$. The client k conducts the gradient update as

$$\begin{aligned} \boldsymbol{w}_{t+1}^{BS(1)} &= \boldsymbol{w}_t - \eta \bar{\boldsymbol{r}}_t, \\ \boldsymbol{w}_{t+1}^{BS(2)} &= \boldsymbol{w}_{t+1}^{BS(1)} - \eta \bar{\boldsymbol{r}}_t, \\ &\cdots\cdots \\ \boldsymbol{w}_{t+1}^{BS(\lceil \frac{D_k}{BS} \rceil)} &= \boldsymbol{w}_{t+1}^{BS(\lceil \frac{D_k}{BS} \rceil - 1)} - \eta \bar{\boldsymbol{r}}_t. \end{aligned} \tag{4.39}$$

When the above process is finished, the local gradient vector is the final gradient vector of the final batch. When the local epoch is still set as 1, the other procedures are the same as with the full-size gradient descent process.

Figure 4.9(a) and Figure 4.9(b) show the test accuracy with different batch sizes for the OTA FL system under the balanced data setting when the noise power is set as −70 dB and −80 dB, respectively. By observing Figure 4.9(a), it is clear to see that when the batch size decreases from All to 256, the test accuracy of the OTA FL system increase. However, when the batch size continuously decreases from 256 to 128 or 64, the test

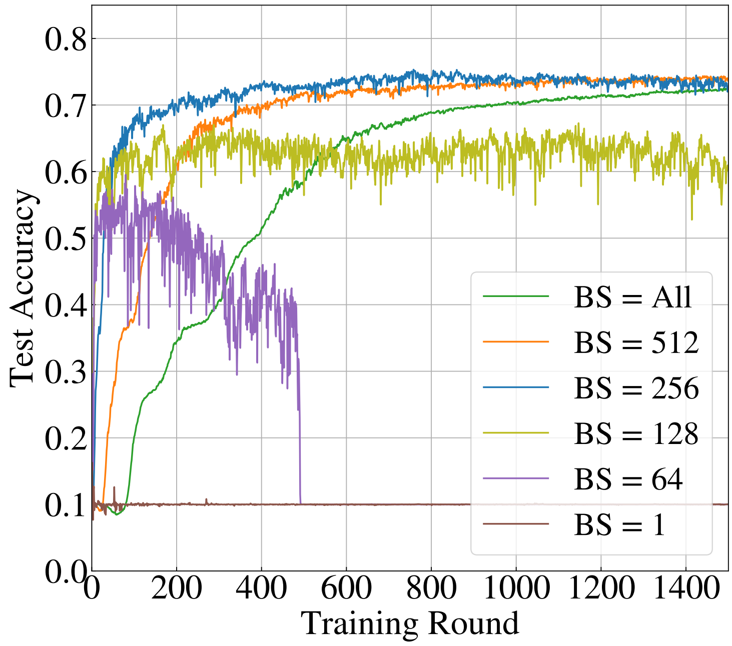

(a) Noise power = −70 dB

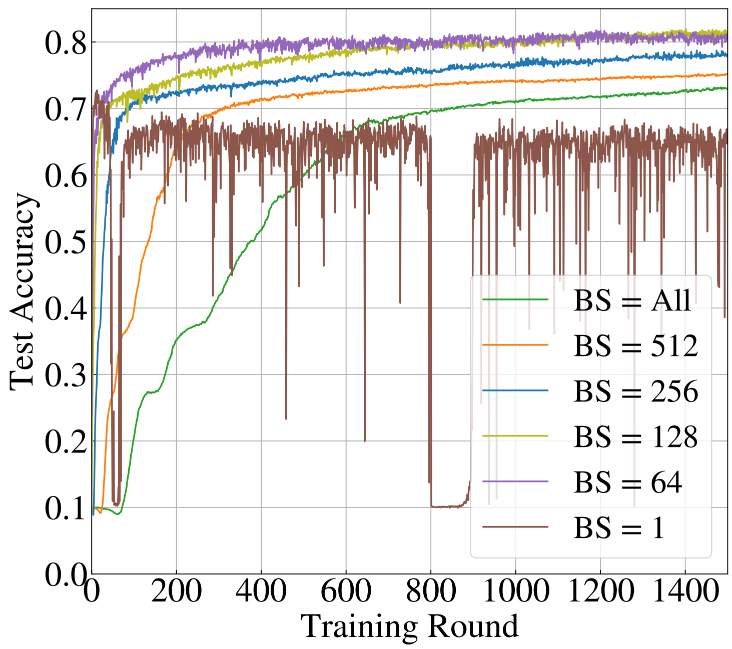

(b) Noise power = −80 dB

Figure 4.9: The test accuracy with mini-batch gradient descent for balanced data.

accuracy will decrease gradually. The OTA FL system even can not converge when the batch size is set as too small such as 64 or 1, and the reason for that is the small batch size may have a larger gradient norm, and the larger gradient norm will make the α_t in formula (4.20) smaller, which will cause the introduced error larger. As a result, the aggregated gradients will deviate from the true values, and the OTA FL system cannot converge.

Figure 4.9(b) has a similar trend compared with Figure 4.9(a). Besides, by comparing Figure 4.9(a) and Figure 4.9(b), it can be seen that when the noise power decrease from −70 dB to −80 dB, the OTA FL system performs better, and the best batch size setting is set as 128 rather than 256 in Figure 4.9(a). Therefore, to get better system performance for the OTA FL system, the batch size is required to be adjusted according to the experimental settings.

4.6 Summary

In this chapter, we focus on the OTA FL system operating in the SIMO setting. We analyze the convergence of the OTA FL system considering energy harvesting, client selection, receive beamforming, and transmission power control. Based on this analysis, we formulate a problem to minimize the optimality gap of the training loss. The goal is to optimize both client selection and receive beamforming design while adhering to energy constraints and transmission power control. To address this problem, we propose a joint optimization method that operates in an online mode. This method combines the CED-based approach for client selection and the SDR-based method for receive beamforming design. By integrating these techniques, our proposed joint optimization method effectively addresses the formulated MINLP problem. It enables us to minimize the optimality gap in the OTA FL system while considering client selection, receive beamforming, energy constraints, and transmission power control.

5
Conclusion

5.1 Concluding remarks

The energy management problem is one of the key issues for the OTA FL system with energy harvesting clients. In this thesis, we have focused on the analysis and optimization for OTA FL with energy harvesting clients while considering the energy constraint and weak channels. We mainly have two objectives in this thesis:

- Objective 1: the analysis and optimization for the OTA FL system with energy harvesting clients under the SISO network setting.

- Objective 2: the analysis and optimization for the OTA FL with energy harvesting clients under the SIMO network setting.

For objective 1, we conducted the convergence analysis of the optimality gap with regard to client selection, the energy constraint, and the noise error channel for the OTA FL system under the SISO network setting. Based on the convergence analysis results, we formulated the online optimization problem to minimize the optimality gap when jointly considering client selection and energy harvesting. The CED-based method is proposed to optimize client selection. The experiments show that our proposed method surpasses the other benchmarks.

For objective 2, we employed the energy harvesting techniques for OTA FL under the SIMO network setting and derived the convergence analysis of the optimality gap regarding client selection, receive beamforming, energy constraint, and transmission power control. Based on the convergence analysis results, we formulated the online MINLP optimization problem to minimize the optimality gap when jointly considering client selection and receive beamforming design. The alternative optimization is developed to solve the MINLP problem. The CED-based method is proposed to optimize client selection decisions, and the receive beamforming is optimized with the SDR method. The simulation results show that our proposed method performs better compared with the other benchmarks.

5.2 Limitations

Despite dedicating a considerable amount of effort to our study, there are still some limitations in our current research.

First, to achieve OTA computation with wireless fading channels, the local client needs to adjust its transmission power based on the current channel state before transmission. The requirement of power scaling relies on having perfect channel state information at the local client. The convergence analysis with imperfect channels is given for the OTA FL system with energy harvesting in Chapter 3, and the convergence analysis results reveal that the OTA FL system still can converge with imperfect channel state information. Nevertheless, if neither the channel state information nor the channel statistics are accessible, the current proposed method cannot be effectively applied to the OTA FL system. The implementation of OTA FL in scenarios where channel state information is unavailable for local clients is regarded as a potential area for future research.

In addition, the successful implementation of OTA computation for FL in our current study hinges on the requirement of precise synchronization among the local clients. It is essential for each client to meticulously adjust their transmission timing to achieve perfect alignment of their signals at the PS. However, achieving such stringent synchronization across multiple clients proves to be immensely challenging and costly in practical scenarios, often leading to residual asynchronies among the signals received from different clients. In future, we intend to address the issue of time misalignments among local clients in the OTA FL system.

5.3 Future directions

The proposed OTA FL system, which incorporates energy harvesting clients, is particularly well-suited for distributed classification or monitoring applications such as wildlife classification [104, 105] or forest fire monitoring [106]. These scenarios often involve remote locations where it is inconvenient to recharge wireless devices, and where ample solar or wind energy resources are available. However, the current communication model for the OTA FL system does not consider the transmission with obstacles and security issues.

OTA FL systems with energy harvesting clients can be further enhanced by introducing privacy-preserving techniques and reconfigurable intelligent surface (RIS). By designing different privacy-preserving techniques in the OTA computation system, more secure OTA computation could be realized. Additionally, the integration of RIS technology will assist in overcoming obstacles and improving the overall performance of the OTA FL system. The subsequent subsections provide a detailed discussion on privacy-preserving OTA and RIS-assisted OTA FL, highlighting the potential benefits and implications of incorporating these advancements into the system.

5.3.1 Toward more secure and privacy-protective OTA computation

The OTA transmission mode utilizes intra-cell interference to protect privacy by hiding individual data within superimposed signals, making it challenging for eavesdroppers to extract specific device information. However, concerns remain about potential leakage of functional computation results. In [107], the authors propose incorporating a jammer into the OTA computation system, which cancels the jamming signal at the intended receiver while appearing as undetectable noise to eavesdroppers. This approach employs coding techniques and channel resolvability to enhance security. Besides, in [108], transceiver designs are also suggested to minimize computation errors at the fusion center while maintaining a certain error threshold for eavesdroppers. These studies motivate further exploration of practical implementation and optimization for various network architectures. Furthermore, the presence of adversarial devices introduces the risk of transmitting irrelevant signals, compromising the receiver's computation. Therefore, designing an attack-resilient OTA FL system is crucial to ensure secure and reliable services even in the presence of adversarial devices.

5.3.2 RIS-assisted OTA FL

RIS has emerged as a promising technology to enable next-generation wireless networks, which has the potential to significantly reduce energy consumption and improve the spectral efficiency of wireless networks. Recently, some studies [81, 82, 94] have been published related to RIS-assisted OTA FL. In [81], the authors consider the heterogenous networks with the simultaneous transmission of NOMA signals and OTA FL signals under the assistance of the RIS. The authors in [82] focus on the challenges of model aggregation and client selection in FL systems that utilize multiple RISs. They propose a joint optimization approach that considers the transmission power, receive scalar, phase shifts, and selection of learning participants to minimize the aggregation error and accelerate the convergence rate of OTA FL. The work in [94] aims to improve the convergence rate of the RIS-enabled OTA FL system by jointly optimizing the client selection, receive beamforming, and the RIS phase shifts of the OTA FL system. However, in prior studies, few works have focused on energy management optimization schemes in RIS-assisted OTA FL systems. Given the impact of RIS on communication energy consumption, optimizing energy management in RIS-assisted OTA FL system is necessary. Therefore, the RIS-assisted OTA FL under the energy constraint can be considered as a future direction.

Bibliography

[1] Brendan McMahan, Eider Moore, Daniel Ramage, Seth Hampson, and Blaise Aguera y Arcas. Communication-efficient learning of deep networks from decentralized data. In *Proc. AISTATS*, Apr. 2017.

[2] Howard H Yang, Zuozhu Liu, Tony QS Quek, and H Vincent Poor. Scheduling policies for federated learning in wireless networks. *IEEE transactions on communications*, 68(1):317–333, 2019.

[3] Mingzhe Chen, Zhaohui Yang, Walid Saad, Changchuan Yin, H Vincent Poor, and Shuguang Cui. A joint learning and communications framework for federated learning over wireless networks. *IEEE Trans. Wireless Commun.*, 20(1):269–283, 2020.

[4] Junqian Kuang, Miao Yang, Hongbin Zhu, and Hua Qian. Client selection with bandwidth allocation in federated learning. In *2021 IEEE Global Communications Conference (GLOBECOM)*, pages 01–06. IEEE, 2021.

[5] Shuhao Xia, Jingyang Zhu, Yuhan Yang, Yong Zhou, Yuanming Shi, and Wei Chen. Fast convergence algorithm for analog federated learning. In *Proc. IEEE ICC*, Jun. 2021.

[6] Kai Yang, Tao Jiang, Yuanming Shi, and Zhi Ding. Federated learning via over-the-air computation. *IEEE Tran. Wireless Commun.*, 19(3):2022–2035, 2020.

[7] Dongzhu Liu and Osvaldo Simeone. Privacy for free: Wireless federated learning via uncoded transmission with adaptive power control. *IEEE Journal on Selected Areas in Communications*, 39(1):170–185, 2020.

[8] Mohammad Ali Sedaghat, Ali Bereyhi, Saba Asaad, and Ralf R Mueller. How to coordinate edge devices for over-the-air federated learning? *arXiv preprint arXiv:2211.03449*, 2022.

[9] Liqun Su and Vincent KN Lau. Data and channel-adaptive sensor scheduling for federated edge learning via over-the-air gradient aggregation. *IEEE Internet of Things Journal*, 9(3):1640–1654, 2021.

[10] Xin Fan, Yue Wang, Yan Huo, and Zhi Tian. Joint optimization of communications and federated learning over the air. *IEEE Trans. Wireless Commun.*, pages 1–1, 2021.

[11] Xiaowen Cao, Guangxu Zhu, Jie Xu, Zhiqin Wang, and Shuguang Cui. Optimized power control design for over-the-air federated edge learning. *IEEE J. Sel. Areas Commun.*, 40(1):342–358, 2021.

[12] Tomer Sery, Nir Shlezinger, Kobi Cohen, and Yonina C Eldar. Over-the-air federated learning from heterogeneous data. *IEEE Trans. Signal Process.*, 69:3796–3811, 2021.

[13] Yuxuan Sun, Sheng Zhou, Zhisheng Niu, and Deniz Gündüz. Dynamic scheduling for over-the-air federated edge learning with energy constraints. *IEEE J. Sel. Areas Commun.*, 40(1):227–242, 2021.

[14] Sennur Ulukus, Aylin Yener, Elza Erkip, Osvaldo Simeone, Michele Zorzi, Pulkit Grover, and Kaibin Huang. Energy harvesting wireless communications: A review of recent advances. *IEEE J. Sel. Areas Commun.*, 33(3):360–381, 2015.

[15] Chengrun Qiu, Yang Hu, Yan Chen, and Bing Zeng. Lyapunov optimization for energy harvesting wireless sensor communications. *IEEE Internet Things J.*, 5(3):1947–1956, 2018.

[16] Yuyi Mao, Jun Zhang, and Khaled B Letaief. Dynamic computation offloading for mobile-edge computing with energy harvesting devices. *IEEE J. Sel. Areas Commun.*, 34(12):3590–3605, 2016.

[17] Fengjun Zhao, Ying Chen, Yongchao Zhang, Zhiyong Liu, and Xin Chen. Dynamic offloading and resource scheduling for mobile-edge computing with energy harvesting devices. *IEEE Trans. Netw. Service Manag.*, 18(2):2154–2165, 2021.

[18] Rami Hamdi, Mingzhe Chen, Ahmed Ben Said, Marwa Qaraqe, and H Vincent Poor. Federated learning over energy harvesting wireless networks. *IEEE Internet Things J.*, 9(1):92–103, 2021.

[19] Başak Güler and Aylin Yener. Energy-harvesting distributed machine learning. In *Proc. IEEE ISIT*, Jul. 2021.

[20] Ozan Aygün, Mohammad Kazemi, Deniz Gündüz, and Tolga M Duman. Over-the-air federated learning with energy harvesting devices. In *Proc. IEEE GLOBECOM*, pages 1942–1947, 2022.

[21] David W Cheung, Jiawei Han, Vincent T Ng, Ada W Fu, and Yongjian Fu. A fast distributed algorithm for mining association rules. In *Fourth International Conference on Parallel and Distributed Information Systems*, pages 31–42. IEEE, 1996.

[22] Hwanjo Yu, Xiaoqian Jiang, and Jaideep Vaidya. Privacy-preserving svm using nonlinear kernels on horizontally partitioned data. In *Proceedings of the 2006 ACM symposium on Applied computing*, pages 603–610, 2006.

[23] Shuang Wang, Xiaoqian Jiang, Yuan Wu, Lijuan Cui, Samuel Cheng, and Lucila Ohno-Machado. Expectation propagation logistic regression (explorer): distributed privacy-preserving online model learning. *Journal of biomedical informatics*, 46(3):480–496, 2013.

[24] Yang Liu, Tao Fan, Tianjian Chen, Qian Xu, and Qiang Yang. Fate: An industrial grade platform for collaborative learning with data protection. *The Journal of Machine Learning Research*, 22(1):10320–10325, 2021.

[25] Ieee guide for architectural framework and application of federated machine learning. *IEEE Std 3652.1-2020*, pages 1–69, 2021.

[26] Jie Xu, Benjamin S Glicksberg, Chang Su, Peter Walker, Jiang Bian, and Fei Wang. Federated learning for healthcare informatics. *Journal of Healthcare Informatics Research*, 5:1–19, 2021.

[27] Shiva Raj Pokhrel and Jinho Choi. A decentralized federated learning approach for connected autonomous vehicles. In *2020 IEEE Wireless Communications and Networking Conference Workshops (WCNCW)*, pages 1–6. IEEE, 2020.

[28] Guodong Long, Yue Tan, Jing Jiang, and Chengqi Zhang. Federated learning for open banking. In *Federated Learning: Privacy and Incentive*, pages 240–254. Springer, 2020.

[29] Ji Chu Jiang, Burak Kantarci, Sema Oktug, and Tolga Soyata. Federated learning in smart city sensing: Challenges and opportunities. *Sensors*, 20(21):6230, 2020.

[30] Wei Yang Bryan Lim, Nguyen Cong Luong, Dinh Thai Hoang, Yutao Jiao, Ying-Chang Liang, Qiang Yang, Dusit Niyato, and Chunyan Miao. Federated learning in mobile edge networks: A comprehensive survey. *IEEE Communications Surveys & Tutorials*, 22(3):2031–2063, 2020.

[31] Latif U Khan, Walid Saad, Zhu Han, Ekram Hossain, and Choong Seon Hong. Federated learning for internet of things: Recent advances, taxonomy, and open challenges. *IEEE Communications Surveys & Tutorials*, 23(3):1759–1799, 2021.

[32] WANG Luping, WANG Wei, and LI Bo. Cmfl: Mitigating communication overhead for federated learning. In *2019 IEEE 39th international conference on distributed computing systems (ICDCS)*, pages 954–964. IEEE, 2019.

[33] Zhida Jiang, Yang Xu, Hongli Xu, Zhiyuan Wang, Chunming Qiao, and Yangming Zhao. Fedmp: Federated learning through adaptive model pruning in heterogeneous edge computing. In *2022 IEEE 38th International Conference on Data Engineering (ICDE)*, pages 767–779. IEEE, 2022.

[34] Tian Li, Anit Kumar Sahu, Manzil Zaheer, Maziar Sanjabi, Ameet Talwalkar, and Virginia Smith. Federated optimization in heterogeneous networks. *Proceedings of Machine learning and systems*, 2:429–450, 2020.

[35] Qianpiao Ma, Yang Xu, Hongli Xu, Zhida Jiang, Liusheng Huang, and He Huang. Fedsa: A semi-asynchronous federated learning mechanism in heterogeneous edge computing. *IEEE Journal on Selected Areas in Communications*, 39(12):3654–3672, 2021.

[36] Dong Wang, Baoqian Wang, Jinran Zhang, Kejie Lu, Junfei Xie, Yan Wan, and Shengli Fu. Cfl-hc: A coded federated learning framework for heterogeneous computing scenarios. In *2021 IEEE Global Communications Conference (GLOBECOM)*, pages 1–6. IEEE, 2021.

[37] Jianyu Wang, Qinghua Liu, Hao Liang, Gauri Joshi, and H Vincent Poor. Tackling the objective inconsistency problem in heterogeneous federated optimization. *Advances in neural information processing systems*, 33:7611–7623, 2020.

[38] Ilqar Ramazanli, Han Nguyen, Hai Pham, Sashank J Reddi, and Barnabas Poczos. Adaptive sampling distributed stochastic variance reduced gradient for heterogeneous distributed datasets. *arXiv preprint arXiv:2002.08528*, 2020.

[39] Jie Xu and Heqiang Wang. Client selection and bandwidth allocation in wireless federated learning networks: A long-term perspective. *IEEE Transactions on Wireless Communications*, 20(2):1188–1200, 2020.

[40] Ahmed Imteaj, Urmish Thakker, Shiqiang Wang, Jian Li, and M Hadi Amini. A survey on federated learning for resource-constrained iot devices. *IEEE Internet of Things Journal*, 9(1):1–24, 2021.

[41] Felix Sattler, Simon Wiedemann, Klaus-Robert Müller, and Wojciech Samek. Robust and communication-efficient federated learning from non-iid data. *IEEE transactions on neural networks and learning systems*, 31(9):3400–3413, 2019.

[42] Yang Chen, Xiaoyan Sun, and Yaochu Jin. Communication-efficient federated deep learning with layerwise asynchronous model update and temporally weighted aggregation. *IEEE transactions on neural networks and learning systems*, 31(10):4229–4238, 2019.

[43] Amirhossein Reisizadeh, Aryan Mokhtari, Hamed Hassani, Ali Jadbabaie, and Ramtin Pedarsani. Fedpaq: A communication-efficient federated learning

method with periodic averaging and quantization. In *International Conference on Artificial Intelligence and Statistics*, pages 2021–2031. PMLR, 2020.

[44] Yibo Jin, Lei Jiao, Zhuzhong Qian, Sheng Zhang, Sanglu Lu, and Xiaoliang Wang. Resource-efficient and convergence-preserving online participant selection in federated learning. In *2020 IEEE 40th International Conference on Distributed Computing Systems (ICDCS)*, pages 606–616. IEEE, 2020.

[45] Youqiang Hu, Hejiao Huang, and Nuo Yu. Device scheduling for energy-efficient federated learning over wireless network based on tdma mode. In *2020 International Conference on Wireless Communications and Signal Processing (WCSP)*, pages 286–291. IEEE, 2020.

[46] Elsa Rizk, Stefan Vlaski, and Ali H Sayed. Optimal importance sampling for federated learning. In *ICASSP 2021-2021 IEEE International Conference on Acoustics, Speech and Signal Processing (ICASSP)*, pages 3095–3099. IEEE, 2021.

[47] Xiaohui Xu, Sijing Duan, Jinrui Zhang, Yunzhen Luo, and Deyu Zhang. Optimizing federated learning on device heterogeneity with a sampling strategy. In *2021 IEEE/ACM 29th International Symposium on Quality of Service (IWQOS)*, pages 1–10. IEEE, 2021.

[48] Wenlin Chen, Samuel Horvath, and Peter Richtarik. Optimal client sampling for federated learning. *arXiv preprint arXiv:2010.13723*, 2020.

[49] Su Wang, Mengyuan Lee, Seyyedali Hosseinalipour, Roberto Morabito, Mung Chiang, and Christopher G Brinton. Device sampling for heterogeneous federated learning: Theory, algorithms, and implementation. In *IEEE INFOCOM 2021-IEEE Conference on Computer Communications*, pages 1–10. IEEE, 2021.

[50] Shiqiang Wang, Tiffany Tuor, Theodoros Salonidis, Kin K Leung, Christian Makaya, Ting He, and Kevin Chan. When edge meets learning: Adaptive control for resource-constrained distributed machine learning. In *IEEE INFOCOM 2018-IEEE conference on computer communications*, pages 63–71. IEEE, 2018.

[51] Zhaohui Yang, Mingzhe Chen, Walid Saad, Choong Seon Hong, and Mohammad Shikh-Bahaei. Energy efficient federated learning over wireless communication networks. *IEEE Trans. Wireless Commun.*, 20(3):1935–1949, 2020.

[52] Nguyen H Tran, Wei Bao, Albert Zomaya, Minh NH Nguyen, and Choong Seon Hong. Federated learning over wireless networks: Optimization model design and analysis. In *IEEE INFOCOM 2019-IEEE conference on computer communications*, pages 1387–1395. IEEE, 2019.

[53] Wenqi Shi, Yuxuan Sun, Sheng Zhou, and Zhisheng Niu. Device scheduling and resource allocation for federated learning under delay and energy constraints. In *2021 IEEE 22nd International Workshop on Signal Processing Advances in Wireless Communications (SPAWC)*, pages 596–600. IEEE, 2021.

[54] Wenqi Shi, Sheng Zhou, Zhisheng Niu, Miao Jiang, and Lu Geng. Joint device scheduling and resource allocation for latency constrained wireless federated learning. *IEEE Transactions on Wireless Communications*, 20(1):453–467, 2020.

[55] Liang Li, Dian Shi, Ronghui Hou, Hui Li, Miao Pan, and Zhu Han. To talk or to work: Flexible communication compression for energy efficient federated learning over heterogeneous mobile edge devices. In *Proc. IEEE INFOCOM*, May 2021.

[56] Guangxu Zhu, Yong Wang, and Kaibin Huang. Broadband analog aggregation for low-latency federated edge learning. *IEEE Trans. Wireless Commun.*, 19(1):491–506, 2019.

[57] Amirhossein Reisizadeh, Isidoros Tziotis, Hamed Hassani, Aryan Mokhtari, and Ramtin Pedarsani. Adaptive node participation for straggler-resilient federated learning. In *ICASSP 2022-2022 IEEE International Conference on Acoustics, Speech and Signal Processing (ICASSP)*, pages 8762–8766. IEEE, 2022.

[58] Hongda Wu and Ping Wang. Node selection toward faster convergence for federated learning on non-iid data. *IEEE Transactions on Network Science and Engineering*, 9(5):3099–3111, 2022.

[59] Haneul Ko, Jaewook Lee, Sangwon Seo, Sangheon Pack, and Victor CM Leung. Joint client selection and bandwidth allocation algorithm for federated learning. *IEEE Transactions on Mobile Computing*, 2021.

[60] Hao Chen, Shaocheng Huang, Deyou Zhang, Ming Xiao, Mikael Skoglund, and H Vincent Poor. Federated learning over wireless iot networks with optimized communication and resources. *IEEE Internet of Things Journal*, 9(17):16592–16605, 2022.

[61] Chunmei Xu, Shengheng Liu, Zhaohui Yang, Yongming Huang, and Kai-Kit Wong. Learning rate optimization for federated learning exploiting over-the-air computation. *IEEE J. Sel. Areas Commun.*, 39(12):3742–3756, 2021.

[62] Li Chen, Xiaowei Qin, and Guo Wei. A uniform-forcing transceiver design for over-the-air function computation. *IEEE Wireless Commun. Lett.*, 7(6):942–945, 2018.

[63] Alphan Sahin and Rui Yang. A survey on over-the-air computation. *arXiv preprint arXiv:2210.11350*, 2022.

[64] Safi Shams Muhtasimul Hoque and Alphan Şahin. Chirp-based majority vote computation for federated edge learning and distributed localization. *IEEE Open Journal of the Communications Society*, 2023.

[65] Pangun Park, Piergiuseppe Di Marco, and Carlo Fischione. Optimized over-the-air computation for wireless control systems. *IEEE Communications Letters*, 26(2):424–428, 2021.

[66] Mario Goldenbaum, Slawomir Stanczak, and Michal Kaliszan. On function computation via wireless sensor multiple-access channels. In *2009 IEEE Wireless Communications and Networking Conference*, pages 1–6. IEEE, 2009.

[67] Omid Abari, Hariharan Rahul, and Dina Katabi. Over-the-air function computation in sensor networks. *arXiv preprint arXiv:1612.02307*, 2016.

[68] Xiugang Wu, Shengli Zhang, and Ayfer Özgür. Stac: Simultaneous transmitting and air computing in wireless data center networks. *IEEE Journal on Selected Areas in Communications*, 34(12):4024–4034, 2016.

[69] Robert Guirado, Abbas Rahimi, Geethan Karunaratne, Eduard Alarcón, Abu Sebastian, and Sergi Abadal. Wireless on-chip communications for scalable in-memory hyperdimensional computing. In *2022 International Joint Conference on Neural Networks (IJCNN)*, pages 1–8. IEEE, 2022.

[70] Mario Goldenbaum, Peter Jung, Miruna Raceala-Motoc, Jan Schreck, Sławomir Stańczak, and Chan Zhou. Harnessing channel collisions for efficient massive access in 5g networks: A step forward to practical implementation. In *2016 9th International Symposium on Turbo Codes and Iterative Information Processing (ISTC)*, pages 335–339. IEEE, 2016.

[71] Ufuk Altun, Semiha T Basaran, Gunes Karabulut Kurt, and Enver Ozdemir. Scalable secret key generation for wireless sensor networks. *IEEE Systems Journal*, 16(4):6031–6041, 2022.

[72] Guangxu Zhu, Yuqing Du, Deniz Gündüz, and Kaibin Huang. One-bit over-the-air aggregation for communication-efficient federated edge learning: Design and convergence analysis. *IEEE Trans. Wireless Commun.*, 20(3):2120–2135, 2020.

[73] Xiaowen Cao, Guangxu Zhu, Jie Xu, and Shuguang Cui. Optimized power control for over-the-air federated edge learning. In *Proc. IEEE ICC*, pages 1–6, 2021.

[74] Naifu Zhang and Meixia Tao. Gradient statistics aware power control for over-the-air federated learning. *IEEE Trans. Wireless Commun.*, 20(8):5115–5128, 2021.

[75] Haibo Yang, Peiwen Qiu, Jia Liu, and Aylin Yener. Over-the-air federated learning with joint adaptive computation and power control. In *2022 IEEE International Symposium on Information Theory (ISIT)*, pages 1259–1264. IEEE, 2022.

[76] Peng Yang, Yuning Jiang, Ting Wang, Yong Zhou, Yuanming Shi, and Colin N Jones. Over-the-air federated learning via second-order optimization. *arXiv preprint arXiv:2203.15488 [cs.IT]*, 2022.

[77] Wei Guo, Ran Li, Chuan Huang, Xiaoqi Qin, Kaiming Shen, and Wei Zhang. Joint device selection and power control for wireless federated learning. *IEEE J. Sel. Areas Commun.*, 2022.

[78] Shusen Jing and Chengshan Xiao. Federated learning via over-the-air computation with statistical channel state information. *IEEE Transactions on Wireless Communications*, 21(11):9351–9365, 2022.

[79] Kai Yang, Tao Jiang, Yuanming Shi, and Zhi Ding. Federated learning based on over-the-air computation. In *ICC 2019-2019 IEEE international conference on communications (ICC)*, pages 1–6. IEEE, 2019.

[80] Huayan Guo, An Liu, and Vincent KN Lau. Analog gradient aggregation for federated learning over wireless networks: Customized design and convergence analysis. *IEEE Internet Things J.*, 8(1):197–210, 2020.

[81] Wanli Ni, Yuanwei Liu, Yonina C Eldar, Zhaohui Yang, and Hui Tian. Enabling ubiquitous non-orthogonal multiple access and pervasive federated learning via STAR-RIS. In *Proc. IEEE GLOBECOM*, pages 1–6, 2021.

[82] Wanli Ni, Yuanwei Liu, Zhaohui Yang, Hui Tian, and Xuemin Shen. Federated learning in multi-RIS aided systems. *IEEE Internet Things J.*, 2021.

[83] Xiaopeng Mo and Jie Xu. Energy-efficient federated edge learning with joint communication and computation design. *Journal of Communications and Information Networks*, 6(2):110–124, 2021.

[84] Qunsong Zeng, Yuqing Du, Kaibin Huang, and Kin K Leung. Energy-efficient radio resource allocation for federated edge learning. In *2020 IEEE International Conference on Communications Workshops (ICC Workshops)*, pages 1–6. IEEE, 2020.

[85] Sihua Wang, Mingzhe Chen, Walid Saad, and Changchuan Yin. Federated learning for energy-efficient task computing in wireless networks. In *ICC 2020-2020 IEEE international conference on communications (ICC)*, pages 1–6. IEEE, 2020.

[86] Abdullatif Albaseer, Mohamed Abdallah, Ala Al-Fuqaha, and Aiman Erbad. Fine-grained data selection for improved energy efficiency of federated edge learning. *IEEE Transactions on Network Science and Engineering*, 9(5):3258–3271, 2021.

[87] Richeng Jin, Xiaofan He, and Huaiyu Dai. Communication efficient federated learning with energy awareness over wireless networks. *IEEE Transactions on Wireless Communications*, 21(7):5204–5219, 2022.

[88] Xin Liu, Xiaoqi Qin, Hao Chen, Yiming Liu, Baoling Liu, and Ping Zhang. Age-aware communication strategy in federated learning with energy harvesting devices. In *2021 IEEE/CIC International Conference on Communications in China (ICCC)*, pages 358–363. IEEE, 2021.

[89] Qunsong Zeng, Yuqing Du, and Kaibin Huang. Wirelessly powered federated edge learning: Optimal tradeoffs between convergence and power transfer. *IEEE Transactions on Wireless Communications*, 21(1):680–695, 2021.

[90] Alessio Zappone and Merouane Debbah. Complexity-aware ann-based energy efficiency maximization. In *ICC 2020-2020 IEEE International Conference on Communications (ICC)*, pages 1–6. IEEE, 2020.

[91] Thi Ha Ly Dinh, Megumi Kaneko, Keisuke Wakao, Kenichi Kawamura, Takatsune Moriyama, and Yasushi Takatori. Towards an energy-efficient dqn-based user association in sub6ghz/mmwave integrated networks. In *2021 17th International Conference on Mobility, Sensing and Networking (MSN)*, pages 645–652. IEEE, 2021.

[92] Feihao Chen and Jin Yeu Tsou. Assessing the effects of convolutional neural network architectural factors on model performance for remote sensing image classification: An in-depth investigation. *International Journal of Applied Earth Observation and Geoinformation*, 112:102865, 2022.

[93] Han Xiao, Kashif Rasul, and Roland Vollgraf. Fashion-MNIST: a novel image dataset for benchmarking machine learning algorithms. *arXiv preprint arXiv:1708.07747 [cs.LG]*, 2017.

[94] Hang Liu, Xiaojun Yuan, and Ying-Jun Angela Zhang. Reconfigurable intelligent surface enabled federated learning: A unified communication-learning design approach. *IEEE Trans. Wireless Commun.*, 20(11):7595–7609, 2021.

[95] Xiang Ma, Haijian Sun, Qun Wang, and Rose Qingyang Hu. User scheduling for federated learning through over-the-air computation. In *Proc. IEEE VTC-Fall*, pages 1–5, 2021.

[96] Saeed Razavikia, Jaume Anguera Peris, José Mairton B Da Silva, and Carlo Fischione. Blind asynchronous over-the-air federated edge learning. In *2022 IEEE Globecom Workshops (GC Wkshps)*, pages 1834–1839. IEEE, 2022.

[97] Jiayu Mao, Haibo Yang, Peiwen Qiu, Jia Liu, and Aylin Yener. Charles: Channel-quality-adaptive over-the-air federated learning over wireless networks. In *2022 IEEE 23rd International Workshop on Signal Processing Advances in Wireless Communication (SPAWC)*, pages 1–5. IEEE, 2022.

[98] Xiaowen Cao, Guangxu Zhu, Jie Xu, and Shuguang Cui. Transmission power control for over-the-air federated averaging at network edge. *IEEE J. Sel. Areas Commun.*, 40(5):1571–1586, 2022.

[99] Caijuan Chen, Yi-Han Chiang, Hai Lin, John CS Lui, and Yusheng Ji. Energy harvesting aware client selection for over-the-air federated learning. In *Proc. IEEE GLOBECOM*, pages 5069–5074, 2022.

[100] Michael Grant, Stephen Boyd, and Yinyu Ye. CVX: Matlab software for disciplined convex programming, 2011.

[101] Qingqing Wu and Rui Zhang. Intelligent reflecting surface enhanced wireless network: Joint active and passive beamforming design. In *Proc. IEEE GLOBECOM*, pages 1–6, 2018.

[102] Zhi-Quan Luo, Wing-Kin Ma, Anthony Man-Cho So, Yinyu Ye, and Shuzhong Zhang. Semidefinite relaxation of quadratic optimization problems. *IEEE Signal Process. Mag.*, 27(3):20–34, 2010.

[103] Zheng Chang, Liqing Liu, Xijuan Guo, and Quan Sheng. Dynamic resource allocation and computation offloading for IoT fog computing system. *IEEE Trans. Ind. Informat.*, 17(5):3348–3357, 2020.

[104] Hung Nguyen, Sarah J Maclagan, Tu Dinh Nguyen, Thin Nguyen, Paul Flemons, Kylie Andrews, Euan G Ritchie, and Dinh Phung. Animal recognition and identification with deep convolutional neural networks for automated wildlife monitoring. In *2017 IEEE international conference on data science and advanced Analytics (DSAA)*, pages 40–49. IEEE, 2017.

[105] Andy Rosales Elias, Nevena Golubovic, Chandra Krintz, and Rich Wolski. Where's the bear? automating wildlife image processing using iot and edge cloud systems. In *Proceedings of the Second International Conference on Internet-of-Things Design and Implementation*, pages 247–258, 2017.

[106] Wiame Benzekri, Ali El Moussati, Omar Moussaoui, and Mohammed Berrajaa. Early forest fire detection system using wireless sensor network and deep learning. *International Journal of Advanced Computer Science and Applications*, 11(5), 2020.

[107] Matthias Frey, Igor Bjelaković, and Sławomir Stańczak. Towards secure over-the-air computation. In *2021 IEEE International Symposium on Information Theory (ISIT)*, pages 700–705. IEEE, 2021.

[108] Changjie Hu, Quanzhong Li, Qi Zhang, and Jiayin Qin. Secure transceiver design and power control for over-the-air computation networks. *IEEE Communications Letters*, 26(7):1509–1513, 2022.